Geochemical Perspectives

Volume 8, number 1 | April 2019

NOBUMICHI SHIMIZU

Big-Picture Geochemistry from Microanalyses – my Four-Decade Odyssey in SIMS

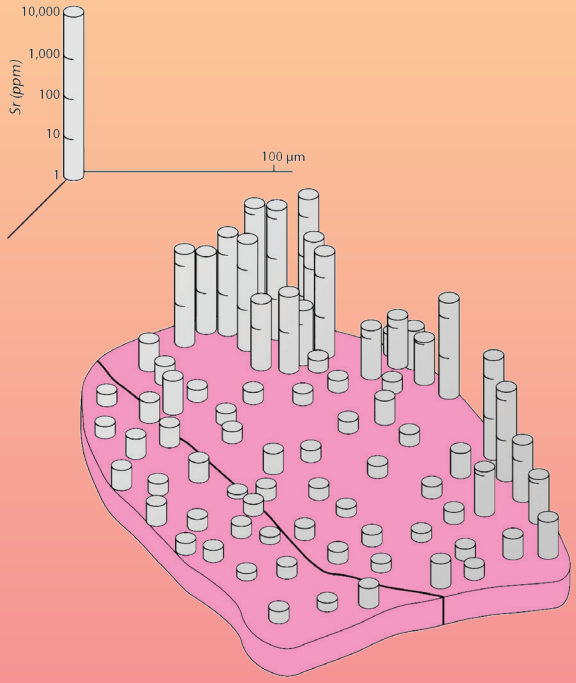

Geochemical Perspectives

Each issue of ***Geochemical Perspectives*** presents a single article with an in-depth view on the past, present and future of a field of geochemistry, seen through the eyes of highly respected members of our community. The articles combine research and history of the field's development and the scientist's opinions about future directions. We welcome personal glimpses into the author's scientific life, how ideas were generated and pitfalls along the way. *Perspectives* articles are intended to appeal to the entire geochemical community, not only to experts. They are not reviews or monographs; they go beyond the current state of the art, providing opinions about future directions and impact in the field.

ISSN 2223-7755 (print)
ISSN 2224-2759 (online)
DOI 10.7185/geochempersp.8.1

Principal Editor for this issue
Janne Blichert-Toft, ENS Lyon, France

Reviewers
Marc Chaussidon, IPGP, France
Tim Elliott, University of Bristol, UK
William White, Cornell University, USA

Cover Layout **Pouliot Guay Graphistes**
Typesetter **Info 1000 Mots**
Printer **Deschamps impression**

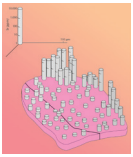
About the cover

The "Down Town Garnet": a bird's eye view of the distribution of Sr in a section of a diamond inclusion garnet from the Mir pipe.

Source: Figure modified from Shimizu *et al.* (1997a).

CONTENTS

DEDICATION

I dedicate this volume to Stan Hart and Claude Allègre, my life-long friends and mentors (see photo on the next page).

Stan received me as a post-doc at DTM in 1971 and continued to be my mentor and friend throughout my career. It was Stan's foresight that made the Cameca IMS 3f, and ion microprobes in general, such a successful tool in geochemistry. Claude gave me a job at IPGP in 1974, where my first encounter with an ion probe happened and my odyssey began. He then patiently watched me struggle with the new technology and supported me throughout my career with enthusiastic friendship. I almost came back to IPGP in 1988 because I so treasured my relationship with Claude.

Nobu Shimizu (middle) with his mentors,
Stan Hart (right) and Claude Allègre (left), at Fall AGU 1996.

PREFACE (OR APOLOGIES)

What you are about to read is my personal story of SIMS applications to geochemistry. Ever since I accepted the invitation by Janne Blichert-Toft to write this, I constantly struggled to decide how I should turn it. Early on, I intended to make this volume useful for a wide range of geochemists by reviewing the history of technical developments and applications in a comprehensive way. But….I changed my mind. It would have been a dry read despite its potential usefulness. Instead, I decided to tell my own struggles, joy of discovery, and my own metanoic moments.

Every volume of the *Geochemical Perspectives* series has been a very interesting read to me, especially because of the authors' personal stories and their accounts of geochemistry and the players of it, and I decided to follow the same line. This inevitably meant then that numerous ion probe studies done by other geochemists had to be almost completely left out, and I apologise deeply to everyone concerned for these omissions. I also had to leave out many things I was directly involved in, not because they were unimportant, but because I wanted to focus on only a few major subjects that I spent most of my time on so as to maintain some semblance of coherence. Apologies therefore are also due to those of my colleagues who were involved in these studies that I have omitted here.

I did my post-doc in the early 1970s, when geochemistry was in a revolutionary period with the plate tectonics theory rapidly developing. I got involved in SIMS in the middle of the revolution, ambitious about developing SIMS applications in geochemistry and contribute to said revolution. Although the technique itself was in its infancy and there were many hurdles to face and overcome, I was

at the IPGP, one of the centres of geochemical revolution at the time, and my enthusiasm was always highly stimulated. At MIT and WHOI, I was surrounded by colleagues with unlimited curiosity and SIMS applications diversified significantly. I maintained the philosophy of an open lab and the "Field of Dreams" approach. Individual geochemical projects I describe here reflect my fundamental curiosity of How Earth Works.

Nobumichi Shimizu
Woods Hole Oceanographic Institution
266 Woods Hole Rd. MS# 23
Woods Hole, MA 02543
USA

ACKNOWLEDGEMENTS

For completing this article, I acknowledge important contributions by several individuals. First and foremost, Janne Blichert-Toft, who not only invited me to write this, but also was a patient editor, helping and encouraging me to be myself. Bill White, Tim Elliott, and Marc Chaussidon provided formal reviews with great suggestions. I thank Natalie Renier of WHOI Graphics Department for reproducing old figures for this article, and Ann Devenish of WHOI-MBL Library for helping me access old papers to be re-read.

BIG-PICTURE GEOCHEMISTRY FROM MICROANALYSES – MY FOUR-DECADE ODYSSEY IN SIMS

ABSTRACT

Secondary Ion Mass Spectrometry (SIMS) is now a well established analytical technique in geochemistry. Its developmental history goes back to the 1970s. Here, I tell the story of how I got involved in its applications to geochemistry in 1974 at the Institut de Physique du Globe in Paris (IPGP) with the Cameca IMS 300 instrument and my ensuing struggles with theories of secondary ion formation processes and the eventual development of the energy filtering approach as an effective method for suppressing molecular ion interferences in silicate minerals and glasses.

The geochemical applications of the techniques that I developed with my colleagues at IPGP, Massachusetts Institute of Technology (MIT), and Woods Hole Oceanographic Institution (WHOI) are summarised in four different categories: (1) trace element zoning of phenocrysts and the kinetics of magmatic crystallisation processes, (2) trace element abundance patterns and geochemical processes

in the mantle, (3) use of trace element abundances in magmatic processes in the mid-ocean ridge system, and (4) use of Sr/Ca ratios in biogenic carbonates in palaeoceanographic studies.

Trace element zoning patterns observed in phenocrysts reveal that crystal growth in magmas can occur with non-equilibrium partitioning of trace elements at the crystal-melt interface. Trace element zoning patterns in augite phenocrysts from Gough Island also indicate repeated drastic changes in magma composition, suggesting a turbulent dynamic state of magma bodies beneath eruptive centres.

Chondrite normalised rare earth element (REE) patterns measured in clinopyroxenes from mantle rocks (peridotites from the Horoman massif and xenoliths in basalts from both oceanic and continental localities) show strong evidence for melt-rock reactions, indicating that lithospheric peridotites depleted in incompatible elements by melt extraction often show evidence of having been subsequently enriched in these elements through melt-rock reaction. The distribution of Sr in garnet inclusions in peridotitic diamonds from South Africa and Siberia is highly heterogeneous over wide concentration ranges, suggesting growth of inclusion garnets as well as formation of these diamonds, occurred shortly before the diamonds were carried to the surface by kimberlite eruptions.

Rare earth element and other trace element abundance patterns measured in clinopyroxenes in abyssal peridotites clearly indicate that melting and melt extraction processes beneath mid-ocean ridges is akin to fractional melting by which small degree melt fractions are progressively extracted from residues as the mantle decompresses and only later mixed, sometimes incompletely, to form mid-ocean ridge basalt lavas erupted on the ocean floor. However, melt-rock reactions between residual peridotites and upwelling melt fractions could significantly alter trace element abundance patterns of originally residual clinopyroxenes. *In situ* analyses reveal very large trace element variations occurring on intra-mineral scales, suggesting that precipitation of clinopyroxene also occurred during melt-rock reactions. It is evident that abyssal peridotites contain complex geochemical histories beyond melt extraction *via* fractional melting.

Sr/Ca variations in coral skeletons (aragonite) reveal strong effects of photosynthesis of symbiont algae in day time growth zones, while those in night time growth zones near centres of calcification record variations of sea surface temperatures (SST) in *Porites lutea.* In *Astrangia poculata*, which experience a large temperature range (-2 – 23 °C), non-symbiotic skeletons faithfully record temperature variations, while symbiotic skeletons display ontogenic effects of algal symbionts. Sr/Ca variations in coccolithophores across the Paleocene-Eocene Thermal Maximum (PETM) display different responses of individual species to the sudden greenhouse environment, and the severity of the response also is dependent on the oceanographic conditions of their habitats.

1. BACKGROUND AND INTRODUCTION (DTM À IPGP)

My SIMS Odyssey began when I moved from Washington, D.C., to Paris, France, in 1974.

Looking back four decades to trace my personal history of involvement in the development of secondary ion mass spectrometry (SIMS) applications to the geosciences, I will try to weave a tapestry with the development of my own scientific interest in modern mantle geochemistry and the development of SIMS technology as crossing threads.

I finished my Ph.D. thesis at the University of Tokyo in 1968 on Pb isotopes in some Japanese granitic rocks and along the way developed a strong interest in studying trace element fractionation during mantle processes. Recognising that Pb isotopic variations observed in basalts (Gast *et al.*, 1964; Tatsumoto, 1966) must be related to fractionation of U from Pb *via* processes in the mantle, I thought that the determination of mineral-melt trace element partitioning at high pressures was one of the most fundamental pieces of knowledge that we needed but did not have. I also thought that documentation of mantle minerals in terms of their trace element abundances should accompany such experimental partitioning data, but the former was largely unknown territory. Although I had an entry level faculty job at the University of Tokyo, the academic environment at the university was not encouraging due to the student-admin confrontation that started in the medical school and grew into a university-wide protest movement, leaving no hope for me to engage in any research projects in the forseeable future at the University of Tokyo. The unrest became part of a larger societal phenomenon that stirred the entire world (from country to country while major societal issues varied, college students played major roles in taking a stand against their respective governments, and Japan was no exception). In addition, my situation was exacerbated by the untimely death of my Ph.D. advisor, Professor H. Kuno, in 1969, so all taken together my future at the University of Tokyo did not at all look promising. I knew that I would not be able to do what I wanted there, and that the only way forward was to go abroad, so I started to write letters to people I would like to work with, proposing some of my ideas. I was extremely fortunate that Stan Hart and colleagues at the Department of Terrestrial Magnetism (DTM) at the Carnegie Institution of Washington were interested in what I proposed to do as a post-doc, and I arrived at the Broad Branch Road campus in August 1971.

I started two projects right away: determining (1) trace element abundances in clinopyroxenes in spinel peridotite xenoliths from Salt Lake Crater, Hawaii, and (2) trace element partitioning between clinopyroxene and melt at high pressures. To do the former, the existing ion exchange column chemistry had to be improved by miniaturising columns and using Teflon tubing and frits, given that purified mineral separates (in this case clinopyroxenes) from small xenoliths would be limited to 10 –20 mg. The efforts were rewarded by reduced chemical blanks to what, at the time, were considered very low levels: K (7 ng), Rb (0.01 ng), Cs

(0.3 pg), Sr (0.2 ng), and Ba (0.8 ng). The isotope dilution approach combined with the new low blank environment was successful for both projects. Stan Hart was instrumental in teaching me microchemistry. He was himself attempting to look at trace element partitioning between clinopyroxene phenocrysts and groundmass, and the low blank chemistry we developed together was later successfully used in his work with Chris Brooks (Hart and Brooks, 1974).

Figure 1.1 Department of Terrestrial Magnetism, Carnegie Institution of Washington, 5241 Broad Branch Rd., N. W., Washington, D.C. Photo courtesy of Carnegie Science.

Encounter with Al Hofmann

Al was George Tilton's post-doc at the Geophysical Laboratory when I arrived at DTM. I did not know which project(s) he was working on but he was a regular member of our lunch club and his compatriot, Borwin Grauert, was my office mate. Borwin was an incredibly hard worker. He was working on zircon dating and was always running around with a sample collection from the Baltimore Gneiss or doing mineral separation with a Wilfrey Table or zircon dissolution chemistry mass spec. runs. In fact, he established a historical record of the largest number of mass spec. runs done in a year. In contrast, I thought Al was lazy: I never saw him work. But, he absolutely amazed me by publishing a paper on chromatographic theory of infiltration metasomatism (Hofmann, 1972) and got into a serious discussion with Korzhinskii. (Al's reply to Korzhinskii: Hofmann, 1973). I knew Korzhinskii's work on open system

thermodynamics because it had been one of the topics we discussed in Miyashiro's Metamorphic Petrology class back at University of Tokyo. This Al, engaging in serious discussions with Korzhinskii? At that moment, he gained my deep respect. He joined the Staff at DTM in 1974 and the three of us, Stan, Al, and I, often sat together in the mass spec. lab discussing geochemistry. Al mentioned at some point that *"here are the world's greatest geochemists together"*. Thanks, Al, for including me!! His leadership quality grew tremendously when he moved to Mainz. The state of geochemistry in Europe in the late 1970s and 1980s was in transition with Claude Allègre doing everything single handedly, but it changed when Al and, later, Keith O'Nions joined Claude in organising EAG, *etc*. so that the European standard in geochemistry became on par with that of the US.

Al and I had a very similar historical experience as well: He and I both spent our childhoods immediately after a loss in WWII and witnessed how American GIs of the occupying force behaved, handing out material riches of victorious America.

Figure 1.2 Geophysical Laboratory on Upton Street, N.W. Washington, D.C. Photo courtesy of Carnegie Science.

For the experimental determination of partition coefficients, I had to go to the Geophysical Laboratory on the Upton Street campus. Luckily, I. Kushiro was there and taught me the intricacies of piston cylinder high pressure experiments

and introduced me to other staff members so I could use their piston cylinders. Trace element analysis of co-existing clinopyroxene and glass was done with the low blank isotope dilution method mentioned above using bulk trace element abundances similar to natural basalts (2200 ppm K, 3.2 ppm Rb, 0.56 ppm Cs, 130 ppm Sr, 250 ppm Ba). The physical separation of clinopyroxene and glass in pure form in experimental charges of approximately 20 mg total was a major obstacle. To get around it, I developed a differential dissolution technique (DDT; Shimizu and Hart, 1973) in which powdered experimental charge was centrifuged with dilute HF repetitively so that the melt phase (hydrous glass) was dissolved before clinopyroxene was attacked. I had to manufacture Teflon centrifuge tubes and each dissolution step required isotope dilution analysis of the leachate. This was a very painstaking and time consuming protocol but I was successful in determining for the first time the partition coefficients of K, Rb, Cs, Sr, and Ba between clinopyroxene and melt at high pressures (Shimizu, 1974).

While I was making progress with the Hawaiian xenolith project, Joe Boyd at the Geophysical Lab published his "pyroxene geotherm" paper (Boyd and Nixon, 1972; Boyd, 1973), and I went to the Geophysical Lab to talk to him. I was surprised when I found that Joe was the guy I saw often in the front yard of the Geophysical Lab, splitting firewood bare-chested. I was curious about trace element abundances in clinopyroxenes and garnets in garnet peridotites, which represented deeper-seated counterparts to my Hawaiian spinel peridotites, and was going to ask him for some samples to analyse. Joe immediately took me into the world of "sheared and granular nodules". In addition, the first Kimberlite Conference was to be held in Cape Town, South Africa, in September 1973, and I was fascinated and excited by the prospect of going to an international conference and present the first trace element mineral data on sheared and granular garnet peridotite xenoliths from kimberlites. Joe was extremely generous in listening to my ideas and giving me samples, including the famous PHN 1611, the sheared garnet peridotite from Thaba Putsoa, Lesotho. Handpicking followed and I soon began to produce abundances of K, Rb, Cs, Sr, and Ba in clinopyroxenes and garnets in sheared and granular peridotitic xenoliths from southern African kimberlites. The difference between sheared and granular xenoliths was stunning. For instance, Sr abundances in clinopyroxene were much higher in the granular than the sheared xenoliths (200 – 560 ppm *vs.* 85-95 ppm), despite the fact that the granular peridotites were depleted in basaltic components relative to the sheared peridotites (Shimizu, 1975a). This brought home to me the puzzling decoupling of major and trace elements pointed out by Fred Frey and colleagues (Frey and Green, 1974, among others), who emphasised the importance of metasomatic processes in the mantle resulting in the enrichment of trace elements in peridotites that were depleted in basaltic components.

Mantle geochemistry/petrology went through a revolutionary period in the 1960s and 1970s with the development and establishment of the plate tectonic theory as the fundamental framework in Earth Sciences. Our knowledge of the Earth's mantle increased rapidly with respect to mineralogy as a function of depth. For instance, the mantle mineral facies concept was developed by

experimentalists that included O'Hara (1967), Ringwood, (1966), Green and Ringwood (1967), and Kushiro and Yoder (1966), among others, who established that garnet peridotite would be stable at greater depths than spinel peridotite. O'Hara (1967) proposed "O'Hara's grid", whereby equilibrium pressure and temperature conditions for natural peridotites could be estimated with reference to experimentally determined variations of mineral chemistry. It was also during this period that experiments showed that partial melting of peridotitic mantle generates basaltic melts (*e.g.*, Kushiro, 1968), and that their solidus melt compositions vary systematically from silica saturated (tholeiitic) to silica undersaturated (alkali basaltic) compositions with increasing pressure. Finally, seismic velocity variations with clear discontinuities (*e.g.*, Anderson, 1965) indicated abrupt changes in mantle densities, reflecting mineralogical changes as a function of pressure.

With respect to isotope and trace element geochemistry, the '60s and '70s were also a period of important breakthroughs. Gast *et al.* (1964) discovered Sr and Pb isotope variations in basalts from Gough and Ascension islands, demonstrating that the mantle source regions for these basalts had been heterogeneous with respect to parent/daughter element ratios (*i.e.* Rb/Sr and U,Th/Pb) for very long periods of time. Tatsumoto (1966) followed up on this by showing that a similar situation existed for the mantle source of Hawaiian basalts. These discoveries were inspiring in that radiogenic isotopes are excellent geochemical tracers reaching far beyond being "just" tools for radiometric dating of rocks and showing that chemical fractionation of parent and daughter elements must have occurred in the mantle long ago to explain the variations of radiogenic isotopes in basalts today. It was shocking to realise that the mantle was chemically heterogeneous and had been so for a long time. Gast (1968) was also the first to show that chondrite normalised rare earth element (REE) abundance patterns were distinctly different between abyssal tholeiites from mid-ocean ridges (mid-ocean ridge basalts; MORB) and alkaline basalts from ocean islands and concluded that the light REE depletion in abyssal tholeiites indicated that they were derived from a mantle source from which melt had been extracted previously (*i.e.* the so-called "depleted mantle source", today a concept we take for granted).

Then came the discovery by Stan Hart at DTM, showing that $^{87}Sr/^{86}Sr$ ratios in basalts were drastically different between abyssal tholeiites from the Reykjanes Ridge and basalts from Iceland. This demonstrated that the mid-ocean ridge and mantle plumes belonged to, or tapped, separate chemical domains in the mantle, domains that had been separate for a very long period of time (Hart *et al.*, 1973).

After successfully miniaturising column chemistry for alkaline and alkaline earth elements, Stan and I agreed to expand our analytical capabilities to include REE. John Philpotts at NASA Goddard Space Flight Center generously shared with us the REE spikes he were using himself as well as important analytical know hows. With REE standard solutions that we prepared at DTM and many mass spec. runs for each individual REE, trying out both double- and triple-filament assemblies, our isotope dilution method for REE got established.

I started to work on a project to measure REE partitioning between garnet and melt (Shimizu and Kushiro, 1975), using the DDT separation of phases. Rare earth element abundance patterns in a suite of basanites and basanitoids from Grenada displayed an interesting constancy for heavy REE coupled with large variations of light REE (Shimizu and Arculus, 1975) indicative of the presence of garnet in the source during melting, which was consistent with the garnet-melt partition coefficients recently established. I also measured REE abundances in handpicked minerals from garnet peridotite xenoliths from kimberlites (Shimizu, 1975a). Between sheared and granular xenoliths, differences in REE abundances are stunning, especially for garnets. While sheared xenolith garnets had smooth light REE depleted patterns, granular xenolith garnets had sinuous patterns with increasing abundances from Ce to Sm, then decreasing towards the heavy REE (see Fig. 1.3).

These patterns indicated equilibrium with extremely fractionated melt, such as kimberlite, and suggested that kimberlitic melts might be involved in metasomatic changes in peridotites. Whole rock REE abundances estimated on the basis of mineral data and abundances of minerals in the rocks showed that the sheared peridotites possessed near-chondritic REE abundances, whereas the granular peridotites were found to be enriched in light relative to heavy REE. Taken together with alkaline and alkaline earth element abundances, these observations indicated that granular peridotites had more complex geochemical histories than sheared peridotites (Shimizu, 1975b).

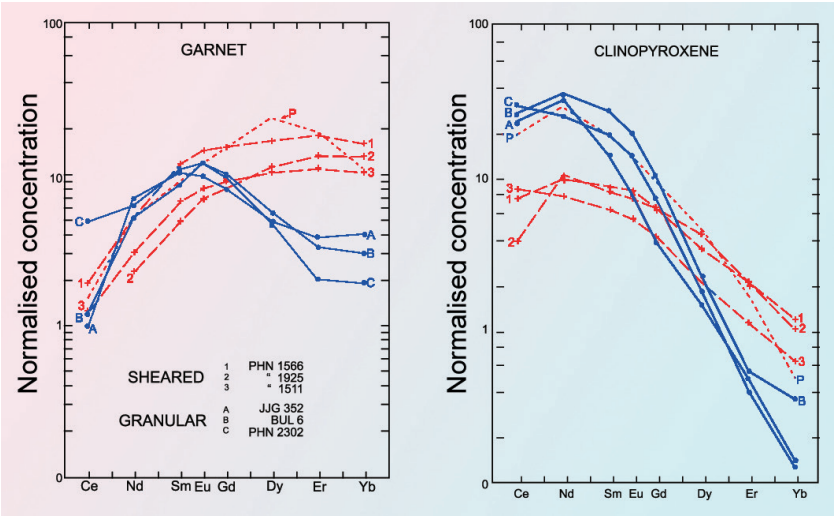

Figure 1.3 Chondrite normalised REE abundance patterns of garnets and clinopyroxenes from garnet lherzolite xenoliths. Modified from Shimizu, 1975b.

The three years I spent at DTM was coming to an end and I had to leave the US due to the J-1 visa regulations. The projects I had worked on had all been successful and the results contributed to significant advances in our knowledge of the distribution of trace elements in mantle minerals and in mantle-basalt systems. However, I realised that the analytical protocol consisting of "handpicking-dissolution-column chemistry-mass spec. analysis" was very labour intensive, as well as stressful, especially the DDT-based projects on experimental partition studies. That was when I was first exposed to the ion microprobe, at a small workshop-type meeting that Stan Hart, Claude Allègre, and others organised in Newport, RI, in 1973. Allègre presented an advertisement for Cameca (IMS 300) showing remarkably clear secondary ion images of rocks, while Ted Bence called the ion microprobe "the ultimate machine". It was not difficult for me to imagine that I could use this machine to pursue my interests in trace element distributions, mineral-melt partitioning, mantle mineral analysis, and possibly trace element zoning of igneous minerals.

While I was at a loss of how to go about my academic future, at the AGU Spring Meeting in Baltimore in 1974, Claude Allègre came to me and said "*I'll give you a job*". I knew that he was a good friend of Stan's but had never spoken to him before. I replied something like "*OK, I'll think about it*", but at that moment I decided to go to Paris and with that my SIMS Odyssey was about to begin.

2. IPGP AND THE PHYSICS OF SECONDARY ION FORMATION PROCESSES

My family and I moved to Paris in August 1974. In the beginning we stayed at a small hotel near the Jussieu campus until a house we could rent was found in the town of Bry-sur-Marne. There were many logistical problems: first of all, there was a postal strike (more than two weeks into the strike, President Giscard d'Estaing declared that it was a political strike … I wondered if there were apolitical strikes!) and the bill of lading was held up so that we could not get our personal stuff, which we had shipped from Washington, through the customs. Then, French bureaucracy came in to play as well: my appointment papers were traveling very slowly from the Ministry of Education and Research to the Ministry of Labor, *etc*., and my first paycheck did not arrive until the end of November 1974. Thus my sojourn in Paris started with camping out in an empty house without our things and without any money from September to the beginning of December.

However, my life at the IPGP (Institut de Physique du Globe de Paris) started out very well. My office was in the middle of a corridor on the third floor, connecting the towers 14 and 24 of the Jussieu campus, and my next door neighbours were Ariel Provost, Jean-François Minster, and Francis Albarède. These brilliant students were the core of the very active geochemistry group that Claude Allègre was leading. Claude came by my office often for discussion by saying "*What news*?". The only problem was that he was so busy that, as soon as he entered my office, his secretaries called him from the end of the corridor: "*Monsieur Allègre, téléphone*!!!" So, I developed a technique to keep him with me a bit longer. When he said something, my first reaction was "*No! That's not right*!". Then he would stay a bit longer to find out why I had said so. It worked and our working relationship was developing very well. One day in the spring of 1975, Claude had just come back from the Lunar Science Conference in Houston, extremely excited about Nd isotopes. He had heard a talk given by Gunther Lugmair on dating of lunar rocks and chondritic meteorites using the Sm-Nd decay system. The reason Claude was excited was not about the dating, but about the potential usefulness of Nd isotopic compositions as a natural tracer. Since ^{147}Sm decays to ^{143}Nd, geochemical processes that fractionate REE would result in variations of Nd isotopic compositions, such that by measuring the Nd isotopic compositions of rocks, we could study the geochemical prehistory of the rock. Unlike the Rb-Sr and U, Th-Pb systems, both the parent and daughter are REE and we knew their fractionation behaviour fairly well, even back then. For me, who had just published mantle-mineral REE distributions (Shimizu, 1975b) and submitted a paper on the partitioning of REE between garnet and melt (Shimizu and Kushiro, 1975), the enormous potential of Nd isotopes as a natural tracer was evident and I was as excited as Claude. Claude then recruited a student, Pierre Richard, who developed the separation chemistry and mass spec. techniques necessary to measure the Nd isotopic compositions of mantle-derived magmas. This was the beginning of the Nd isotope tracer (Richard *et al.*, 1976) and every day at the lab was exciting and very productive.

Encounter with Don DePaolo

In the Spring of 1975, Claude Allègre came back from the Lunar Science Conference in Houston all excited about a new thing: the Sm-Nd system. ^{147}Sm decays to ^{143}Nd, and Gunther Lugmair at Scripps used it for chronology of lunar rocks and meteorites. What excited Allègre more, however, was not the chronological aspect of the Sm-Nd system, but the possibility of using it as a natural tracer by measuring the Nd isotopic compositions of mantle-derived rocks. I was excited about this immediately because I had just published a paper on REE distribution between mantle garnets and clinopyroxenes (Shimizu, 1975b) and REE partitioning between garnet and melt (Shimizu and Kushiro, 1975), and was very familiar with REE fractionation. So, Nd isotope variations in nature as a consequence of Sm-Nd fractionation were of primary interest to me. Allègre recruited a student, Pierre Richard, to find out how to chemically separate Nd from Sm and how to use mass spectrometry to measure Nd isotopes in some oceanic basalts. Our primary target was MORB glasses because Nd isotopic compositions of MORB would be an unequivocal test of Paul Gast's theory (Gast, 1968) that MORB melts were derived from a mantle source already depleted by previous melt extraction. I wrote a letter to Fred Frey at MIT asking for MORB samples (Fred forwarded my letter to Geoff Thompson at WHOI with a scribble saying that "*Shimizu is trying Nd isotopes on MORBs which he (Fred) doubted would be a success*"). We got the samples and the results were what we had anticipated. So we wrote a paper and sent it to EPSL (Richard *et al*., 1976). As it happened, Gerry Wasserburg was also thinking the same thing, and he put Don DePaolo on it for his Ph.D. thesis at Caltech (although Don said somewhere that it was his idea) and got basically the same results as we did. At an AGU Spring Meeting in 1976, Don's paper and ours were presented back to back. The room was packed. People were interested in hearing about the latest development in isotope geochemistry. Now came a race to publish the first geochemistry paper on Nd isotopes: our paper got very favourable reviews with some minor revisions to take care of. I left the manuscript on my desk for three weeks. One day, Allègre barged into my office, enraged, and said, "*You lazy son of a bitch!*". While I had left our manuscript on my desk, the Caltech group published the first Nd isotope paper in Geophysical Research Letters (DePaolo and Wasserburg, 1976). Actually, when we looked at the submission dates, ours was earlier than theirs, but they beat us to the publication, and Don was awarded all the accolades (he got medals for it) and launched his very successful career.

While this was going on, I also started to work on the geochemical applications of secondary ion mass spectrometry using the first generation Cameca IMS 300. Michel Semet introduced me to the machine and showed me its basic functions. Partly due to my naïveté, I was deeply curious about the physics of secondary ion formation processes and was secretly ambitious about devising a scheme of converting secondary ion mass spectra into quantitative information on concentrations of major and trace elements in silicate minerals and glasses. The IMS 300 was a commercial version of a secondary ion imaging instrument based on Georges Slodzian's thesis (Slodzian, 1964). Secondary ion intensities were measured by a photomultiplier, which was saturated very easily. Using this instrument as a quantitative tool had to wait until a major change in ion optics was implemented with the addition of an electrostatic sector and an electron

multiplier detector. The resultant instrument became a double-focusing machine with reverse geometry (an electrostatic sector after a magnetic sector) and was called the IMS 300-RG.

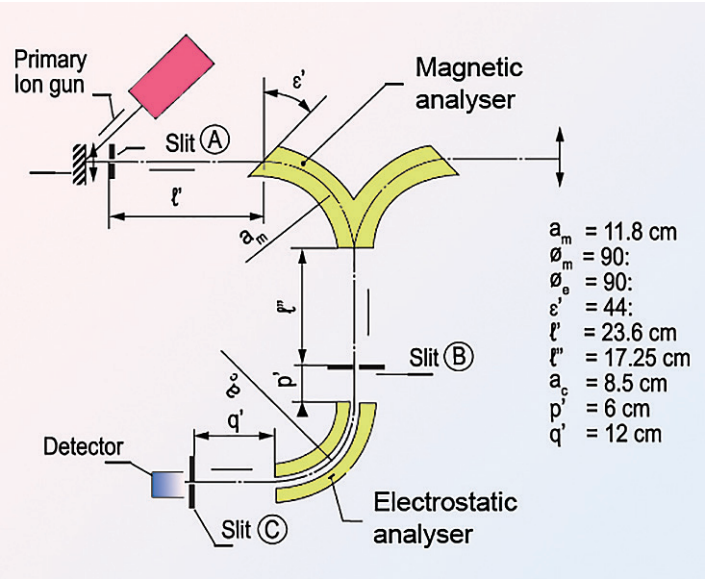

Figure 2.1 A plan view of the IMS 300-RG; instead of reflecting at a mirror, the ion beam goes through an added electrostatic analyser (ESA) and is detected by an electron multiplier. Image courtesy of Cameca.

I want to acknowledge at the outset the contributions made by Georges Slodzian, who did his Ph.D. thesis on designing a SIMS instrument and wrote many seminal papers on the physics of ionisation, the ion optics involved in SIMS instruments, and a wide range of applications of the technique.

Figure 2.2 Georges Slodzian, the inventor of the Cameca SIMS machines.

Techniques for chemical and isotopic analysis of solid surfaces were developed in the 1960s (*e.g.*, Liebl and Herzog, 1963; Long, 1965) and Liebl (1967) described one of the first commercially available instruments (the ARL machine), which was to be used by Andersen and Hinthorne (1973) for serious geochemical applications. Independently, Georges Slodzian's secondary

ion imaging instrument (Slodzian, 1964) became commercialised by Cameca as the IMS 300. While these early instruments had rather low mass resolving power, the necessity for high mass resolution instruments was pointed out by Bakale *et al*. (1975) and Bill Compston at the ANU in Canberra. With the aim of determining U-Pb ages of zircons *in situ*, ANU scientists built a high mass resolution instrument known as the SHRIMP (Sensitive High Resolution Ion Micro-Probe; see Compston and Clement (2006); also see Foster (2010) for a historical perspective of SHRIMP development). The acronym SIMS (Secondary Ion Mass Spectrometry) was coined by Benninghoven (1970). Fundamentally, SIMS is mass spectrometry, and intensities of secondary ions, representing various elements, are measured relative to a reference element (Si for silicates, for instance). In practice, isotopes representing various elements are measured against ^{28}Si.

From the point of view of the analyst, the secondary ion intensity of an element (in practice, an isotope) is a measure of the number of ions detected *per* unit time at the end of an instrument and depends on a number of factors. For sputtered secondary ions, this can be expressed as follows:

$$I_i = N_i * P_i * \eta \tag{2.1}$$

where N_i is the number of sputtered particles containing element *i* (sputtered particles can be single atoms as well as clusters, such as dimers, oxides, and complex polyatomic molecules) in a unit volume of sputtering site *per* unit time, P_i the probability of ionisation of element *i* as singly charged positive ions (number of ions relative to number of sputtered particles containing the element), and η the transmission of the instrument. A bulk sputtering coefficient, S, can be defined for a given sample as the number of particles sputtered from the sample *per* incident ion:

$$N_i = C_i * S \tag{2.2}$$

where C_i is the atomic concentration of element *i*. Since S is a bulk coefficient, *i.e.* the number of particles sputtered integrated over energy and angle *per* incident ion, the chemical composition of the population of the sputtered particles is assumed to be identical to that of the bulk sample.

$$I_i = C_i * S * P_i * \eta \tag{2.3}$$

This equation establishes a direct relationship between measured intensity and chemical composition of a sample, and is self-evident for single component materials such as pure metals for which theories of sputtering and early ionisation models were developed.

Sputtering is a dynamic destructive process and is complex for poly-component materials such as silicate minerals and glasses. Historically, the physics of sputtering was studied on clean surfaces of pure metals bombarded with noble gas ion beams. It was Peter Sigmund (Fig. 2.4) who developed the random collision cascade theory, which has come to be widely accepted as a leading theory for sputtering (Sigmund, 1969). The time scale of collision cascades (of the order of

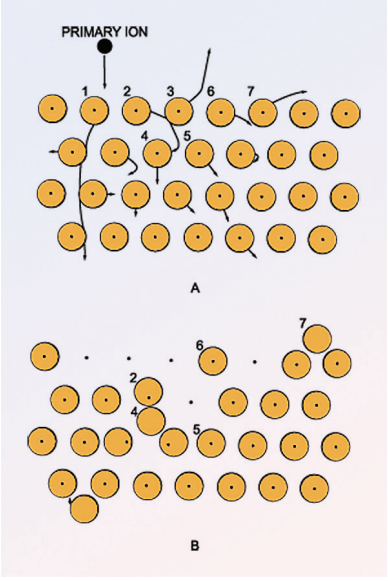

Figure 2.3 A cartoon of how sputtering works. The upper panel shows how atoms would move upon bombardment of a primary ion (black dot), while the lower panel shows where atoms are after 10^{-10} seconds of bombardment. Modified from Shimizu and Hart (1982b), modified from Williams (1979).

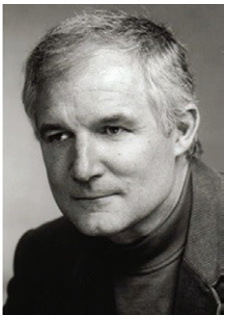

Figure 2.4 Peter Sigmund, who laid the foundation for the physics of sputtering.

10^{-13} seconds) is much shorter than that of the impingement of successive primary ions onto a sputtering site with primary ion beam currents commonly being used (Sigmund, 1974; Werner, 1974) such that there is no overlap between two successive cascades. In other words, a collision cascade is completely finished before the bombardment by another primary ion beam ion. It has also been argued that emitted ions originate within a few nanometres of the surface after relatively small numbers of collisions. Sputtered particles leave a sample surface with various kinetic energies, reflecting, among others, prehistories of collision cascades. The distribution of kinetic energy among sputtered particles is predicted by Sigmund's theory and is approximated by the inverse square of kinetic energy (E^{-2}) (Thompson, 1968).

Based on the analysis of surfaces after sputtering through Auger electron analysis, Rutherford back scattering depth profiling, and other techniques, it has been observed that sputtering results in chemical and isotopic fractionation of the surface in question (Kelly, 1978, 1980; Betz, 1980; Watson and Haff, 1981; among others). It is understood that fractionation is caused by energy transfer between colliding atoms during cascades and the effects of differences in surface binding energies. For instance, light isotopes are preferentially sputtered relative to heavy isotopes, such that the sputtering site will be enriched in heavy isotopes. It should be emphasised, however, that this type of isotopic and chemical fractionation occurs as a transient phenomenon. As sputtering proceeds, chemical and isotopic fractionation diminishes because of recoil implantation, mixing, and diffusion, with the result that the chemical and

isotopic compositions of sputtered particles approach the bulk composition at steady state (for instance, see Shimizu and Hart, 1982b; Fig. 9). Therefore, equation (2.2) is valid as long as the analysis is carried out under steady state sputtering conditions. The validity of equation (2.2) makes it possible to ascribe any chemical and isotopic fractionation observed in populations of secondary ions to have originated from the ionisation process through probability of ionisation.

By measuring the intensity ratio against a reference element, R, the instrumental transmission is eliminated:

$$I_i/I_R = \left(N_i/N_R\right) * \left(P_i/P_R\right) \tag{2.4}$$

As long as (2.4) is valid,

$$I_i/I_R = \left(C_i/C_R\right) * \left(P_i/P_R\right) \tag{2.5}$$

If P's can be assumed to be constant for a given set of materials (a mineral solid solution or, defined a little more loosely, silicate glasses of similar compositions),

$$I_i/I_R = \left(C_i/C_R\right) * \alpha \tag{2.6}$$

where α is P_i/P_R.

For a set of materials in which C_R is quasi-constant and hence I_R is reproducible, I_i can be converted to concentration in a straightforward fashion. Particularly for trace elements for which P_i is constant, *i.e.* independent of concentration, we obtain a simple linear relationship between the intensity ratio and concentration (working curve) in the form:

$$C_i = a * \left(I_i/I_R\right), \tag{2.7}$$

where *a* is the slope of the working curve and is called the sensitivity factor. As an example, and for my own historical reason, I show Figure 2.5 here, which was the first trace element working curve I obtained for Sr in clinopyroxenes in 1976.

This approach has been a success story when it comes to applying SIMS techniques to trace element geochemistry. However, it should be recalled that it is valid only when P_i/P_R in equation (2.5) is constant. The experience of Geo-SIMS practitioners reveals that this ratio varies for different mineral solid solutions, and between basaltic and high silica glasses, a phenomenon known as "matrix effects", making it necessary to perform a standardisation procedure, involving many homogeneous well documented minerals and glasses, and is a major obstacle to easy quantification of SIMS data.

Variations of P_i/P_R as a function of composition in a given set of materials have been shown by several authors for binary alloys, demonstrating that enhancement of ionisation of an element occurs due to the presence of the other. In other words, P's for individual elements vary, depending on the chemical composition of the sample (Brochard and Slodzian, 1971; Pivin *et al.*, 1978, 1979; Yu and Reuter, 1981a,b among others). These authors noted that variations of

P_i/P_R in binary alloys occur as a function of composition when the atomic concentration of an end member element is no longer "trace". It is also noticeable that these studies of binary alloys were made in the presence of oxygen, either by a primary oxygen beam or under ambient oxygen conditions. For oxygen-rich materials such as silicates with an O^- primary beam, variations of P_i/P_{Si} can also occur in a similar fashion. Yu and Reuter (1981a) noted that in a binary alloy A-B, where A forms a stronger oxide bond than B, the presence of A enhances the ionisation of B. This indicates that Si-induced enhancement of ionisation can occur in silicates because Si forms the strongest oxide bond in silicates. My study of Ca-Al-silicate glasses showed the Si-induced enhancement of ionisation of Ca and Al (Shimizu, 1986).

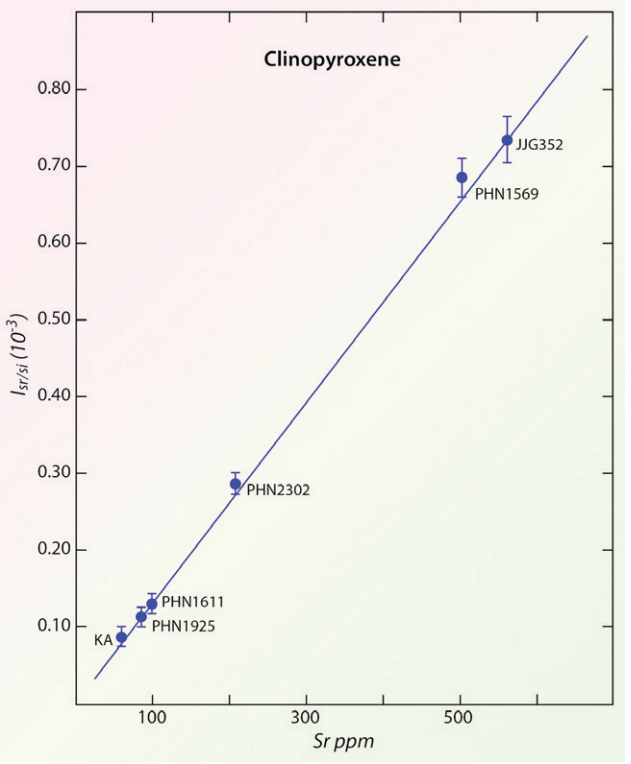

Figure 2.5 The first working curve for a trace element (Sr) in silicate minerals (CPX) obtained using the IMS 300 (1976). Modified from Shimizu *et al.* (1978).

In an early part of my SIMS odyssey, I was completely baffled by my observations. I had carefully chosen to study the simplest solid solution, olivine (Mg_2SiO_4 – Fe_2SiO_4), in the hope that any systematic variations observed might be easy to understand for mineral solid solutions. I measured Mg/Si and Fe/Si intensity ratios against known atomic ratios. To my surprise, I found a quadratic relationship between the Mg/Si intensity ratio and the Mg/Si atomic ratio in olivines. The Mg/Si intensity ratio increased from forsterite (Fo_{100}) to Fo_{75}, then decreased toward fayalite. This was very confusing. Why did the Mg/Si intensity ratio have to increase when the Mg/Si atomic ratio decreased? I also found that the Ca/Si intensity ratio increased from diopside ($CaMgSi_2O_6$) to hedenbergite ($CaFeSi_2O_6$), although the Ca/Si atomic ratio remained constant.

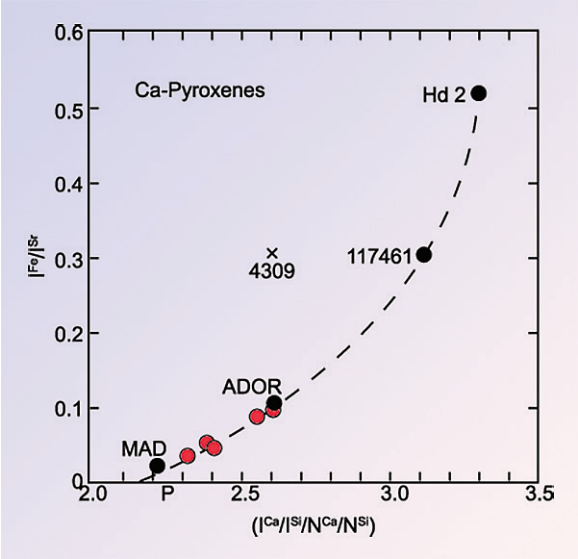

Figure 2.6 The effect of Fe on the ionisation of Ca in Ca-rich clinopyroxenes. Note that the Ca/Si intensity ratio increases with the Fe/Si intensity ratio. Modified from Shimizu *et al.* (1978).

This was a very confusing beginning for me: P_i appeared to be dependent on the concentration of other element(s) in a single mineralogical matrix. This meant that there were "interactions" between atoms of different elements, playing important roles in the ionisation process. How do ionisation models explain these observations? I found the ionisation models of the 1970s and 1980s simply confusing and disappointing. I was expecting that existing models could explain my observations so as to render achievable the quantitative analysis of silicate minerals and glasses.

One prominent model developed into a scheme of quantitation was known as the Local Thermal Equilibrium model (LTE; Andersen and Hinthorne, 1972, 1973). This model assumes that a sputtering/ionisation site resembles a plasma in thermodynamic equilibrium, in which

$$M^0 = M^+ + e^-, \tag{2.8}$$

where M^0 denotes a neutral atom, M^+ a positive ion, and e^-—an electron. The equilibrium constant for this reaction can be written as

$$K = \frac{n_{M+} n_{e-}}{n_{M0}} \tag{2.9}$$

where n_{M+}, n_{M0}, and n_{e-} represent the numbers of positive ions, neutral atoms of element M, and electrons in unit volumes. The equilibrium constant also can be written using the Saha-Eggert equation as:

$$K = \left(\frac{2\pi m_{M+} m_{e-}}{h^2 m_{M0}} kT \right)^{3/2} \left(\frac{B_{m+} B_{e-}}{B_{M0}} \right) \exp\left(-E/kT\right) \tag{2.10}$$

where m's are mass, B's are internal partition functions for M^+, M^0, and electrons, h the Planck's constant, k the Boltzmann's constant, T plasma temperature, and E the ionisation potential of element M. By combining (2.9) and (2.10), we get

$$\frac{n_{M+}}{n_{M0}} = \left(\frac{2\pi m_{M+} m_{e-}}{h^2 m_{M0}} kT \right)^{3/2} \left(\frac{B_{m+} B_{e-}}{B_{M0}} \right) \exp\left(-E/kT\right) \ / n_{e-} \tag{2.11}$$

Taking $n_{M+}/n_{M0} = P$, (2.3) can be rewritten as:

$$I_{M+} = \left[\eta I_P C_M A \left(B_{m+}/B_{M0} \right) \exp\left(-E_M/kT\right) \right] / n_{e-} \tag{2.12}$$

where A is the proportionality factor (includes $B_{e-} = 2$), which is assumed to be the same for all elements. This means that secondary ion intensity can be related directly to concentration with the knowledge of plasma temperature, electron density (n_{e-}), and B's (also a function of temperature; for example, see de Galan *et al.*, 1968). Andersen and Hinthrone (1973) developed a method for quantitative SIMS analysis with this approach in which plasma temperature and electron density were estimated using two internal reference elements of known concentrations. The rest of the element concentrations were calculated based on (2.12).

It is evident from (2.12) that intensity-concentration conversion can be achieved with the knowledge of plasma temperature and B's (also functions of plasma temperature), and that the secondary ion intensity of any element should depend on its ionisation potential in a negative exponential fashion. Indeed, numerous studies made at that time by Andersen and Hinthorne (1973), Werner (1974), Morgan and Werner (1976, 1977, 1978), among others, showed the negative

exponential relationship between intensity and ionisation potential as supporting evidence for this approach. However, there were fundamental problems: for instance, a serious question was raised about the validity of the assumption that the ionisation site can be approximated by a plasma in local thermodynamic equilibrium. Sroubek (1974) stated that the assumption of local thermodynamic equilibrium is not consistent with the accepted concept of sputtering as a dynamic non-equilibrium process, and the energy distribution of secondary ions with "high-energy tails" is inconsistent with the equilibrium energy distribution. Slodzian (1975) also stated that many collisions are required for equilibrium to be reached, whereas secondary ions are generated after a small number of collisions, thus making the equilibrium model unrealistic. As shown by Morgan and Werner (1976), for instance, the plasma temperature had to be adjusted to gain negative log-linear relations with ionisation potentials when secondary ion populations of different energies came from the same sample. This implied that if a plasma existed at a sputtering site, the temperature inside the plasma was heterogeneous for ionisation of a given element depending on the velocity of the particle. This clearly contradicts the equilibrium assumption. In Morgan and Werner (1977) and others, the plasma temperature in equations (2.10 – 2.12) becomes a fitting parameter, thereby completely losing its physical meaning. For the purpose of devising an empirical scheme for converting secondary ion intensities into concentrations, this situation is permissible (Morgan and Werner, 1976), but to me, nevertheless, it was a fatal blow to the LTE approach. Efforts to improve errors associated with LTE continued well into the 1980s (*e.g.*, Kuroda and Tamaki, 1986). These authors examined errors in computing the partition functions as a function of temperature for several elements and showed that errors in concentrations could amount to 20 % for Zr in Ni-based alloys.

There were more disappointing shortcomings of the LTE approach: Secondary ion formation of an element was considered as element specific, just the probability of ionisation as a function of electron density and temperature of the plasma. This explanation completely avoided the type of observation that I mentioned above, the apparent interaction of atoms of different elements during ionisation. This, again, was a huge disappointment to me because I was seeking a solution to my puzzle in the ionisation model. Another fundamental shortcoming was the complete disregard of secondary ion energy in the probability of ionisation. This is perhaps unfair to Andersen and Hinthorne (1973) as the energy dependence of ionisation was not noted until the late 1970s (Blaise and Nourtier, 1979; Norskov and Lundqvist, 1979) and early 1980s (Yu, 1981).

There was one more reason why I was suspicious of the quantitation efforts at that time. Although not related to the physical basis of the approach, it was equally fundamental: the identity of secondary ion peaks. In those early days of SIMS, the mass resolving power (MRP) of mass spectrometers was rather low (IMS 300, which was widely used at that time, had an MRP of 300) so that molecular ion interferences were not at all resolved. Therefore, intensities used for the correction scheme might have been overwhelmed by interferences and not have been representative of the elements in question. In fact, a close examination

of Morgan and Werner (1977) revealed that for the NBS 610 glass, the estimated chemical composition of a low energy ion population displayed larger deviations from the true values relative to a high energy population, indicating that molecular ion interferences were particularly severe for low energy secondary ions.

An alternative to the LTE model for analysis of silicate minerals and glasses is the Bond Breaking Model: during collision cascades atoms collide and some are ionised *via* the breaking of bonds. Slodzian and Hennequin (1966), Slodzian (1975), and Slodzian *et al.* (1980) presented the basic concept involved. Observations on Cu^+ and O^- emissions from copper oxide were parallel to each other as a function of time (depth into the sample), suggesting that Cu^+ and O^- were formed by a single mechanism, *i.e.* the breaking of bonds. Mathematical formulation for this model had to wait until 1987, when Yu (1987) presented it. The physical model expressed in Slodzian *et al.* (1980) and formulated by Yu (1987) is based on the assumption that the atomic collisions that lead to secondary ion formation resemble molecular dissociation by atomic collisions in gas, in which the Landau-Zener potential curve crossing can be applied. In other words, the model is based on the crossing of two potential energy curves: one for covalent $M^0 + X^0$ and one for ionic $M^+ + X^-$ at a critical distance from the surface as shown schematically in Figure 2.7 (Fig. 1 of Yu, 1987).

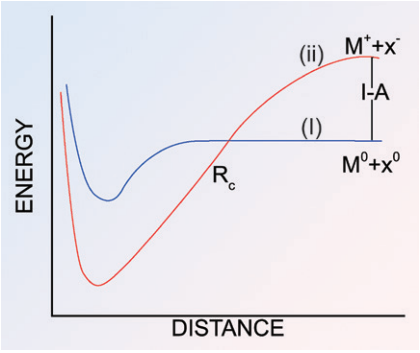

Figure 2.7 The Landau-Zener potential energy crossing in atomic collisions in gas as applied for the Bond Breaking Model during sputtered ion formation. Modified from Yu (1987).

Physically, this involves sputtering of M that creates a vacancy on the surface, which in turn traps excess electrons in the time frame of sputtering (~10^{-13} secs), and M^+ is emitted. According to this model, the probability of ionisation, P^+, is expressed in the general form:

$$P^+ = \exp\left(-\frac{G}{v(r_c)}\right) \tag{2.13}$$

where G is a constant and $v(r_c)$ is the velocity of a given ion at the critical distance where crossing of potential energy curves occurs. Furthermore,

$$v(r_c) = \left(\frac{2}{M}\left(E_k + I - A\right)\right)^{1/2} \tag{2.14}$$

where M is mass, E_k kinetic energy, I ionisation potential, and A the electron affinity of the cation vacancy in the sample created by the leaving ion (oxygen for silicates). It is clear from this expression that the Bond Breaking Model predicts that the probability of ionisation is dependent on kinetic energy, ionisation potential, and the mass of the sputtered particle. Note that the probability of ionisation would be greater for higher energy particles, consistent with the observations made by Lundquist (1979), Norskov and Lundqvist (1979), and Yu (1981), and smaller for elements with higher ionisation potential, similar to the LTE model. In fact, Yu (1987) discussed that isotopic fractionation predicted by this model agrees with observations as well. However, quantitative applications of this model to the interpretation of secondary ion mass spectra have not been made because of the difficulty involved in defining G. It centres on the knowledge of electron wave functions for neutral and ionised particles related to the transient state of the vacancy during sputtering.

While those leading models of secondary ion formation were completely confusing and disappointing to me, I continued my own experiments with the IMS 300. One thing I noticed was that the isotope ratios I measured for any elements were wrong. This simple fact baffled me… why a mass spectrometer could not measure isotope ratios correctly? So, I decided to find out a specific set of machine parameters with which the isotope ratios of a pure tungsten filament could be measured correctly, hoping that any systematic variations I could reproduce would tell me something fundamental about the process of secondary ion formation. The one machine parameter that allowed me to obtain reproducible results happened to be the secondary ion acceleration potential. The Cameca instrument had an independent circuit for applying "energy offset", which is the reduction of the acceleration potential from 4.5 kV. Measuring $^{182}W/^{184}W$ as a function of energy offset clearly showed that the measured ratio was too high at zero offset (*i.e.* 4.5 kV) but decreased toward the natural abundance ratio of 0.865 with increasing energy offset. The results indicated that isotopic fractionation occurred in secondary ion formation, and that its magnitude was a function of secondary ion energy. A low energy ion population measured at zero offset possessed a more fractionated isotopic composition than a high energy ion population measured at greater offsets. In retrospect, this became clear later when Stan Hart and I did a systematic study of isotope fractionation in sputtered ion formation (Shimizu and Hart, 1982a), but it was an important revelation to me at the time. Then I stumbled onto an article about measuring energy distribution of secondary ions (Jurela, 1973). Jurela (1973) used a single focusing mass spectrometer with a sputtering source (Jurela and Parovic, 1968) and a retarding potential lens at the end of the machine, so that the energy distribution of mass-analysed ions was measured as a function of retarding potential (up to 330 V). What I was doing instead was reducing acceleration potential, but the IMS 300-RG was a double focusing mass spectrometer, and I was measuring ion intensities as a function of "excess" energy. In other words, the greater the offsets, the greater the excess energy. In addition to the energy distributions of several metal ions from pure targets, Jurela (1973) also reported comparisons of energy distributions of

single atom ions and molecular ions (dimers, *etc.*). It was evident that molecular ions displayed a much narrower energy distribution relative to single atom ions. The encounter with Jurela's work and the realisation of what I was observing in physical terms changed my life. For one thing, the variations of W isotope ratios as a function of energy offset were understood as reflecting different ionisation probabilities for isotopes as a function of energy. For another, there was a stunning systematic difference in energy distribution curves between single atom ions and molecular ions, and I intuitively latched onto that observation as a possible avenue to proceed with SIMS analysis of silicates because it seemed possible that abundant molecular ions (mainly oxides and complexes) emerging from silicates could be screened off by energy offset even for secondary ions of trace elements. This possibility excited me to no end. The first thing I tried was to measure Sr abundances in clinopyroxenes for which I had my own isotope dilution data (Shimizu, 1975b) and the result was a success as shown in Figure 2.5. I was particularly happy that these measurements were carried out when Tony Erlank was visiting me in Paris. Tony was the one who donated some of the garnet peridotite xenoliths I used in establishing the Sr working curve and he looked very impressed when the figure was constructed. This approach based on the systematic difference in secondary ion energy distribution between single atom and molecular ions had provided a credible trace element working curve for the first time, a major breakthrough for geochemical applications of SIMS techniques. The potential usefulness of this approach was suggested by Herzog *et al.* (1973) in their paper on secondary ion energy distributions of clusters (molecular ions), but the way I stumbled onto it was through the processing of my own experiments in the perspective of Jurela's work. In Shimizu *et al.* (1978), we reported secondary ion energy distributions in silicate matrices, establishing the difference between single atom and oxide ion species, and data on isotope ratios of selected elements as a function of energy offset. These observations completely support the basic tenets of the energy filtering method.

Although I was more than satisfied with the success of the energy filtering method, I felt that this approach was something like "resolving problems without knowing them". In other words, molecular ion interferences were suppressed without identifying exactly what they were. With the low mass resolving power of the IMS 300 and the subsequent generations of f-series instruments, this issue remained but the energy filtering approach was a successful and practical solution to complex materials such as minerals and glasses. However, the effectiveness of the energy filtering method was demonstrated mass spctrometrically only much later on with the IMS 1280.

While coverage of trace elements amenable to analysis expanded as more users came needing more elements to be analysed, I was still stuck with my old puzzle of "matrix effects" expressed as the chemically variable P^+ in equation (2.3). My experience showed that Fe was one of the culprits as mentioned earlier, but I was worried that Si may be causing a similar effect as well and decided to study it in a series of glasses that Seifert *et al.* (1982) had used to study variations of the structure of silicate melts as a function of chemical compositions. This study

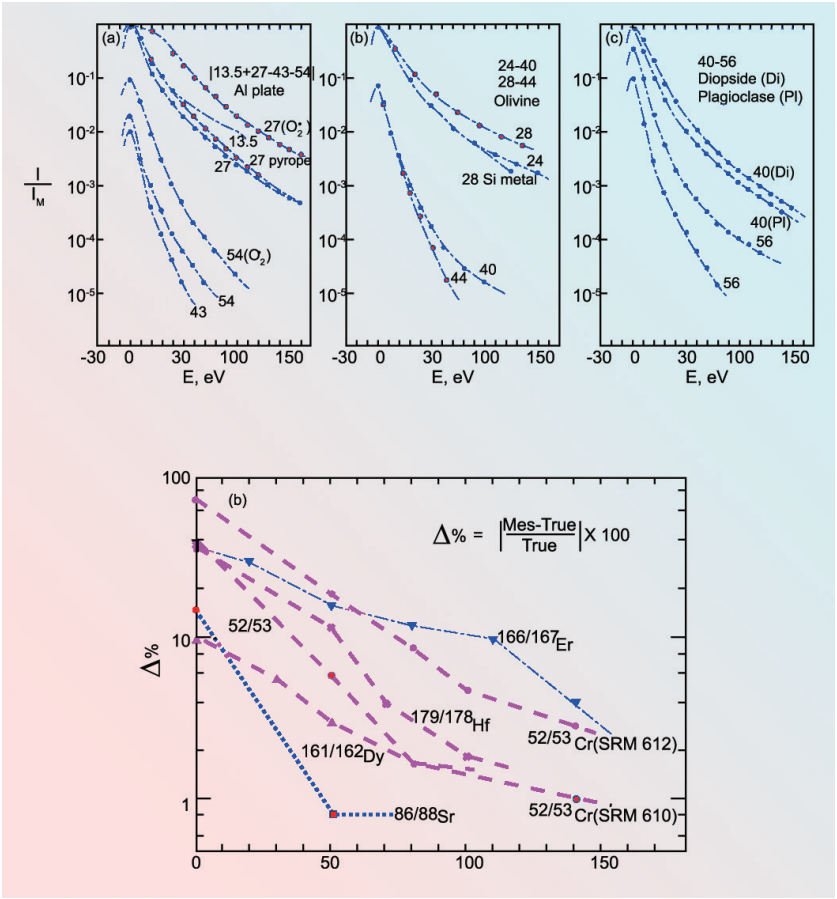

Figure 2.8 **Upper panel: (a)** energy distributions of secondary ions of Al^+, Al_2^+, Al^{2+}, and AlO^+ emitted from an aluminum plate; **(b)** energy distributions of Mg^+, Si^+, MgO^+, and SiO^+ from olivine; **(c)** energy distributions of Ca^+ and CaO^+ from diopside and plagioclase. Note that molecular ions show narrower energy distributions than single atom ions. For all panels, the horizontal axis is the excess energy of secondary ions, measured by lowering acceleration potential (energy offset). E = 0 means zero offset, and ions have an energy of 4500 eV. Modified from Shimizu *et al.* (1978). **Lower panel:** decrease of the displacement of measured isotope ratios from the true values as a function of energy for Cr, Sr, Dy, Er, and Hf in a silicate glass NBS 610. Note that all the measured ratios approach their true values with increasing energy. Modified from Shimizu *et al.* (1978).

was carried out in the mid-1980s, when trace element work with the IMS 3f was already flourishing but my mind still remained stuck with the old puzzle of matrix effects (Shimizu, 1986). The glass I studied was in a binary system $CaAl_2O_4$-SiO_2, with end member compositions CA9S1W with Si 8.98 atomic %, Al 60.9 %, Ca 30.1 % to CA2S14 with Si 82.4 %, Al 11.8 %, Ca 5.85 %. Two principal observations were made: (1) Al ionisation was increasingly enhanced with increasing Si contents from CA9S1W to Ca2S14, despite the fact that the atomic concentration of Al decreased. Ca ionisation was enhanced more than Al, (2) along with the enhancement of ionisation of Al and Ca, the energy distributions of Al, Ca, and Si ions changed: the energy spread at the half maximum intensity (full width at half maximum or FWHM) decreased for $^{27}Al^+$ and $^{40}Ca^+$. In other words, the energy distributions of Al and Ca ions sharpened with increasing Si. In contrast, the energy distribution of $^{28}Si^+$ broadened with decreasing Si abundance. These two observations were qualitatively in complete agreement with the observations made on binary alloys by Yu and Reuter (1981a,b) who studied ionisation systematics on binary alloys and concluded that: (1) for a binary alloy A-B, in which A forms a stronger bond with oxygen than B, the presence of A enhances ionisation of B, while the presence of B suppresses ionisation of A, and (2) the presence of A sharpens the energy distribution of B, while the presence of B broadens the energy distribution of A. In the system I studied, Si forms a stronger oxide bond than Ca and Al, and acts as element A in Yu and Reuter's alloys. Slodzian *et al*. (1980) also reported that the FWHM for $^{40}Ca^+$ in calcite was greater than that in feldspar, *i.e*. sharpening of the Ca^+ energy distribution in the presence of Si, consistent with Yu and Reuter (1981a,b) and Shimizu (1986).

The similarity of ionisation systematics between binary alloys and silicates was encouraging, but there was no satisfactory physical or mechanistic explanation. What I suspected was the existence of binary collisions during ionisation, in which oxygen and charge are exchanged in the form:

$$MO + Si^+ \rightarrow SiO + M^+ \qquad (2.15)$$

M represents either Al or Ca in my glasses. If the right hand side of the equation is more stable, then more M^+ would be produced with increasing Si^+. Additionally, if kinetic energy distributions are more or less maintained among colliding partners, then M^+ would maintain the energy distribution of MO, which is sharp, resulting in sharpening of the energy distribution of M^+ with increasing Si, as observed in my glasses. Enhancement of ionisation due to Fe as discussed by Shimizu *et al*. (1978) can also be explained by a similar reaction, with Fe replacing Si in equation (2.15). In this case, instability of Fe^+ in an oxygen-rich environment might kinetically make the reaction proceed.

I intended to carry on with the idea of ionisation enhancement in a given matrix so that matrix effects could be directly related to the physics of ionisation. I thought that one of the ideal systems is pyroxenes in the pyroxene quadrilateral, in which "interactions" of Ca, Mg, and Fe can be studied at constant Si. Lunar

pyroxenes are known to vary their compositions widely within the quadrilateral and could present an ideal case. Unfortunately, I did not do this project because I was pessimistic about how funding agencies might consider a proposal like this.

Havette and Slodzian (1980) were the first to attempt a mathematical approach to matrix effects. Their scheme was to consider that the ion yield of a given element in a matrix is a function of the concentrations of all the elements in the matrix,

$$r_\alpha\left(M_j\right) = \sum_{l=1}^{n} X_{jl} C_{\alpha l} \tag{2.16}$$

where $X_{jl} = k_{jl}/k_{11}$, a coefficient of ion yield relative to an internal standard, in this case Si. In other words, the ion yield of element M in a matrix α is expressed as the sum of "inter-element interaction terms" multiplied by element concentrations. With sufficiently large numbers of standards with known cation atomic concentrations, X_{jl} can be established. Havette and Slodzian (1980) showed that the errors involved in relative ion yields in all matrices they examined were within ±6.5 %. This approach has not been further developed to encompass most of the silicate matrices encountered in geochemistry/petrology. One of the obvious reasons why not is that major element analysis has become more readily accessible with electron microprobes, hence eliminating the need to use ion microprobes for this purpose. Although this approach completely ignores physics, it is a pity in my opinion that it has not been developed further.

Shimizu and Hart (1982b) showed that atomic abundances of major elements calculated directly from intensity ratios (against Si by assuming that total is 100 %) in a given matrix is dependent on the energy of the ions, and that displacements of calculated ionic abundances from atomic abundances decrease with increasing energy, suggesting that the magnitude of matrix effects could decrease with increasing energy. In fact, a common practice for SIMS analyses of trace elements in silicates was to use a high silica glass standard (NBS 610) for all silicate matrices by analysing high energy secondary ions (energy offset of -90 eV, for instance).

Thus, my journey through secondary ion formation has been mostly a struggle in darkness. Without email (remember this was in the mid-1970s) I could not ask Peter Sigmund questions about sputtering, although I wrote to him, exposing my fundamental misunderstanding of physics! I did not speak with Slodzian, although he was at Orsay, just outside Paris. The only way for me to move forward was to stubbornly remain an experimentalist and think about what I saw instead of what I read in papers. Progress was very slow, but based on the level of confusion and misunderstanding, it gave me time to correct my strategy. Claude Allègre was patiently watching me struggle in darkness, and I thank him for that. When I stumbled over Jurela's paper, I finally saw a light shining through and the foundation of my thinking, energy dependence of everything, was established. It was 1976, the hottest and driest summer I had in Paris.

Two years later, I moved from IPGP to MIT, and a new phase of my odyssey began. Circumstances of my move will be told in the next section. As soon as the IMS 3f was installed at MIT and major bugs were taken care of, serious measurements of isotopes got underway. Stan was interested in isotopically zoned galena crystals from Mississippi Valley–type ores (Hart *et al.*, 1981), and Stan and I started to look at isotopic fractionation as a function of energy in 12 pure metal samples over a mass range from B (10) to Pb (208). When we started working on this project in 1979, there was no study of this type, and we thought that isotopic fractionation would be the key to understand the physics of secondary ion formation process, because it was just mass fractionation of a given matrix. Under steady state sputtering conditions, three major observations were made: (1) light isotopes were always preferentially ionised relative to heavy isotopes, (2) the magnitude of isotopic fractionation was dependent on energy, and each of the 12 metals studied displayed variable energy dependence (see Fig. 4 of Shimizu and Hart, 1982a); and (3) maximum isotopic fractionation over the observed mass range (10 – 208) was approximated by M_L/M_H.

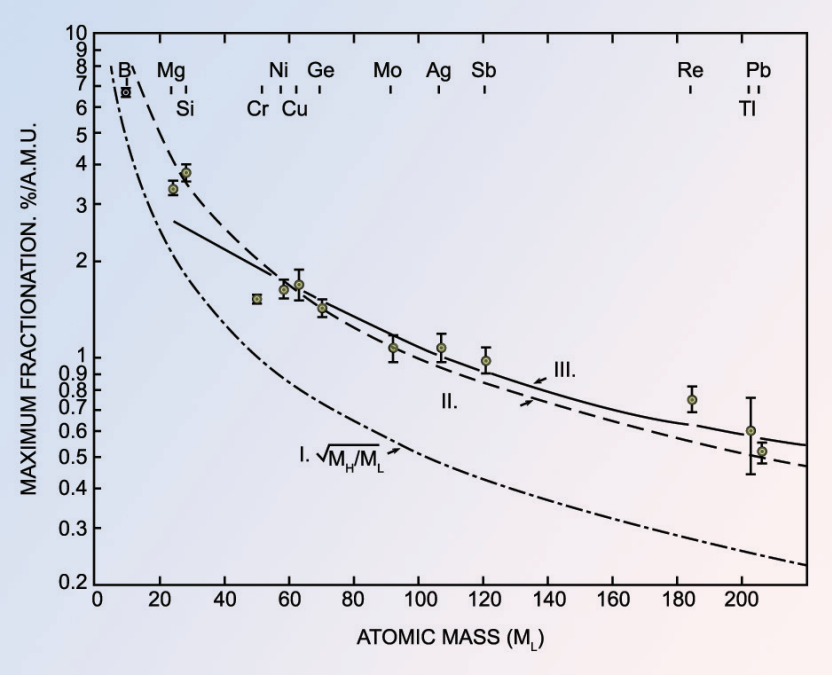

Figure 2.9 Maximum observed isotopic fractionation (% *per* amu) in pure metals bombarded by an O^- primary beam as a function of atomic mass. Curve I is the square root of the mass ratio (M_H/M_L) and Curve II is M_H/M_L. Modified from Shimizu and Hart (1982a).

Interpreting the results was a difficult task because there were no models for isotopic fractionation in secondary ion formation. As it turned out, Slodzian and his group were working on the same subject in secret competition with us. Slodzian *et al*. (1980) had made the same observation as ours, observation (1) above, and the energy dependence, observation (2) above, was such that isotopic fractionation decreased with increasing energy. The difference with respect to our observations on pure metals might be related to the fact that they did their study on minerals with an oxygen primary ion beam, creating an oxygen oversaturated environment. Based on their observations, they proposed a bond breaking model for secondary ion formation, using the Landau-Zener potential energy crossing model. They also stated that the energy distribution of $^{40}Ca^{+}$ was sharper for feldspar than for calcite, and that the Ca ion yield for feldspar was five times that for calcite. This was consistent with the Si-related matrix effects discussed above. In addition, their observation of the magnitude of Si isotope fractionation in olivine as a function of energy was qualitatively similar to what we observed for Si metal (Shimizu and Hart, 1982a). Although their discussion was qualitative, it is evident that their ideas bore fruit some years later in the form of the Yu (1987) formulation of the bond breaking model.

3. MIT AND THE KINETICS OF MAGMATIC CRYSTALLISATION

Encouraged by the promise of the energy filtering approach, I was beginning to feel that my time at IPGP was a success, and I started to think about the future. Although I was happy at IPGP, I wondered if the French education system was good for my kids. I did not want my kids to be put through the Japanese education system, which was a continuous selection process. I did not particularly like the French system either, mostly because it was similar to the Japanese system and a selection between general and vocational courses had to be made at a young age. This made me look for job opportunities in the US. Stan Hart had moved to MIT from DTM in 1975 and was leading a very productive geochemistry group. He was very much aware of research possibilities through SIMS techniques and decided to obtain funding from NSF to establish a SIMS laboratory. He invited me to be part of his group.

Once NSF funding was secured, I applied for an Immigrant Visa at the US Embassy in Paris. At MIT, Stan asked the Department Chair, Dr. Frank Press, to write a letter of reference for my visa application. At the time (in early 1978), Frank was at the White House as President Carter's Science Advisor. So, a letter of reference written on White House letterhead arrived at the US Embassy, recommending an Immigrant Visa for me. The Ambassador was very impressed and summoned me immediately. *"Ah, Dr. Shimizu, you must be a famous guy!"* the Ambassador exclaimed as soon as I walked into his office. So, my visa problem was solved, I thought, but then did not hear from them for interviews for a long time, and when I inquired about it, they found out that my papers had been lost somewhere between the State Department and the Embassy! I was frantic and tried to reach Stan, but in vain, because MIT was closed for a week due to the blizzard of 1978. After this psychological torture, interviews were eventually conducted and visas were issued in late spring of 1978.

I finally arrived at MIT in August 1978, and Cameca's first commercial production of the IMS 3f arrived in November that year under a consortium arrangement involving MIT, Harvard, and Brown. As a first commercial production instrument, it was in a far-from-complete state, with cables hanging out everywhere on the backside of the chassis, some circuit boards were there but not usable, and the software had numerous issues. The Cameca engineer responsible for the development of the 3f, Michel Lepareur, was nevertheless superbly confident and believed that the instrument was capable of anything (Lepareur, 1980). It took the Cameca team more than four months to complete the installation and acceptance tests, but soon after that, three students started their Ph.D. thesis work on the machine: Glenn Ray on the partitioning of trace elements between diopside and melt in the Di-Ab-An system (Ray *et al.*, 1983), Mark Sneeringer on diffusion of Sr and Sm in diopside (Sneeringer *et al.*, 1984), and Scott Meddaugh on the Pb isotopic compositions of galenas from Archean uraninite ores (Meddaugh *et al.*, 1982). Ray and Sneeringer were Stan Hart's

students at MIT, and Meddaugh was Dick Holland's student at Harvard. Bruno Giletti represented Brown University and was a frequent user of the instrument, working on diffusion of oxygen, alkaline and alkaline earth elements in quartz and feldspars in hydrothermal experiments followed by ion probe depth profiling (*e.g.*, Giletti and Yund, 1984).

Encounter with Gerry Wasserburg

My first encounter with Wasserburg was in 1979, I believe, when he visited Stan at MIT. I knew that he had purchased a Cameca IMS 3f and was completely reconfiguring it to his liking with tremendous difficulty. He came into the 3f lab while I was analysing CPX standards for trace elements. He said, "*Can you make it limp?*". I was hurt. I was not only making it limp, I was making it run! I was aware of his reputation as an aggressive cynic, but this was too much, and I hated him. I believed that he reviewed our NSF proposals negatively over a number of years, and that did not change my view of him for a long time.

Many years later, in the late 1990s, I represented the US side of the US-French collaboration on geochemical studies of the Oman ophiolite through an NSF International Program, and Gerry was a part of it too. Adolphe Nicolas was the French representative. So, we gathered in Oman, with Adolphe leading us to major outcrops around the Wadi Tayin area. One day, we were moving from one place to another in a four-wheel drive vehicle, with my student Ken Koga driving. I was on the front passenger seat and Gerry was on the backseat. We were animated by discussions about one thing or other, when Ken wanted to pass a slow moving truck. But he saw an oncoming car and tried to steer sharply… too sharply it turned out and our car careened to roll over on the elevated highway. Gerry and I were badly hurt with scrapes. Small pieces of glass were embedded in my scalp and Gerry's hand was in such a bad shape that he insisted to be taken to the University Hospital near Muscat. I was treated at a local clinic and went back to our hotel. I realised that Gerry and I had almost died together. This realisation made us close. After that time, Gerry always approached me at meetings, saying, "*How you doin', Bud*?"

With routine analytical protocols based on energy filtering established, I started developing strategies for the best use of SIMS techniques in geochemistry. The uniqueness of the ion probe for depth profiling was important for diffusion studies, but I thought that the high sensitivity of the ion probe with a finely focused beam should be used to bring petrographical context to trace element geochemistry. I had already published work on trace element abundances in mineral phases (*e.g.*, Shimizu, 1975a,b), but the *in situ* capability of the ion probe should make it possible to obtain data without destroying the petrography of the rocks. A preliminary example of this was Shimizu and Allègre (1978) on the analysis of kimberlite xenolith minerals for transition elements, which provided the starting point for many mantle mineral studies to be discussed later in this article.

Recognising that minerals in igneous rocks often show chemical zoning with respect to major elements, I was interested in documenting mineral zoning with respect to trace elements with the notion that trace element zoning could tell us a lot more about how igneous crystallisation processes work. A preliminary

study I did in Paris on trace element zoning of plagioclase provided intriguing results that made me wonder whether trace element partitioning at the interface of growing crystals was what we thought it to be and could perhaps provide new insights into the kinetics of magmatic crystallisation. Thus, I decided to embark on studies of augite phenocrysts in volcanic rocks because trace element abundances in augites were high enough to obtain meaningful (meaning precise enough) data with a satisfactory spatial resolution.

For analysis of heterogeneous samples, the spatial resolution of data points is one of the keys, but also where a compromise had to be struck: gathering zoning data on as many trace elements as possible had to meet, on the one hand, requirements on intensities (count rates) to be statistically meaningful, and, on the other hand, the spatial resolution to be adequate. Although energy filtering could effectively suppress molecular ion interferences, ion intensities had to be sacrificed. For this reason, I intentionally separated a group of trace elements in clinopyroxenes, Sc, Ti, Cr, V, Sr, and Zr, from REE. For these elements, an energy offset of -90 v typically was applied and a beam size of 5 – 8 microns was used.

Trace element abundances in phenocrysts are essential information for understanding magmatic differentiation processes, but it was not well known how they were distributed in phenocryst phases and whether they could be used to predict how differentiation processes operated in specific magmatic systems. My interest in this topic grew as the usefulness of the IMS 3f in trace element analysis became more firmly established, leading to expansion of opportunities, and decided to look at trace element zoning in phenocrysts. I was vaguely expecting that phenocrysts would display normal zoning in support of the Rayleigh fractionation model. Oscillatory zoning of plagioclase had long been known and I was wondering how trace elements would fit in the picture. Sector-zoned pyroxenes were also attractive from the trace element point of view. Albarède and Bottinga (1972) were the first to apply kinetic theories of impurity redistribution between a growing crystal and medium to geochemical systems, and I followed a similar path with special emphasis on *in situ* analysis of trace elements in crystals so that applicability of models to nature could be directly tested.

Among the theories and models of crystallisation kinetics developed in the field of materials science at that time were ones for studying distribution of impurities upon crystallisation. For instance, Smith *et al*. (1955) formulated a solidification model in one dimension, whereby the distribution of an impurity can be predicted as a function of the crystal growth rate (V), the diffusion coefficient of the impurity in the melt (D), and the distribution coefficient of the impurity at the crystal-melt interface (k) in a semi-infinite system as shown in the following equation,

$$\frac{\partial C_L}{\partial t} = D\frac{\partial^2 C_L}{\partial x^2} + V\frac{\partial C_L}{\partial x};\ x > 0, t > 0 \qquad (3.1)$$

where C_L denotes the concentration of the impurity in the melt, x the position in the system measured from the interface (x > 0 for t > 0), and t the time. This is written in such a way that position (x) is the distance from the interface, such that x = 0 at the interface and elsewhere increases with crystal growth. The distribution of an incompatible element in this system is that enrichment in the melt at the interface could affect the concentration in the subsequent solid if D is not sufficiently large relative to V. In such a case, the concentration in the solid at the interface would continue to increase with time. For a compatible element, depletion in the melt at the interface would result in gradual decrease of the concentration in the solid with time. With boundary conditions, *i.e.*,

$$\begin{aligned} C_L(x,0) &= C_0 ; x \geq 0 \\ C(\infty,t) &= C_0 ; t \geq 0 \end{aligned} \tag{3.2}$$

and

$$D\left(\frac{\partial C}{\partial x}\right)_{x=0} = VC(0,t)(k-1) \tag{3.3}$$

where C_0 denotes initial concentration of the impurity in the melt and k the partition coefficient ($k = C_{solid}/C_{liquid}$). Elements with k > 1 are called compatible elements, whereas those with k < 1 are incompatible, as is general practice in geochemistry. The steady state solution to the equation was obtained by Tiller *et al*. (1953) and Burton *et al*. (1953). It is important from the point of view of trace element zoning of crystals that it is a transient solution to the equation, not a steady state solution, although there might be cases for steady state crystallisation in nature as discussed by Shimizu (1978), for instance. The concentration of the impurity (a trace element) in the solid at the interface is:

$$C_S = kC_L(0,t) = \frac{C_0}{2}\left[1 + erf\,\frac{Vt}{2\sqrt{Dt}} + (2k-1)\exp\left\{k(k-1)Vt\frac{V}{D}\right\} erfc\,\frac{(2k-1)Vt}{2\sqrt{Dt}}\right] \tag{3.4}$$

By defining x′ = Vt, a half size of the crystal, and $f = (V/D)x'$, following Smith *et al*. (1955), trace element zoning patterns can be described as:

$$C_S = \frac{C_0}{2}\left[1 + erf\,\frac{\sqrt{f}}{2} + (2k-1)\exp\left\{k(k-1)f\right\} erfc\,\frac{(2k-1)\sqrt{f}}{2}\right] \tag{3.5}$$

Figure 3.1 shows how trace element zoning would evolve with time as a function of the partition coefficient (Shimizu, 1983).

In this model (Smith *et al*., 1955), it is assumed that the equilibrium partition coefficient prevails at the interface and stays unchanged as crystallisation proceeds in a semi-infinite system (perhaps corresponding to the initial stage of magmatic crystallisation where magma size is sufficiently large relative to the growing crystals). It is evident that the trace element concentration in the solid asymptotically approaches a value with which the partitioning of the

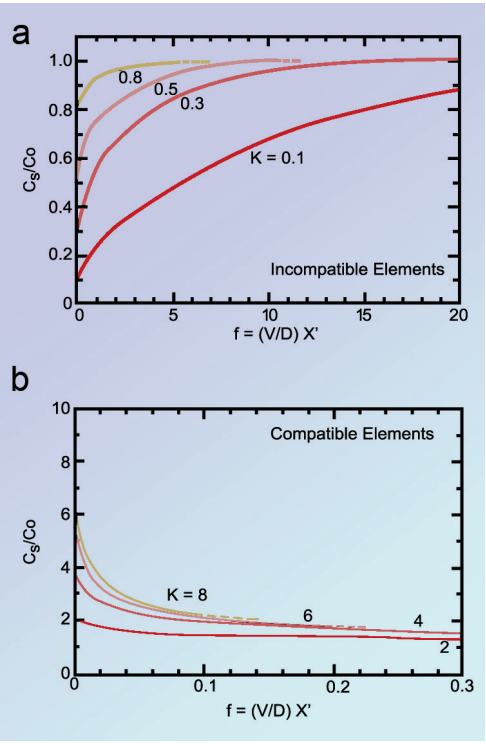

Figure 3.1 Zoning of trace elements in a growing crystal relative to the initial concentration in the liquid. **(a)** Incompatible elements with partition coefficients ranging from 0.1 to 0.8. **(b)** Compatible elements with partition coefficients ranging from 2 to 8. Modified from Shimizu (1983).

element between the crystal surface and the main part of the melt is unity at steady state. In other words, $C_S = C_0$. This simple model could apply to natural magmatic systems where a magma body can be approximated by an infinite reservoir; in other words, early stages of crystallisation. The predicted crystal zoning patterns (Fig. 3.1) are "normal zoning", but they should not be confused with evidence of Rayleigh fractionation because, in the present case, the system evolves toward a steady state, while in a closed (and finite) Rayleigh system, a bulk mass balance should always be maintained.

In this crystallisation model, a non-dimensional parameter, f = (V/D)x', is used. Available data on diffusion of elements in silicate melts and measured crystal growth rates should be combined to assess how natural magmatic crystallisation processes compare with the model. For instance, Shimizu (1983) used Hofmann's (1980) data on diffusion and crystal growth rate data of Grove and Bence (1977, 1979) and Grove and Raudsepp (1978) and estimated the V/D ratio to be of the order of 0.1 for major and divalent trace elements and of the order of unity or less for tri- and quadrivalent elements. It is thus suggested that for augite growing at T ~ 1200 °C, the *f* value in the equation above should be between 0 and 0.01 for divalent elements and between 0 and 0.1 for other elements for a crystal with a half size up to 1 mm. Thus, it is clear from Figure 3.1 that natural magmatic crystallisation is far from a steady state when equilibrium partition coefficients prevail at the interface.

The question of whether partitioning at the interface is in equilibrium adds another dimension to the problem. The affinity of a trace element, which is the difference in chemical potential of the trace element between melt and crystal, is zero at equilibrium, but it could deviate from zero during crystal growth. If the deviation remains small, however, the equilibrium partition coefficient can be used as an approximation, and this is a general practice. If, however, the affinity deviates significantly from zero, then the partition coefficient at the interface must be re-defined. One approach is to express it as a function of crystal growth rate, as it is imaginable that partitioning at the interface under very rapid crystal growth conditions could significantly deviate from an equilibrium value and tend to unity. If incorporation of trace elements into a growing crystal is *via* adsorption (attachment), the partition coefficient should involve kinetics of attachment and detachment. If, however, incorporation is through chemical reaction, involving assembly of melt components to form trace element end member molecules (such as $SrMgSi_2O_6$, Sr-diopside molecule), the kinetics of its formation reaction should play an essential role.

When I started to look at trace element zoning of phenocrysts, I thought that interface kinetics could be significant in magmatic systems in modifying interface partitioning relative to equilibrium and therefore decided to look at phenocrysts formed under obvious disequilibrium conditions. Sector-zoned augites were a case in point where growth sectors were known to have different chemical compositions for major elements (Dowty, 1976; Nakamura, 1973). One such example in basalt from Truckee, California (T79-10) was analysed by the IMS 3f. Among many sector-zoned grains in a thin section, I chose to study the one cut through its centre. The results of the ion probe analyses are shown in Figure 3.2.

Although it was imaginable that trace element concentrations could be different between sectors, the results were puzzling. The fast growing basal sector [$\bar{1}11$] was lower for all trace element concentrations relative to the slow growing prism sector [100] irrespective of element compatibility. When the interfaces were exposed to a common liquid, then when they advanced, was incorporation of trace elements into the basal sector more deviant from equilibrium partition coefficients and closer to unity, or was partitioning at both interfaces controlled by some mechanism other than just growth rates? It is noted that both compatible (Cr) and incompatible (Ti, Sr) elements are enriched in the slow growing prism sector, indicating that the growth rate is not the only factor defining the interface partition coefficients. The results were interpreted based on the "protosite concept" (Nakamura, 1973) and its significance in growth of sector zoned augites (Dowty, 1976). On the surface of a growing augite crystal, there are certain numbers of half-formed cation sites (protosites), the crystal side of which are bonded with oxygen but the liquid side of which represents concentration of negative charges due to half-bonded oxygen to which cations can be attracted (Dowty, 1976). Then, difference in numbers of protosites between growth directions, *i.e.* the basal sector *vs.* the prism sector, becomes crucial in determining which sector is more enriched in trace elements, and the field

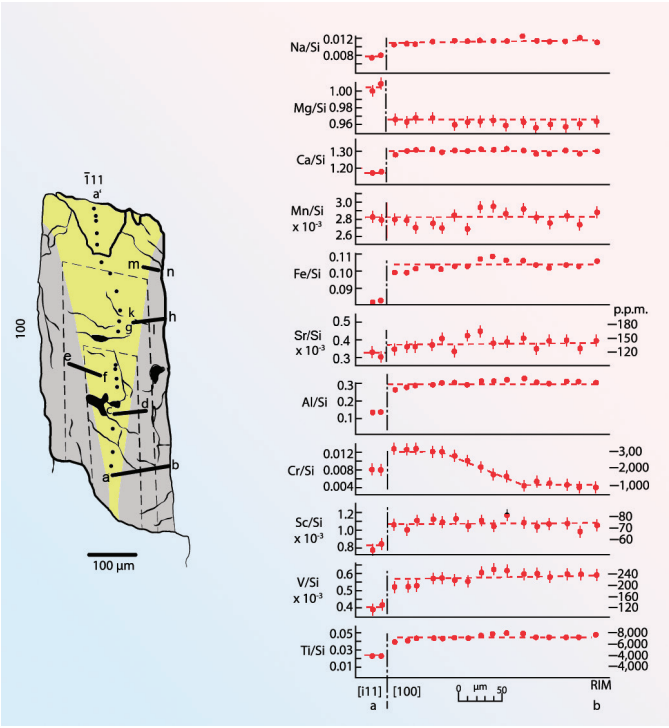

Figure 3.2 **(a)** A crystal of sector-zoned augite. Ion probe traverses conducted are labeled a-a', a-b, c-d, *etc.* and the data is shown only for the traverse a-b. Shaded area is the [100] prism sector, which is optically dark as well. **(b)** Analytical data along the traverse a-b, starting with the basal sector [$\bar{1}$11]. Intensity ratios against Si are shown for all elements with concentrations calculated for some trace elements. Modified from Shimizu (1981).

strength of ions plays a significant role in determining inter-sector enrichments of elements (Nakamura, 1973; Dowty, 1976). In fact, for elements going into the M_1 sites of augite, the field strength (ionic charge/ionic radius squared or Z/r^2) is positively correlated with [100]/[$\bar{1}$11] ratios (Fig. 3 of Shimizu, 1981), indicating that the Coulomb interaction between ions in the melt and at the growing crystal surface is key to trace element incorporation into magmatic minerals. From the point of view of kinetics, however, rates of attachment of SiO_3 chains and the Coulomb-type ion adsorption (and desorption) should be known before a quantitative understanding of the process can be gained. It was nevertheless an exciting learning experience for me in realising that trace element distribution between melt and growing crystal is controlled not just by the interplay between growth rate and diffusion of elements in the melt but also by the rate of interface processes and, therefore, the separation of phenocrysts from melt may result in

trace element trends in successive melts that are very different from what a simple fractional crystallisation model would predict. In this way, I started to be skeptical about phenocryst-groundmass partition coefficients as "equilibrium" values, and I even doubted whether fractional crystallisation processes as we learn them in petrology classes, actually operated in nature.

It is still important to document how much partition coefficients of trace elements can deviate from equilibrium values during crystallisation. As mentioned above, the growth rate-induced change would be in the direction of modifying partitioning at the interface toward unity as growth rate increases. But, what if processes at the interface came into play upon incorporation of trace elements in a growing crystal? The protosite concept mentioned above is an example of interface processes, in which kinetics of attachment/detachment of elements onto protosites dictates element incorporation. It is also possible that incorporation of trace elements in growing crystals occurs through formation reactions of trace element "end member" molecules. Here again, literature in materials science provides some insights.

For instance, Hall (1953) studied incorporation of incompatible trace elements (Sb, Ga) into growing Ge and Si crystals from their own melts with adsorption/desorption of trace elements on the surface in mind and came up with a definition of the interface partition coefficient as:

$$K = K_{eq} + \left(K_S - K_{eq}\right)\exp\left(-V_i/V\right) \tag{3.6}$$

where K_{eq} denotes the equilibrium partition coefficient, K_S the interface partition coefficient, V_i the velocity of the interface process (in the case of the sector-zoned augite mentioned above, adsorption/desorption), and V the crystal growth rate. For very fast interface processes (relative to the growth rate), $K = K_{eq}$, and for very fast growth (relative to the interface process), $K = K_S$. Hall's data indicates that K_S for Sb in Ge could be 4.5~6 times greater than K_{eq}. This suggests that rimward increase in concentration would be greater for incompatible elements and steady state can be reached at smaller f values. For compatible elements, rimward decrease in concentration would be accentuated with elevated partition coefficients.

Could something like this happen in growth of natural silicate crystals? If it did, geochemical consequences would be significant in using phenocryst-matrix partition coefficients for modelling magmatic crystallisation. For incompatible elements, the degree of fractionation would be reduced, and the effect of crystallisation would not be felt strongly in the residual liquid. For compatible elements, however, effects of crystallisation would be accentuated by stronger depletion in the residual liquids. At the crystal-liquid interface, stronger depletion in compatible elements would result in stronger chemical zoning of the crystal for compatible elements, whereas the liquid would not be strongly enriched at the interface for incompatible elements. In terms of the crystallisation model mentioned above, it would become easier for incompatible elements to reach a steady state, whereas much more crystal growth would be required for compatible elements to reach a

steady state (see Fig. 3.1). These reasons led me to verify whether elevated interface partitioning can happen in growth of silicate minerals in magmas, and my search for crystal growth experiments soon found interesting examples. Results of dynamic crystallisation experiments (when crystals are grown under controlled cooling rates) showed that for both incompatible (Ti, Al) and compatible (Cr) elements partition coefficients were elevated relative to equilibrium values during clinopyroxene growth studied by Grove and Bence (1979) and Tsuchiyama (1981). In the former, the partition coefficients for Ti and Cr in dynamic (crystal growth during cooling) experiments on the Luna 24 composition were found to be more than a factor of 2 greater than equilibrium partition coefficients obtained by Grove and Vaniman (1978). In the latter, the Al partitioning was elevated by a factor of 10 relative to equilibrium in the $Di_{80}An_{20}$ composition (Tsuchiyama, 1981). For the sector-zoned augite, the Cr content of the rim of the [100] sector is 1610 ppm (Table 1; Shimizu ,1983) and that of the groundmass is 30 ppm, the [100] interface partition coefficient is 54, vastly elevated from the equilibrium value of 2 – 3 (Irving and Price, 1981; Huebner *et al*., 1976). The decrease in Cr content in the augite (by a factor of 3 over a distance of 220 μm; see Fig. 3.2) can then be reconciled with the semi-infinite reservoir crystal growth model with this elevated interface partition coefficient (Shimizu, 1983).

It was a surprise to me to discover that elevated partition coefficients in silicate systems occur during dynamic crystallisation experiments, which led me to believe that it could actually occur in natural crystallisation processes as well, although cooling rates in natural systems were much slower than those of dynamic crystallisation experiments. Looking back at my preliminary study of plagioclase zoning (Shimizu, 1978), where a plagioclase grain from the Skaergaard Intrusion showed an apparent partition coefficient for K near unity, the observation could be explained as an example of an elevated partition coefficient for K at the interface. If this were the case, elevated interface partition coefficients occur in natural systems not only for clinopyroxene but also for plagioclase. I was encouraged to continue trace element studies of phenocryst zoning with the ion microprobe, as trace element petrography could provide unique information about the workings of magmatic processes.

Augites from ocean island basalts presented excellent case studies as they commonly occur as phenocrysts. Some augite phenocrysts occur in picritic rocks and hence could reflect conditions and processes of the early stage of magmatic crystallisation. However, a collaborative work on Gough Island basalt phenocrysts with Anton le Roex of University of Cape Town (Shimizu and le Roex, 1986) provided yet another dimension of the complexity of nature. Figure 3.3a and 3.3b summarise varieties of trace element zoning patterns observed in Gough Island augites. Several salient features can be summarised as follows: (1) many crystals display concentric growth zones with abrupt changes (to within the spatial resolution of the study of 5 – 8 μm) in the concentrations of both compatible and incompatible elements; (2) trace element variations appear to override element compatibility, *i.e.* a compatible element (*e.g.*, Cr) can vary either sympathetically or antithetically with incompatible elements (*e.g.*, Ti and Sr); (3) the magnitude of

trace element changes at a given growth zone transition over a distance of 10 μm can be as large as a factor of 2 or more; (4) individual phenocrysts from a given lava can display different zoning patterns (see three phenocrysts from ALR26G), suggesting that they might have grown from chemically different magmas; (5) trace element changes are always accompanied by changes in major elements, whether with respect to Mg/Fe ratios or the Ca-Tschermak's component; and (6) apparent partition coefficients of Ti and Cr calculated against groundmass concentrations are all elevated relative to the respective equilibrium values by a factor of 2 – 6 for Ti and a factor of 20 – 30 for Cr for the picritic basalt ALR26G, whereas those for Sr are approximately equal to the equilibrium value.

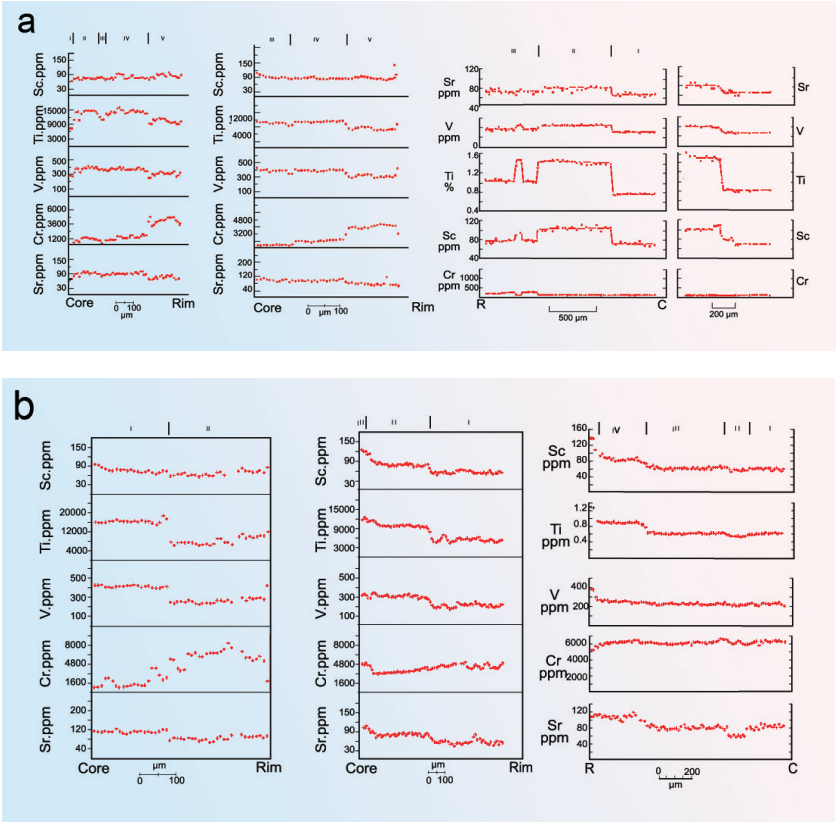

Figure 3.3 **(a)** Trace element zoning patterns of augite phenocrysts from ALR 51G (two left transects) and ALR 49G (two right transects). For ALR 51G: In phenocryst A-111 (left), five growth zones (I to V) are recognised, with each internally homogeneous and with sharp transitions between zones. In phenocryst A-1 (right) three growth zones are recognised which correspond to zones III, IV, and V of A-111, suggesting that A-1 is younger than A-111. For ALR 51G: In

phenocryst AB-2 (left), three growth zones are recognised, and phenocryst AB-21 (right) displays two growth zones I and II. A very sharp transition between zones I and II is seen, with Ti increasing by a factor of two. Note also that two compatible elements, Sc and Cr, are behaving antithetically. **(b)** Trace element zoning patterns of three augite phenocrysts from ALR 26G, AS-1 (left), AB-1 (centre) and A-2 (right). In A-2, four growth zones (I – IV) are defined principally by sympathetic changes in two incompatible elements, Ti and Sr, and a rim, where Cr decreases and Sc increases. It is noticeable that Cr stays constant at ~6000 ppm throughout the growth zones. In AB-1, three growth zones are recognised and element abundances of its outer zone (III) match those of the rim in A-2. Cr behaves differently from A-2. In AS-1, there are two major growth zones (note that the core-rim orientation of this figure is reverse to that of the other two figures). Element behaviour in this phenocryst seems very different from the other two phenocrysts in ALR 26G, indicating that this crystal might be a xenocryst.

Sudden simultaneous changes in trace element abundances irrespective of their compatibility are not likely to be produced by sudden changes in the kinetics of the interface process during crystal growth, but rather reflect changes in the chemical composition of the magmas. If this interpretation is correct, then phenocryst zoning could also provide information about the dynamic state of the magma body itself. A growing crystal is surrounded by two types of boundary layers: one is the fluid dynamic boundary layer in which there is no relative motion between crystal and magma, and the other is the diffusion boundary layer in which mass transport is by diffusion only. If it is assumed that the diffusion boundary layer is much thinner than the fluid dynamic boundary layer, then, gravitationally sinking phenocrysts would drag the entire diffusion boundary layer with it and gravitational separation of phenocrysts would have no chemical effects on the main part of a sufficiently large magma body. If, however, turbulent current exists in a magma body in which an old magma is mixing with a new batch, the fluid dynamic boundary layer would be thinned, and a growing crystal could be exposed to a different magma. If this type of magma mixing takes place multiple times in a given magma body during augite growth, multiple stages of growth zones could ensue in a given crystal. If this picture holds in nature, the Gough phenocrysts indicate a magma body with repeated introduction of magmas of different chemistry under turbulent conditions. It is also noticeable from the figures that each growth zone appears to be homogeneous internally with interface partition coefficients elevated relative to equilibrium values. As noted above, high (~6000 ppm) and homogeneous Cr concentration in an augite phenocryst (A-2 in ALR 26G) yields an apparent partition coefficient of 38 relative to the groundmass (Shimizu, 1983; Shimizu and le Roex, 1986). The observations summarised above provide evidence to support a contention that partition coefficients at crystal-melt interfaces could be significantly elevated relative to equilibrium values even during natural magmatic crystallisation processes.

Studies of phenocryst zoning that started with a sector-zoned augite (Shimizu, 1981) also led me to examine more disequilibrium crystal growth cases such as oscillatory zoning of trace elements. Oscillatory zoning of plagioclase has

long been known with several theories attempting to explain the phenomenon. For instance, Haase *et al*. (1980) used a crystal growth model in which crystal growth rate was dependent on melt and crystal compositions at the interface as well as on transport of components in melt, and argued that a positive feedback for crystal compositions could be created. In other words, their model predicted a situation where an anorthite-rich crystal surface incorporates more anorthite-rich plagioclase, and resulting depletion of Al in the melt eventually begins to crystallise albite-rich plagioclase. Then, more albite-rich composition would be incorporated until aluminum-rich, anorthite-rich melt composition is reached and the system completes a cycle. The cycle would continue, producing oscillatory zoning. Crystal growth of augite from a basaltic melt is much more complex with more melt components than in the albite-anorthite system, but a similar positive feedback could be considered for various trace elements. Suppose, for instance, that Cr is incorporated as $CaCrAlSiO_6$ and Ti as $CaTiAl_2O_6$. Behaviour of the system for incorporation of those trace element end member components could mimic the albite-anorthite system in that a positive feedback could be formed between those components. If so, oscillation of Cr would be antithetic to oscillation of Ti. Haase *et al*. (1980) also pointed out that plagioclase oscillatory zoning is a phenomenon far from equilibrium, and it is assumed here that oscillatory trace element zoning in augite is also a disequilibrium phenomenon.

An augite phenocryst in a primitive basalt from Lihir Island, Papua New Guinea, displays spectacular oscillations in many elements over large concentration ranges in a transect over a distance of ~500 μm. Variations of Cr and Ti are shown in Figure 3.4 (Shimizu, 1990). Note that Cr varies more than a factor of 40 over a very short distance, and oscillations of short wavelengths are predominant. Also note that the lowest concentrations are about the same (near 100 ppm), whereas high Cr peak concentrations vary. Ti variations are antithetical to those of Cr, with an additional trend of increasing concentration toward the rim.

These trace element variations are in contrast to a relatively small range in Mg# of the augite (the high Cr part has an Mg# of 89.3, whereas the low Cr part has an Mg# of 72.5) and hence require a complex model of crystal growth with significant variations in interface processes. Take the Cr oscillation for instance. From the low Cr core (72.5 ppm Cr), a gradual increase in Cr content over a distance of ~100 mm is followed by strong oscillation over the subsequent 400 μm. The oscillation appears to begin with low (~100 ppm) Cr, whereas high Cr peak concentrations vary. It is remarkable that an apparent partition coefficient for Cr relative to the bulk rock (158 ppm; Kennedy *et al*., 1990) varies from 0.46 (Cr behaves as an incompatible element!) for the low Cr end of the oscillation, and in the core of the grain, to a maximum of 25 (the highest Cr is 3995 ppm). If the concept of the theory of Haase *et al*. (1980) is applied to this case, once Cr incorporation started, it is further accelerated by a positive feedback mechanism until the Cr peak is reached, then the trend reverses itself. At that point, an incompatible element such as Ti becomes preferred and incorporation of Ti is accelerated by a positive feedback mechanism, and oscillation repeats itself. The large variation of the apparent partitioning of Cr reflects the fact that the oscillations are

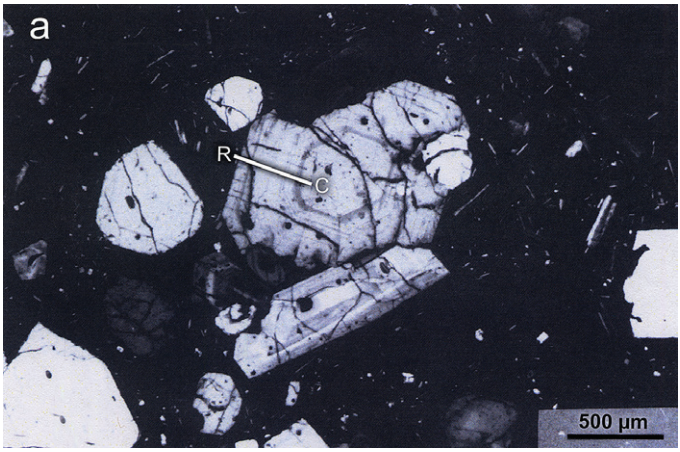

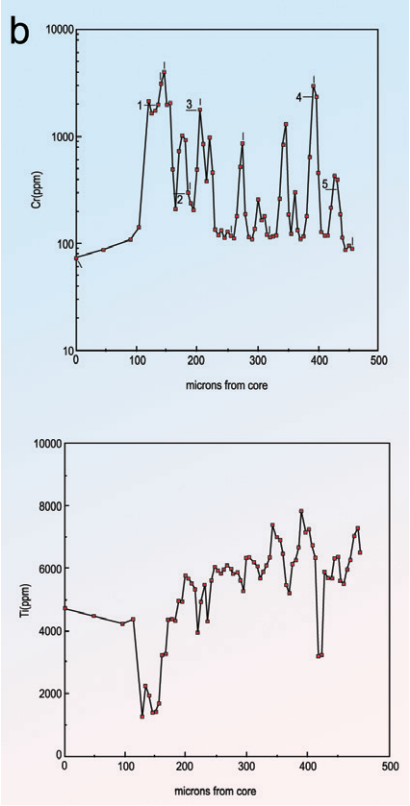

Figure 3.4 **(a)** Photomicrograph of the augite grain analysed here, with a line R-C denoting the location of the ion probe traverse. **(b)** Core-to-rim transect of an augite phenocryst in a primitive alkali basalt from Lihir Island, Papua New Guinea. Top: zoning of Cr from the core (position 0) toward the rim (~450 μm). A broad low Cr core growth is followed by strongly oscillatory variations of high frequency. The oscillation appears to be between the "fixed" low Cr end of at ~100 ppm and the high Cr peaks of >1000 ppm occur many times. Bottom: zoning of Ti. Ti oscillation is antithetic to Cr oscillation and is accompanied by rimward increase in concentrations. Modified from Shimizu (1990).

phenomena far from equilibrium. Likewise, the apparent partition coefficient for Ti varies from 0.22 to 1.5, relative to the equilibrium value of 0.1 – 0.25 (Grove and Vaniman, 1978). The antithetic relationship between Cr and Ti suggests that incorporation of these elements is coupled in a feedback mechanism, just as for albite and anorthite components in plagioclase as discussed by Haase *et al.* (1980). However, the irregularity in oscillation indicates involvement of other melt components and clinopyroxene end member components in complicating the feedback mechanism. Although it is uncertain whether these oscillations represent an example of geochemical self-organisation, a reaction-transport kinetics approach developed by Ortoleva *et al.* (1987) could be applied to the system of crystal growth with multi-component feedbacks.

Overall, my thoughts on silicate crystallisation from magma developed through the study of trace element zoning of augite phenocrysts as presented above and can be summarised as follows. Fundamentally, igneous crystal growth takes place with certain degrees of supercooling and can be considered as a phenomenon far from equilibrium. Growth of augite from a basaltic magma requires assembly of clinopyroxene end member components at the surface, while the growth rate and composition of the crystal are defined by the reaction rates of the formation of the endmember components. For instance,

$$
\begin{aligned}
&R_{Di} = R\left(CaO + MgO + 2SiO_2\right)\\
&R_{Hd} = R\left(CaO + FeO + 2SiO_2\right)\\
&\vdots\\
&R_{Sr} = R\left(SrO + MgO + 2SiO_2\right)\\
&R_{Ti} = R\left(CaO + TiO_2 + Al_2O_3\right)\\
&R_{cr} = R\left(CaO + CrO_{1.5} + AlO_{1.5} + SiO_2\right)\\
&\vdots
\end{aligned}
$$

where R_{Di} *etc.* denote rates of formation of individual end member components, including trace element pyroxene end members, and it is assumed that in the magma oxides are melt components. Individual R's reflect affinities of these formation reactions and are a function of temperature (and pressure), or, more precisely, a function of supersaturation (thermal as well as constitutional). At a given set of conditions, the sum total of progress of all individual reactions in a unit time determines growth rate, while relative reaction progress defines chemical composition. Therefore, growth rate and chemical composition of growing crystals are interrelated. Of course, diffusion of chemical components in magma comes into play when a reaction rate involving slow diffusing components, *e.g.*, R_{Ti}, becomes high and melt will then become depleted in those components. This will reduce constitutional supersaturation and results in decrease in R_{Ti}. The interface process mentioned above can also be interpreted as rates of specific end member component formation reactions. Incorporation of Sr, for instance, will be determined by $R_{Sr}/\Sigma(R)$. Experimental determinations of R's under isothermal and

dynamic crystal growth conditions will be essential for advancing this approach. Oscillation of chemical compositions as shown above could also be interpreted quantitatively by expanding this approach to involve transport of components in magma with feedbacks. Under certain disequilibrium conditions this type of system could evolve into a bifurcation and chemical oscillation could begin.

As mentioned above, trace element zoning of phenocrysts could provide unique information pertaining to the dynamics of magma bodies. The Gough Island case was an unexpected outcome of my study of trace element petrography. A joint work with Jon Blundy, when he was visiting MIT in the 1980s, was another example of gleaning the dynamics of a magma body through trace element zoning of minerals. The data on Sr and Ba distribution in plagioclase crystals over a large range of rocks from hornblende gabbro to granitoid from the Adamello Massif, Italy, indicated that early formed An-rich plagioclase crystals were "recycled" in a vigorously convecting magma body during differentiation (Blundy and Shimizu, 1991). The observations presented in this chapter imply that physical and chemical processes in magma bodies can be much more complex than indicated by traditional igneous petrology. It is my belief, however, that observations on microscales could provide important first steps toward a better understanding of how natural igneous processes work. In this context, a recent review by Cashman *et al*. (2017) presents encouraging signs of significant progress being made in volcanology and igneous petrology.

Trace element petrography as advocated in this chapter goes beyond igneous rocks. Its application to metamorphic petrology is demonstrated by a study of trace element distributions in metamorphic garnets (Hickmott and Shimizu, 1990) in contact metamorphosed rocks in the Kwoiek area, British Columbia, where Hollister (1966, 1969a,b) did the classical work.

Hollister (1966, 1969a) proposed that Mn zoning profiles could be explained by a simple Rayleigh fractionation model, but our data on trace elements (see Fig. 3.5) indicated that many do not conform to the Rayleigh model. Elements such as Li, Na, Y, Ti, V, Cr, and heavy REE (not shown) show inflection midway through the profile, suggesting that garnet growth during contact metamorphism and trace element distributions between garnet and matrix in the Kwoiek region were complex. The Ti profile is particularly interesting; because Ti in the system was buffered by the presence of ilmenite, the Ti profile would require sudden change in temperature and/or pressure during garnet growth if equilibrium partitioning prevailed. This is unlikely for contact metamorphism, and suggests that garnet growth took place under disequilibrium conditions. It is proposed that rapid garnet growth at the beginning due to large overstepping of a garnet growth reaction resulted in elevated incorporation of Ti in the core, followed by growth under gradually decreasing affinity and growth rate. At the inflection, growth rate suddenly increased and Ti incorporation was increased probably due to a sudden increase in pressure (as evidenced by kyanite replacing andalusite according to Hollister,1969b). Thus, our data suggest that the explanation of Mn zoning by Hollister (1966, 1969a) is no longer tenable, but rather

that incorporation of trace elements into rapidly growing garnets was controlled by interface processes with resultant disequilibrium partitioning of elements between garnet and its growth medium.

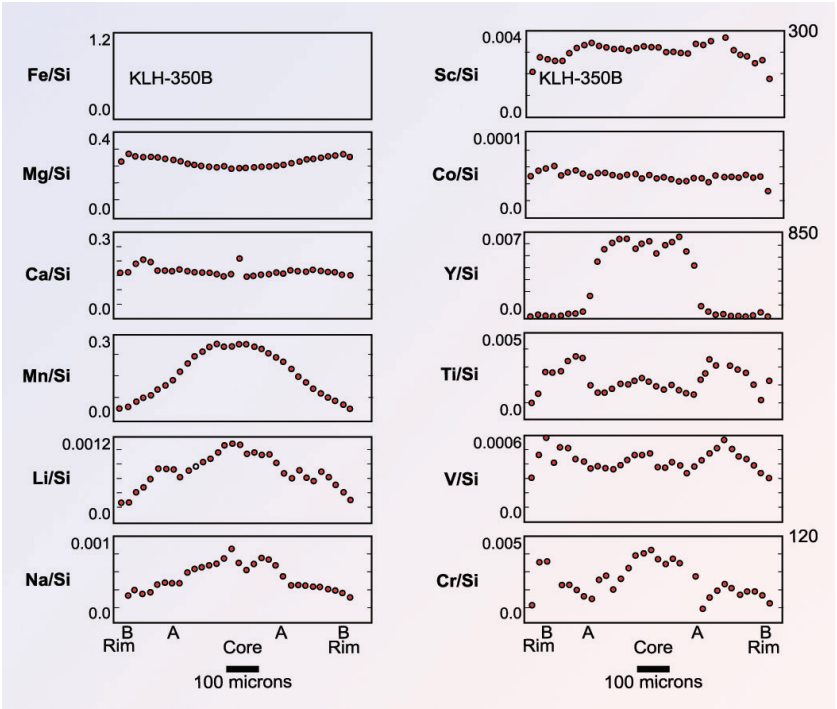

Figure 3.5 Major and trace element zoning profiles expressed in intensity ratios against Si of a garnet in sample 350B from the Kwoiek area, British Columbia. Trace element concentrations are given for some elements based on the pyrope-based working curves. Modified from Hickmott and Shimizu, 1990.

Here again, it is clear that ion probe-based trace element petrography could provide unique information to advance our understanding of the growth of silicate minerals under a wide range of temperatures and pressures.

4. MIT-WHOI: APPLYING SIMS TO MANTLE GEOCHEMISTRY

One of my major motivations for getting into geochemical SIMS was analysing mantle minerals for trace elements *in situ*. Combined with our increasing knowledge during the 1970s on mineral-melt partitioning, I thought it was important to document mantle minerals for their trace element abundances. Peridotite xenoliths had always been important sources of insights into mantle petrology and mineralogy and a significant volume of literature already existed on this topic since the late 1960s (for instance, see Wyllie's book published in 1967: *"Ultramafic and Related Rocks"*), but trace element and isotope geochemistry on peridotite xenoliths lagged behind due essentially to delayed technological developments. Early efforts were made on whole rock peridotites from alpine massifs (also known as high temperature peridotites) and xenoliths in basalts and kimberlites. Noticeable among those early studies was an important discovery by Frey and Green (1974) of apparent decoupling of trace elements from major elements; large ion lithophile element abundances were often much higher in peridotites that were more depleted in basaltic components relative to more Fe-rich "fertile" peridotites. In their view, this situation came about when peridotitic residues left after partial melting (lithospheric peridotite) were modified by infiltrating small degree melt and recrystallisation. They called the lithospheric part Component A and the infiltrating melt Component B, which they thought to represent small degree melts and thus enriched in P, K, Ti, light REE, Th, and U. I thought that analysing peridotite minerals that carried a significant mass balance of incompatible elements would contribute to a better understanding of the process of lithospheric enrichment. My early study of mantle xenoliths (Shimizu, 1975a,b) confirmed Frey's notion that incompatible element concentrations were higher in clinopyroxenes from peridotites more depleted in major elements relative to fertile peridotites. My first SIMS study of mantle xenoliths (Shimizu and Allègre, 1978) further confirmed this idea and convinced me that SIMS could prove powerful for this type of enquiry.

Encounter with Tony Erlank

I knew who Tony was before I arrived at DTM in 1971, because he and Kushiro did an experimental study to determine the stability of K-richterite, which was considered by some to be a major carrier of potassium in the mantle. Tony was Stan's post-doc before I arrived and visited Washington more than twice while I was there and our friendship grew because we had shared scientific interests. His vast knowledge of kimberlite xenoliths helped me greatly. After the first kimberlite conference in Cape Town (1973), we discussed the possibility of collaborative projects, focusing on mineral trace element chemistry. Tony was following my struggle with the IMS 300 with interest, and was, in fact, visiting me in Paris in 1976 when I produced the first trace element working curve. He witnessed it and shared my excitement. After I moved to Woods Hole, he visited me again and we collaborated on a project on variations of mineral trace element abundance patterns in a series of garnet peridotite xenoliths for establishing trends with increasing degree of metasomatism.

Infiltration of fluid/melt into a peridotitic substrate that results in modifications of the bulk chemistry of peridotite is widely known as "mantle metasomatism" and could occur in different forms: (1) exchange of trace elements between fluid/melt and existing minerals without modal changes; (2) precipitation or addition of the same minerals that already existed in the peridotite; (3) precipitation of minerals that were new to the peridotite; and (4) dissolution of minerals into fluid/melt and precipitation of minerals from fluid/melt. The occurrence of phlogopite and/or K-richterite in kimberlite-borne peridotite xenoliths was one of the remarkable types of metasomatism with enrichment in K and Rb without changing the depleted nature of the major element composition of the rock. Metasomatism without modification of the mineralogy (or mineral assemblage) is called cryptic metasomatism and occurs much more broadly. In fact, as will be shown below, SIMS analysis of mantle minerals has revealed trace element abundance patterns characteristic of cryptic metasomatism and made significant contributions to the understanding of the processes of fluid/melt-mantle interactions on grain to outcrop scales. The concept proposed by Navon and Stolper (1987) that the Earth's mantle acts as an ion exchange column with infiltrating fluid/melt has been proven to be correct, and mathematical models developed by Bodinier and his colleagues (*e.g.*, Bodinier *et al.*, 1990; Vasseur *et al.*, 1991, among others) have been instrumental in the quantitative understanding of the process.

My journey into this domain began innocently; the distribution of trace elements in mantle minerals, combined with mineral-melt partitioning experiments, would be fundamental to the quantitative understanding of mantle melting and evolution of basaltic magmas, and I was going to provide the observational link to natural systems. However, I immediately encountered trace element abundance patterns that were unexpected from the known partition behaviour of elements, reflecting complexity in the natural processes. Those unusual patterns gave me opportunities for a better understanding of nature but with a lot of headaches and sleepless nights.

4.1 Are Diamonds Forever?

In the early 1980s, Steve Richardson came to join the Stan Hart group at MIT as a graduate student. He developed into a superb microchemist and did his Ph.D. working on garnet inclusions in diamonds. His greatest discovery was that Nd and Sr isotopic compositions of the sub-calcic peridotitic garnet inclusions in diamonds had radiogenic Sr ($^{87}Sr/^{86}Sr$ ranging from 0.7115 to 0.7211) and unradiogenic Nd ($\varepsilon^{143}Nd$ as low as -15), indicating that the model ages were as old as 3.5 Ga (Richardson *et al.*, 1984). These authors interpreted the model ages as the formation ages, and the antiquity of diamonds in the continental lithosphere became a topic of intense research activity. I was unsatisfied with the interpretation of model age = formation age but was very much interested in the fact that the garnets had a long-term residence in an environment with low Sm/Nd (*i.e.* a LREE enriched environment). Actually, I was shocked to see that these

garnets had $[Sm/Nd]_n$ < chondrite; I had never seen any garnets like that before (*cf.*, garnets I had analysed in garnet peridotite xenoliths, for instance: Shimizu, 1975b). If the garnets really were 3.5 Ga old, the processes responsible for their formation must have been very different from those we encounter commonly in the mantle. Because Richardson's data showed that garnets had low Sm/Nd, I decided to study trace element abundances in diamond inclusion garnets in some detail with the ion probe. Individual inclusions left over from Richardson's study were mounted in epoxy and analysed by the IMS 3f.

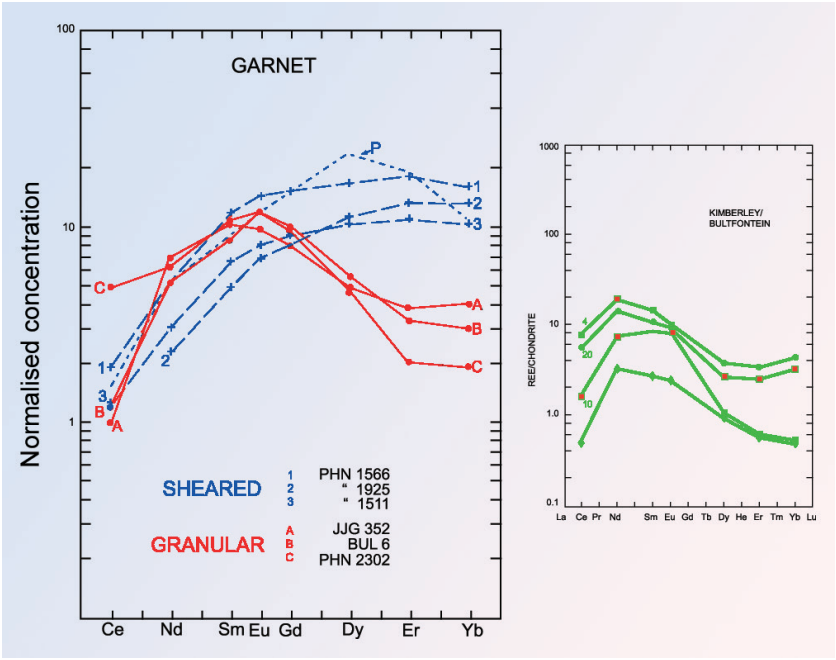

Figure 4.1 **Left panel:** Chondrite normalised REE patterns of garnets in peridotite xenoliths. Modified from Shimizu (1975b). **Right panel:** Chondrite normalised REE patterns of garnet inclusions in diamonds. Modified from Shimizu and Richardson (1987).

The results shown in Figure 4.1 were extremely puzzling: the LREE enriched patterns were found to be common; chondrite normalised abundances increased from La to Nd, then decreased toward Yb, reminiscent of the sinusoidal patterns I had found in some garnets in low temperature metasomatised garnet peridotites (Shimizu, 1975b; also see figure above). This resemblance suggested a geochemical commonality between some garnet peridotite xenoliths and diamonds. Another shock was unusually high Sr contents (up to 10 ppm) in agreement with Richardson's isotope dilution data (Richardson *et al.*, 1984), in

spite of the fact that these garnets were unusually low in CaO (many so-called G-10 garnets are ~1 – 3 wt. % CaO, relative to ~6 wt. % in garnets in peridotites). Why do these low Ca garnets contain unusually high Sr (10 ppm, in contrast to less than 1 ppm in garnets in peridotites)? How is this explained? Even if metasomatic reactions between garnet and melt/fluid modified the garnet chemistry, it was beyond imagination for garnet to gain 10 ppm Sr in equilibrium partitioning.

The oddity of the chemistry of the diamond inclusion garnets and their potential connection to mantle metasomatism were the main motivation for my plans to develop ion probe studies of diamond inclusion garnets of diverse composition and occurrence. John Gurney was very kind to respond to my request by giving me his collection of peridotitic garnets from the Finsch pipe, and Rory Moore wanted to know whether trace element chemistry of ultra-deep majoritic garnet inclusions from the Monastery Pipe diamonds was in any way unusual. It turned out that the majoritic garnets had normal REE patterns and low Sr contents (Moore *et al.*, 1991), but many G-10 garnets from Finsch reproduced early results based on Richardson's samples (Shimizu and Richardson, 1987). While this was going on, the Russian group, Nick Sobolev and Nick Pokhilenko, proposed a similar study of trace elements in diamond inclusion garnets from some Russian kimberlites. They lent me epoxy mounts with a large number of garnets to analyse and I started to look at those from the Udachnaya, Mir, and other pipes. This led to a stunning discovery: some garnets were found to be highly heterogeneous with respect to Sr concentrations.

As shown (Fig. 4.2), the distribution of Sr is highly irregular; the grain centre looks homogeneous with low concentration, whereas high concentrations (up to 535 ppm) are found around the grain edges (the upper corner area in the figure seems to be particularly high in Sr). When chemical heterogeneity was sought in a diamond inclusion garnet, a special strategy had to be invented. Imagine a garnet grain beginning to grow in a diamond; the "core", or the starting point of growth of the grain, would rest on the host and would not become the centre of a full-grown crystal but become a "corner" of a grain because an inclusion would not be suspended in a growth medium like igneous crystals. Of course, the epoxy mount of a grain may not expose the "corner", and I had to analyse many grain margins before discovering any high Sr corners. This strategy was found only after making a number of futile rim-to-rim transects. The figure shows several rim-to-rim transects, representing earlier attempts that led to the establishment of the strategy. My first reaction was that if these garnets were indeed 3.5 Ga old, having resided under mantle conditions that long, diffusion would have homogenised the Sr distribution within the garnets. The fact that significant heterogeneity still existed on μm scales suggested that the garnet and host diamond were young. This conclusion fundamentally deviated from Richardson's contention of the antiquity of diamonds, but in my mind, it presented a possible solution to the model age *vs.* formation age issue. Experimental data on Sr diffusion in garnet was taken from Richard Coghlan's thesis at Brown (Coghlan, 1990), which indicated that a garnet grain with a radius of 100 μm would be homogenised in 7×10^4 years at 1000 °C. In other words,

the materials from which garnet and diamond formed were ancient (3.5 Ga old continental lithosphere), but the formation of diamond and inclusion garnet had occurred recently (as recent as the eruption of the host kimberlite at 350 Ma).

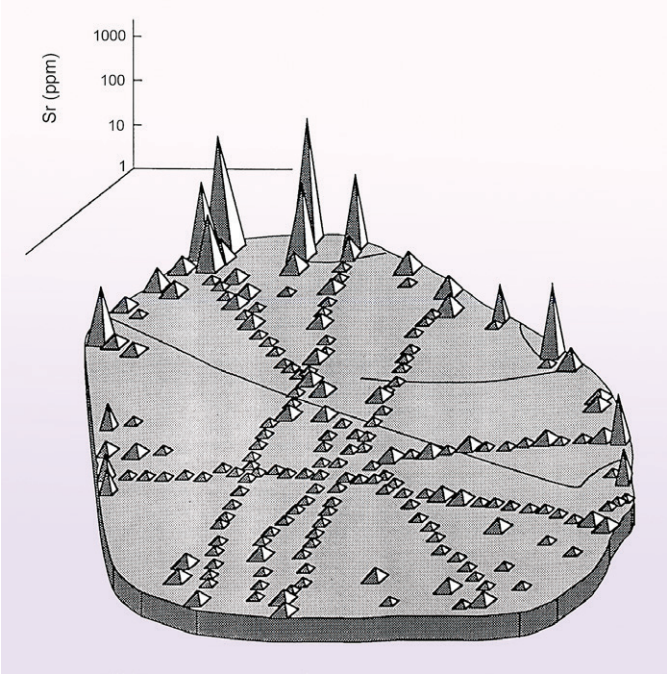

Figure 4.2 Distribution of Sr in a garnet inclusion in diamond from Mir, a bird's eye view. The highest concentration is 535 ppm. From Shimizu and Sobolev (1995).

My second reaction was the difficulty of accepting the absurdly high Sr concentrations. My data on Sr partitioning between clinopyroxene and melt was around 0.1 (Shimizu, 1974), and Sr partitioning between clinopyroxene and garnet was approximately 90 to 1. Shimizu (1975a) reported 89.3 ppm Sr in clinopyroxene and 0.98 ppm in coexisting garnet so that the garnet/melt partition coefficient should be around 10^{-3}. In order to produce garnet with 500 ppm Sr would require melt/fluid with 50 wt. % Sr! I thought this argued very strongly against equilibrium partitioning of Sr during growth of a garnet "corner".

A paper (Shimizu and Sobolev, 1995) describing this discovery was published in *Nature* just before the International Kimberlite conference in Novosibirsk (Russia), and significant hostility was waiting for me there. I knew that a potential criticism could be focused on the detailed distribution of Sr in some garnets; in the garnet grain described in Shimizu and Sobolev (1995), high Sr

appeared to be on grain edges, and some might argue that it resulted from exposure of garnet to high Sr fluids when the host diamond cracked, and thus was not a primary feature. As mentioned above, however, that this putative fluid had to contain 50 wt. % of Sr made this criticism unrealistic. In any case, because I anticipated such criticism, I brought more convincing data to the conference: a G-10 garnet inclusion from the Mir kimberlite pipe analysed for more than 200 spots with a corner area about 30 x 50 μm where Sr was highest (the highest concentration was 2307 ppm) and sharply dropped to a 1 ppm level within a 10 micron distance (Shimizu *et al.*, 1997a).

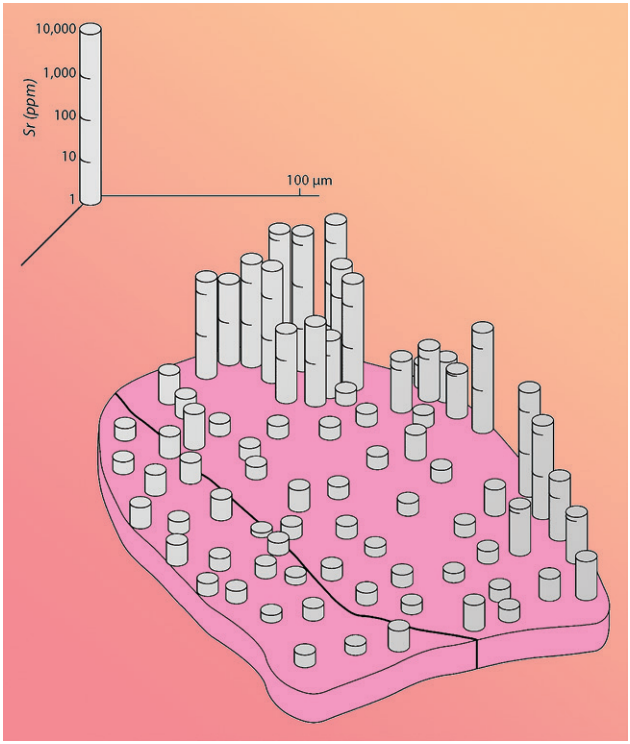

Figure 4.3 "The downtown garnet", three dimensional (bird's eye view) presentation of the distribution of Sr in a section of a garnet inclusion in diamond from the Mir Pipe (Av49, Grain #14). The highest Sr concentration in this grain is 2307 ppm. Modified from Shimizu *et al.* (1997a).

In a 3-dimensional (a bird's eye view) diagram of the Sr distribution in this garnet it resembled a downtown area of a city with tall buildings, and therefore I called it the "downtown garnet" (fig. 4.3). People in opposition to young diamonds attempted to discredit my results by saying that high Sr was due to a

secondary process. They even imagined that the high Sr edge might have been created during burning of the host diamond to liberate its inclusions. The downtown garnet was a strong defense on my part, but my critics still maintained their attitude. The point of contention really was on the validity of Richardson's conclusion that the model age = formation age, and my observations presented an alternative to this view.

Much more work was needed to argue either way: diffusion of Sr in pyropic garnet had not been studied experimentally (Coghlan's work was made on almandine garnet), and reasons for having high Sr in strong contrast to low Ca in G-10 garnets also were among the contentious issues. For the high Sr areas of the garnets, REE patterns were decidedly strange: more sinusoidal than others, while the low Sr areas in the downtown garnet had normal REE patterns (low LREE gradually increasing toward HREE in a chondrite normalised pattern). Nick Pokhilenko was working on diamond exploration in Canada, using the chemistry of detrital garnet grains, and asked me to look at the trace element patterns in some of them. Nick Sobolev continued to feed me with sub-calcic garnets from the Siberian pipes.

With more data collected, an idea began to form, based on the partitioning of Sr between fluid/melt and garnet: Consider that growth of garnet (and its host diamond) started under highly disequilibrium conditions and fast crystal growth rate and that the system (peridotite – fluid/melt) approached equilibrium as growth continued with reduced rates. Element partitioning under highly disequilibrium conditions could deviate in the direction of elevated partition coefficients (see arguments in Section 3). When crystal growth rate overwhelms the kinetics of element partitioning, the interface partition coefficient could approach unity. As the system evolved toward equilibrium as garnet growth continued, growth rate was reduced and element partitioning approached an equilibrium value. This could explain the unusually high Sr and highly sinusoidal REE at the beginning of garnet growth and rapid approach to low Sr and normal REE as growth continued, reflecting the progress of the reaction. From this point of view, even 2307 ppm Sr at the beginning of growth of "The downtown garnet" is not unusual, as for instance, the Sr contents of South African kimberlites range from 183 to 1520 ppm (Fesq *et al.*, 1975). If this were the case, a collection of as many REE patterns in G-10 garnets as possible in a single locality might form a continuous trend of fluid-rock reaction progress, and this argument would be strengthened if a single zoned garnet displayed a continuous variation in REE patterns from sinusoideal at the beginning to normal at the end. For this purpose, my Russian colleagues and I started to look at trace element abundance patterns of diamond inclusion garnets from three Siberian kimberlite pipes, Mir, Udachnaya, and Aikhal. Twenty garnet grains from 7 diamonds from Mir, 9 grains from 7 diamonds from Udachnaya, and 1 grain from each of 4 diamonds from Aikhal. Thirteen of 33 garnet grains showed Sr variations of more than a factor of 2 within individual grains, and 6 out of 33 showed more than a factor of 10 variation. Recalling the random orientation of epoxy mounts, this statistic reveals the common nature of chemical heterogeneities of diamond inclusion garnets in general. Looking

at chemical heterogeneities on more restricted spatial scales, we note: (1) REE patterns in garnets from individual diamonds share general features as shown in Figure 4.4. This suggests that on micrometre-millimetre scales (*i.e.* within individual diamonds), environments and mechanisms of garnet growth were similar. (2) Variability within individual pipes is much larger, indicating that growth environments and mechanisms (and timings) could have varied within individual pipes. (3) Figure 4.4b shows that Sr co-varies with light REE. Unusually high Sr contents in low Ca garnets appear to show a decoupling between two geochemically similar elements, but it could also just be a "red herring". The co-variation of Sr with light REE shown in Figure 4.4b would suggest that high Sr is a reflection of the environment and mechanism of garnet growth, and the apparent decoupling with Ca would simply mean that the bulk system in which garnet formed was strongly depleted in Ca. This implies that diamond

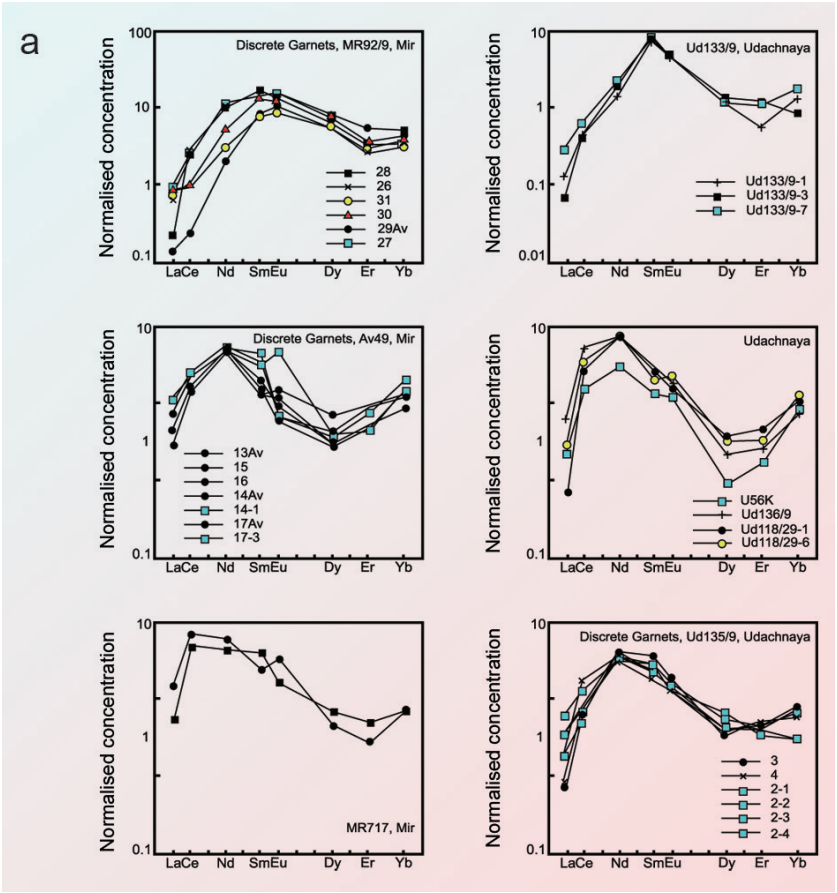

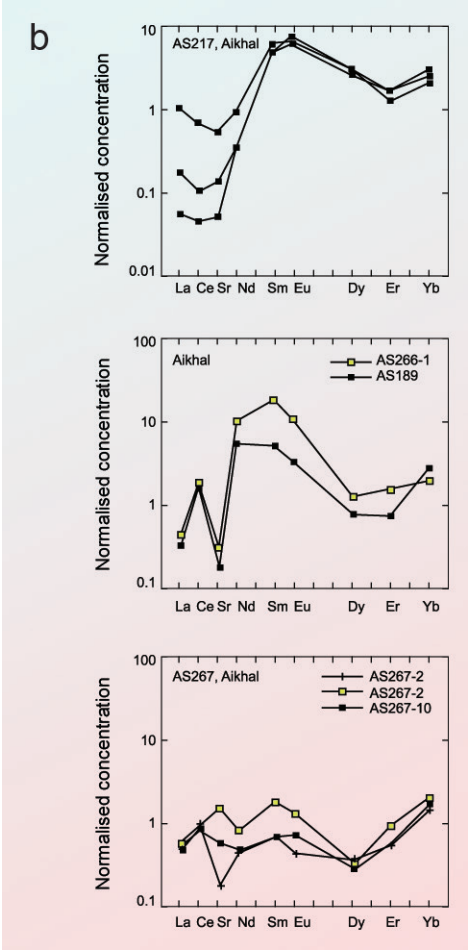

Figure 4.4 Chondrite normalised REE patterns in diamond inclusion garnets from Mir, Udachnaya, and Aikhal. Modified from Shimizu *et al.* (1997a).

inclusion garnets formed in the absence of clinopyroxene in a harzburgitic to dunitic substrate. Pokhilenko *et al.* (1991) described megacrystalline olivine-rich peridotites as the host of Siberian diamonds, and the vast majority were clinopyroxene-free, consistent with the implications mentioned above. In contrast to the large variations in Sr, elements such as Ti and Zr are relatively uniform. For instance, sample Av49 (one of the garnets in "the downtown garnet" in which Sr varies from 1.6 to 2307 ppm) has Ti around 210 ppm with Ti/Zr of 31 ± 3.

It is important to recognise that the peculiarity of REE patterns of diamond inclusion garnets is shared by purple garnets in garnet peridotite xenoliths, indicating commonality of their processes of formation. The data of Shimizu *et al.* (1997b) on garnets from peridotite xenoliths from the Udachnaya pipe completely overlaps with diamond inclusion garnets from the same pipe (see Fig. 4.5). Similarities between diamond inclusion and peridotite xenolith garnets also include Ti, Sr, Y, and Zr abundances and abundance ratios. Unfortunately, the observations made on separate garnet grains did not provide a compelling case for a specific geochemical mechanism responsible for the peculiarity of REE patterns. To get at this, a detailed study of chemically zoned garnet crystals was needed.

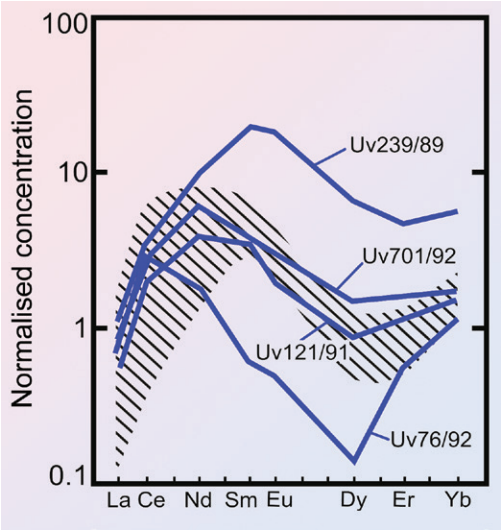

Figure 4.5 Comparison of REE abundance patterns in garnets between diamond inclusions and peridotites from Siberia. Shaded area represents diamond inclusion garnets as shown in Figure 4.4, others are garnets in garnet lherzolite xenoliths from the Udachnaya kimberlite pipe. Modified from Shimizu *et al.* (1997a).

One such example is shown below for a garnet dunite xenolith from the Udachnaya kimberlite pipe, Uv4/76. This grain is approximately 3 mm across and consists of a core (~1.5 mm across) and a mantle. The core is characterised by low CaO (~3 wt. %) and high Cr (7.98 wt. %) concentrations. Titanium and Sr are heterogeneous and roughly antithetic to each other within the core; there appears to be a high Sr (~7 ppm), low Ti (~300 ppm) ring within the core, while the centre is low in Sr (~0.8 ppm) and high in Ti (~450 ppm). The core displays highly sinusoidal REE patterns. The mantle has higher CaO (~6 wt. %), higher Ti (~900 – 1200 ppm), and lower Sr (~0.8 ppm). REE patterns in the mantle vary rim-ward toward more normal garnet REE patterns.

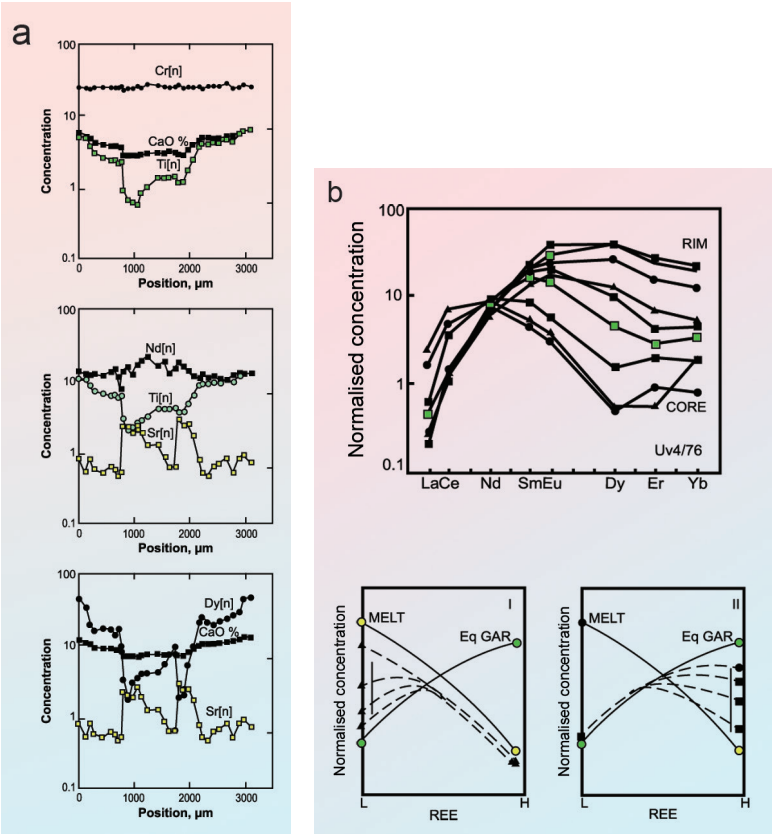

Figure 4.6 **(a)** Rim-to-rim zoning patterns of a garnet from the garnet dunite from Udachnaya (Uv4/76). Normalising factors are: 2660 ppm for Cr, 436 ppm for Ti, 7.8 ppm for Sr, and 0.452 ppm for Nd. **(b)** Chondrite normalised REE patterns of the same garnet (upper panel), and a possible explanation for how the REE variations occurred. Starting with a LREE enriched pattern (strong disequilibrium), LREE concentrations decreased toward equilibrium values (left), while HREE concentrations increased (right) during crystal growth. Modified from Shimizu *et al.* (1997a).

Note that highly incompatible light REE (La and Ce) concentrations decrease outward from the core, whereas more compatible middle-heavy REE concentrations increase outward (Fig. 4.6b). In other words, the entire REE zoning is "reverse", indicating that crystal growth occurred under disequilibrium conditions. As discussed in Section 3, interface partition coefficients can be elevated relative to equilibrium values, but it appears that in this case partition coefficients for incompatible light REE are elevated while those for compatible heavy REE are

suppressed, simultaneously. The Sr distribution in the core (Fig. 4.6a) suggests that this could have been a skeletal crystal at the beginning with a high Sr concentration in the central part of the crystal and that Sr partitioning changed toward the equilibrium value as growth continued. It is also noticeable that the highest Sr coincides with the lowest Dy.

Based on the idea that core crystal growth started under highly disequilibrium conditions, the decrease of light REE can be interpreted to mean that element partitioning gradually approached equilibrium with a light REE enriched and heavy REE depleted melt/fluid. The increase rim-ward of middle-heavy REE also can be a trend toward equilibrium partitioning of REE. The idea of a skeletal crystal core likewise suggests growth under highly disequilibrium conditions. Extending this interpretation, chemical zoning of garnets (as both peridotite and diamond inclusions) can be seen as phenomena associated with crystal growth from melt/fluid. This interpretation differs from that suggested by Hoal *et al.* (1994), as well as that of Shimizu (1999), whereby sinusoidal REE patterns are formed *via* melt/fluid-rock reaction by increasing light-middle REE from a highly refractory precursor with very depleted light-middle REE. In chromatographic melt/fluid-rock reactions, incompatible elements move toward equilibrium faster than compatible elements, and at the stage where light REE are equilibrated, middle-heavy REE still possess some refractory precursor and sinusoidal patterns therefore will ensue. This mechanism is plausible for unzoned peridotitic garnets, but is not applicable to zoned garnets as shown above.

The common occurrence of zoned garnets as diamond inclusions and discrete grains in peridotitic substrates also indicates the timing of garnet formation to be young. For instance, Griffin *et al.* (1989) and Smith *et al.* (1991) argued that overgrowth of Fe-rich garnet on a more pyrope-rich core took place in the lithosphere beneath the Colorado Plateau with subsequent diffusional annealing producing "S-shaped" zoning patterns over a timescale of 60 – 240 years at 1200 – 1300 °C. Similarly, Shimizu (1999) analysed a zoned garnet from Udachnaya (Uv246/89) and argued that Ti zoning can be produced by exchange between the garnet surface and melt and subsequent diffusive penetration of Ti inward over a period of 35 years. Those time scales argue strongly against the notion that everything we have in lithospheric peridotites is ancient (3.5 Ga old, for instance), and if garnet was added to the peridotitic (or harzburgitic) substrate during young event(s), peridotitic bulk compositions might not be representative of Archean lithosphere.

A fundamental difficulty of working on diamond inclusions and xenoliths is to gain a geologic perspective of the processes of interest. In this particular case, I had difficulty relating the geochemical characteristics (peculiarities) of diamond inclusion and xenolith garnets to mantle-fluid/melt interaction processes in a geological context. Was this process lithosphere-wide, or highly localised, perhaps even being constrained to within an individual kimberlite pipe? Did this process always occur in temporal proximity to kimberlite eruption? If the crystal growth hypothesis proposed above were correct, it would mean that garnet was a new phase added to the peridotitic/dunitic substrate. Accepting this, I became

increasingly suspicious of bulk rock peridotite xenoliths as representing Archean lithospheric compositions. In order to explore this disturbing thought further, I decided to look for direct evidence of the occurrence of G-10 garnets in rocks. In Siberian kimberlites, it was known that diamonds were sometimes discovered in megacrystic garnet dunites (*e.g.*, Pokhilenko *et al.*, 1991) and I was interested in looking at sub-calcic garnets in garnet dunites as a geological proxy for garnet inclusions in diamonds. Some of the garnets in garnet dunites were found to be revealing. For instance, in some of these rocks, garnet grains occurred in strings, not as discrete grains, indicating that they formed in a pathway of fluid and fluid-rock reaction resulting in growth of garnets. Individual garnet grains were in some cases chemically zoned with respect to Sr and REE.

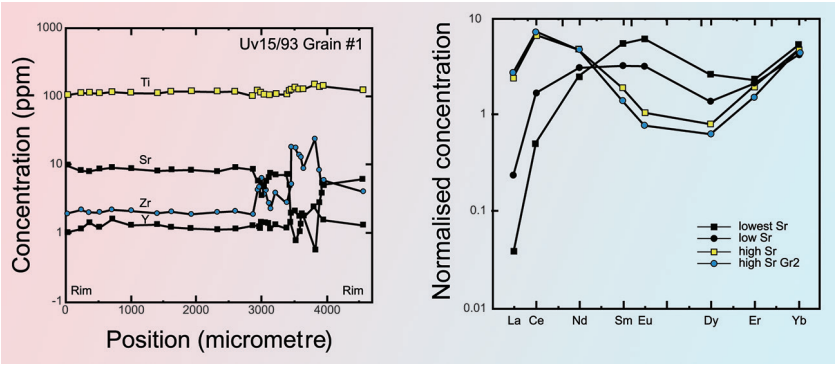

Figure 4.7 Rim-to-rim transect of a garnet in garnet dunite (Uv15/93) from Udachnaya for Ti, Sr, Zr, and Y (left panel), and chondrite normalised REE patterns for some representative points (right panel). Near the right hand side rim is a zone with low Sr where other trace element abundances also vary. For the REE patterns, note that high Sr portions display highly sinuous patterns. Modified from Shimizu *et al.* (1999).

This remarkable example (Fig. 4.7) was described in Shimizu *et al.* (1999), where a trace element transect reveals a structure inside the grain that suggested it might have started its growth as a skeletal grain and then grew inward. This hypothesis is based on the Sr distribution. As shown above, the Sr content is high and constant around 10 ppm in most of the grain but drops precipitously to less than 1 ppm in a small area of the grain where Zr, Y, and REE abundances are all drastically different. Mineral-melt and CPX-Gar partitioning of Sr indicate that "equilibrium" Sr in pyrope-rich garnets should be around 1 ppm, suggesting that this small area crystallised near equilibrium conditions. This structure can be considered as a skeletal grain, which, under conditions of highly disequilibrium element abundances, grew inward and ended up with near equilibrium growth at the end, filling the "pit". The figure also shows that REE patterns started out as highly unusual with high light REE abundances in high Sr zones, whereas they are near equilibrium patterns in the "pit", supporting the interpretation based on Sr.

Overall, my thoughts about diamond genesis in particular and mantle metasomatism in general developed into one coherent point: it is a reaction between fluid/melt and peridotitic substrate, which was melt depleted and trace element enriched in the Archean. The age of the fluid/melt-peridotite reaction could be any time, and, at least at the beginning of the reaction, took place under highly disequilibrium conditions, and hence anomalous chemistry ensued. Looking at peridotite xenoliths from this perspective, it would be extremely difficult to find any primordial ancient piece of mantle anywhere. Even some of the "fertile" peridotite xenoliths could have been affected by interactions between peridotite and fluids/melts. In fact, it had already been known that garnets in fertile xenoliths often were found to be chemically zoned (*e.g.*, Smith *et al.*, 1993). While I was looking at fertile high temperature garnet peridotite xenoliths from the Premier Pipe (thanks to Joe Boyd's collection of large xenoliths of representative bulk rock major element chemistry), I found garnet in sample FRB 1350 to be somewhat like a radial aggregate as shown in Figure 4.8.

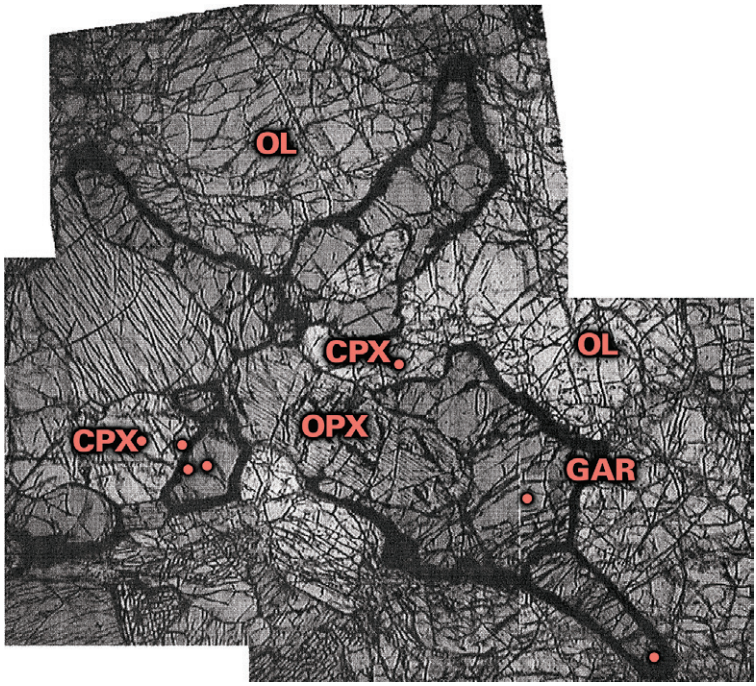

Figure 4.8 Photomicrograph of a garnet peridotite (FRB 1350) from Premier. Note that garnet grains surrounded by kelyphitic rims outline a radial aggregate. From Shimizu (1999) with permission from the Geochemical Society.

This is not a typical equilibrium texture that one would expect for a high temperature mantle rock. As it turned out, these garnet grains were chemically zoned, and REE distributions in a attached clinopyroxene grain were not in equilibrium (Shimizu, 1999). This indicated addition of garnet to the peridotitic substrate through a secondary fluid/melt-rock reaction. The fact that the Sm-Nd mineral isochron age of this specimen coincided with the age of the host kimberlite eruption indicated that reactions with precursor fluids related to the host kimberlite magma could have been responsible for precipitation of radial aggregate garnet grains. If this interpretation is correct, then even major element compositions of garnet peridotites can be secondary, a later modification of its ancient progenitor. This cautions against the common practice of estimating Archean continental lithosphere based on the chemical compositions of mantle xenoliths. A recent work by Dimitri Sverjensky shows that some silicate minerals could also form during diamond forming reactions between peridotite substrate and Carbon-Hydrogen-Oxygen-Nitrogen-Sulfur (CHONS) fluids, and one of the silicate minerals commonly formed is garnet (Sverjensky and Huang, 2015). If this type of work can be extended to include trace element characteristics of silicate minerals, it might prove that the strange chemistry I found for G-10 garnets could be explained once and for all, and my puzzle of diamond genesis would be forever solved.

4.2 Geochemical Processes of Lithospheric Enrichment

As the diamond story unfolded in the late 1980s and 1990s, usage of the IMS 3f ion probe multiplied, in particular for the documentation of trace element abundances in the minerals of mantle rocks.

In addition to Kevin Johnson's thesis on abyssal peridotites (completed in 1990; see Section 5 on MORB), which dealt with trace element variations during melt extraction beneath mid-ocean ridges, documentation of mantle clinopyroxenes for trace elements revealed the workings of fluid/melt-mantle interaction in detail. One of the examples is Eiichi Takazawa, who came to MIT in 1991 to do his Ph.D. with Fred Frey on the petrology and geochemistry of the Horoman peridotite massif, Hokkaido, Japan. The Horoman massif is a large layered ultramafic massif in which a dunite-harzburgite-lherzolite-plagioclase lherzolite sequence is observed. The age of the massif is constrained by Rb-Sr isotope systematics of phlogopite-bearing peridotites to be 23 Ma (Yoshikawa *et al.*, 1993). The typical interpretation for the origin of the layering was sequential precipitation of olivine-orthopyroxene-clinopyroxene-plagioclase from a basaltic magma (*e.g.*, Niida, 1974; Obata and Nagahara, 1987). Takazawa's tasks with the ion probe were to analyse clinopyroxenes in representative rock types of the layered massif. He selected a section of the massif where layers of dunite, harzburgite, spinel lherzolite, and plagioclase-bearing lherzolite were observed in almost continuous outcrops so that geochemical changes could be put into geological context. Very

early on during this project, REE abundance patterns in clinopyroxenes displayed puzzling transitions between lherzolite and harzburgite. Figure 4.9 shows the gist of the transition as a function of sample position.

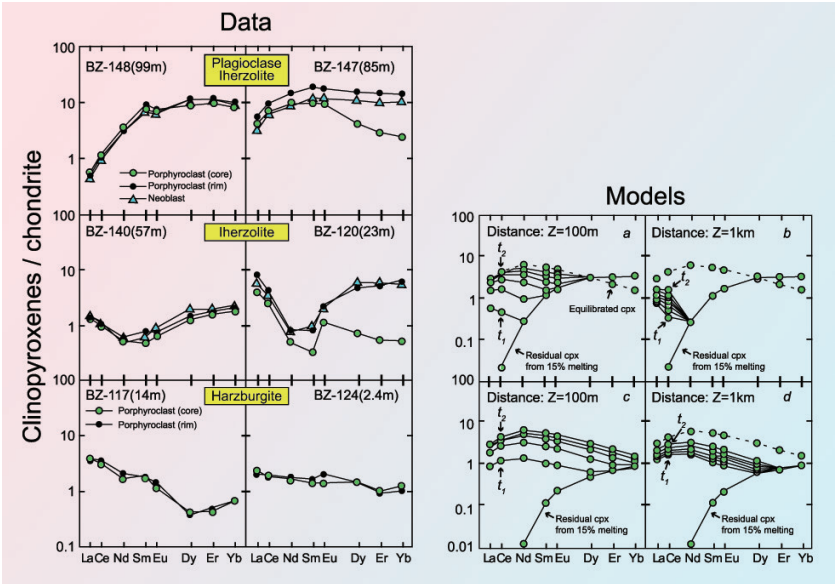

Figure 4.9 Chondrite normalised REE patterns of clinopyroxenes from representative positions in a ~100 m stratigraphic section of the Horoman peridotite massif, Hokkaido, Japan. **Left panel:** sample positions in metres are measured from the olivine gabbro-harzburgite contact. Harzburgite covers a distance of 0 – 22 m, lherzolite 22 – 77 m, and plagioclase lherzolite 77 - ~100 m. **Right panel:** modifications of REE patterns in clinopyroxenes through chromatographic fractionation of REE during melt infiltration and reaction calculated with the model of Vasseur *et al.* (1991). Time t_2 is set to 2 x 10^4 years for all models and t_1 = 670 years for *a* and *c* and 2 x 10^3 years for *b* and *d*. Modified from Takazawa *et al.* (1992).

A big surprise we had was sharply inflected REE patterns found in clinopyroxenes in lherzolites near the harzburgite boundary. They were completely unexpected for clinopyroxenes precipitated from a basaltic magma or those left after melt extraction (*e.g.*, Johnson *et al.*, 1990) and were not at all consistent with the hypotheses of the origin of the layered massif. Our interpretation was that these inflected REE patterns represent intermediate stages of reaction between percolating light REE enriched melt and originally light REE depleted clinopyroxene (Takazawa *et al.*, 1992), based on the chromatographic melt-rock reaction model conceived by Navon and Stolper (1987) and developed by Bodinier and his colleagues (Bodinier *et al.*, 1990; Vasseur *et al.*, 1991). The gist of the theory is based on how the degrees to which clinopyroxene exchanges REE with

percolating melt depend on the partition coefficients of REE between clinopyroxene and melt. In this process, light REE with highly incompatible behaviour will approach equilibrium partitioning more readily than heavy REE, and partly reacted light REE parts and unreacted heavy REE enriched original patterns will produce inflected patterns as shown in the figure. Furthermore, the degrees to which original REE patterns are modified also depend on distance from the melt as the reaction front progresses into the host rock. In this sense, the discovery of inflected REE patterns and the interpretation presented above for the Horoman massif clinopyroxene provided evidence for melt migration and reaction through the upper mantle and presented opportunities for examining whether peridotite samples from other occurrences were also subject to reactions with percolating melt. In other words, here was a way to explore geochemical processes of interaction between Components A and B (Frey and Green, 1974), and thus processes of lithospheric enrichment.

For instance, a study of peridotite xenoliths from Hawaii by Sen *et al.* (1993) showed that clinopyroxenes from lherzolitic xenoliths from the Pali, Kaau, and Kalihi vents possess very large ranges of variations in REE abundance patterns from light REE depleted to light REE enriched with inflected and spoon-shaped patterns between. Lanthanum concentrations in these clinopyroxenes varied by a factor of 100 for Pali and 50 for Kaau. Such large variations are interpreted to represent various stages of melt-rock reaction similar in general to the Horoman case mentioned above.

In some samples, clinopyroxene grains were zoned with respect to REE, with cores representing earlier stages of reaction relative to rims, indicating that the progress of the reaction front is observed in individual grains. These clinopyroxenes testify to a lithospheric enrichment process. In the Horoman case, the simple model of chromatographic element exchange without modal changes was used. Is the same model applicable to the zoned clinopyroxenes described by Sen *et al.* (1993)? If there were no modal change during the process, it would mean that the grain surface exchanged REE with melt/fluid at some stage of the chromatography and REE then diffused toward the grain core. Since heavy REE (Yb) diffuses faster than light REE (La), light REE enrichment would reach the core later than heavy REE. In fact, using diffusivities given by van Orman *et al.* (2001), Yb would require 3.2×10^5 years to penetrate diffusively a distance of 100 μm (at 1050 °C), whereas it would take 9.5 Ma for La to penetrate the same distance. Because of this difference in diffusivities, the signature of the mineral-melt exchange at the surface, such as an inflected REE pattern, would be significantly subdued during diffusion. This suggests that direct applications of chromatographic melt-rock reaction models to zoned clinopyroxenes could be complicated. For instance, as far as penetration into the lithospheric substrate, more incompatible La is faster than less incompatible Yb, and enrichment in La on a grain surface could be achieved faster than for Yb. But, subsequent diffusive penetration into the grain would be substantially slower for La than Yb as shown above. Thus, zoned clinopyroxenes with inflected REE patterns might be explained more easily by postulating crystal growth during melt-rock reaction,

rather than reaction under constant modal mineralogy. An important consequence of this interpretation is that melt-rock reaction resulted in an increase in the mass of clinopyroxene in the peridotite substrate.

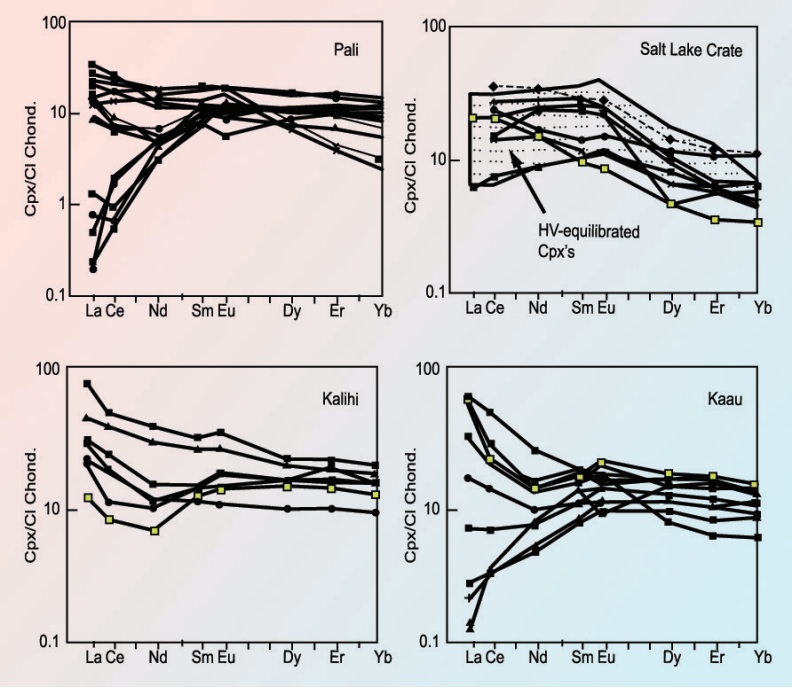

Figure 4.10 Chondrite normalised REE patterns of clinopyroxenes from spinel lherzolite xenoliths from Pali, Kalihi, Salt Lake Crater, and Kaau, Oahu, Hawaii. Note the large LREE variations for Pali and Kaau, ranging from LREE depleted patterns typical for oceanic lithosphere (Johnson *et al.*, 1990) to variably LREE enriched and spoon-shaped patterns, indicating chromatographic reactions between lithospheric peridotites and melt/fluid. Modified from Sen *et al.* (1993).

Another important but difficult point is the identity of "melt" composition. In the Hawaiian case, a magma composition of the Honolulu Volcanics, which hosts the xenoliths, was assumed as a reactant. Not only are trace element variations compatible with this view, but so is also the time frame of reaction inferred from zoned crystals. It is not clear, however, whether the host magma (the magma that carries xenoliths to the surface) is always the reactant directly associated with the observed geochemical changes in xenoliths.

Another example of enrichment of the oceanic lithosphere was described by a study conducted by Hauri *et al.* (1993) on peridotite xenoliths from Savaii and Tubuai islands. These xenoliths are harzburgites of the oceanic lithosphere with

secondary patches of clinopyroxene-spinel ± apatite ± glass, formed by interaction with carbonatitic melt. Trace element abundance patterns of clinopyroxenes are characterised by strong light REE enrichment and negative anomalies for high-filed strength elements, such as Ti and Zr as shown in Figures 4.11 and 4.12.

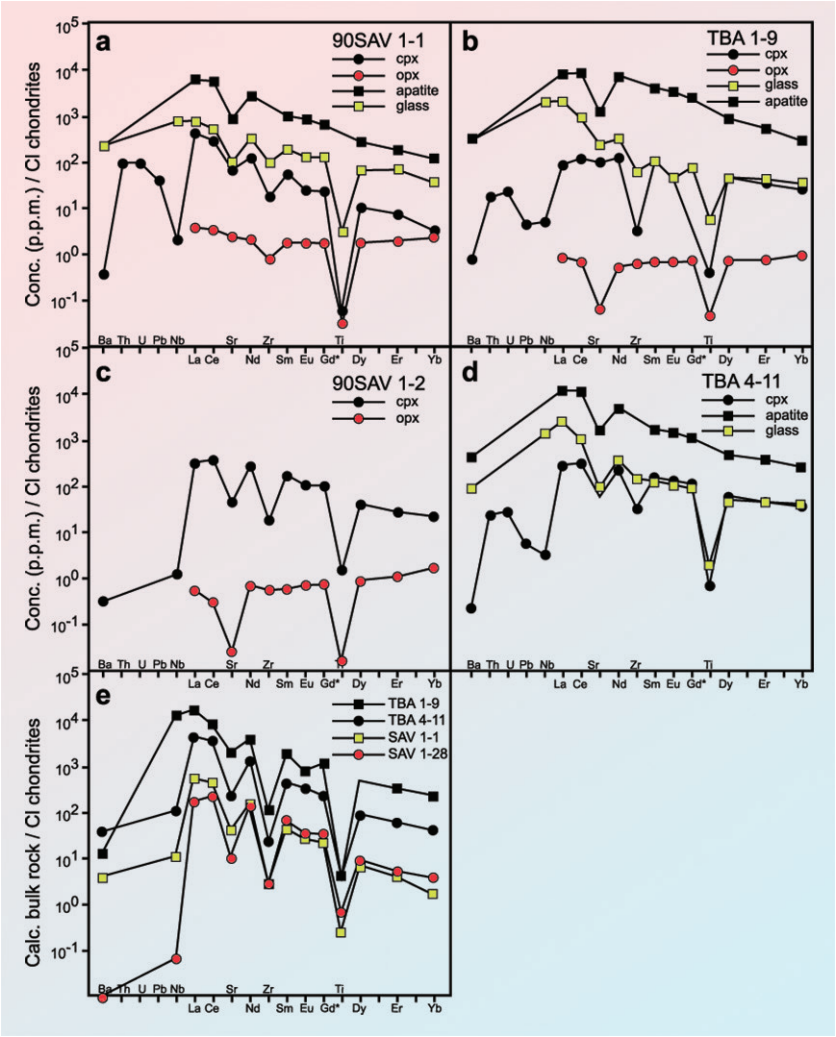

Figure 4.11 Chondrite normalised abundance patterns of xenolith minerals and glasses from Savaii and Tubuai (Hauri *et al.*, 1993). Whole rock pattern (calculated) is shown in panel *e*. Note characteristic depletions in Ti, Zr, and Nb relative to neighbouring REE. Modified from Hauri *et al.* (1993).

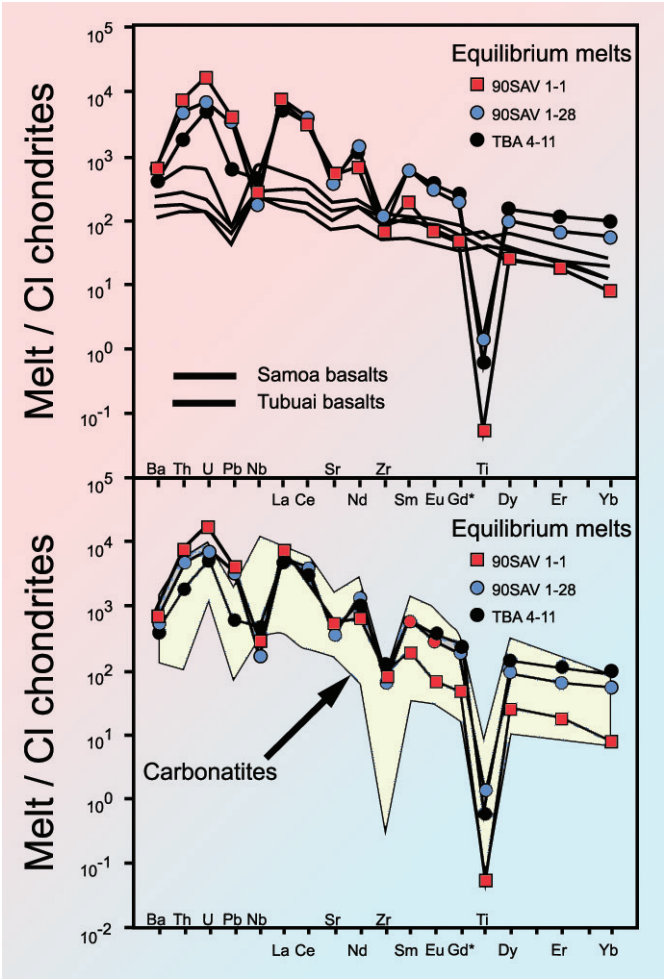

Figure 4.12 **Top:** trace element patterns calculated for putative melts in equilibrium with clinopyroxenes from xenoliths. **Bottom:** comparison with carbonatites. Modified from Hauri *et al.* (1993).

As shown here, melts in equilibrium with clinopyroxenes possess trace element characteristics of carbonatites, including light REE enrichment and depletion of Ti, Zr, and Nb relative to neighbouring REE. This indicates the origin of clinopyroxenes during carbonatite-lithosphere interaction. A remarkable conclusion of this study was that a carbonatitic magma was clearly implicated as a reactant in lithospheric enrichment processes in the oceanic region. Another

important conclusion of this work is the isotopic characterisation of the carbonatitic component as recycled crust (HIMU), indicating that deeply recycled crust could be brought back up to the surface *via* mantle plumes. Ion probe analysis of clinopyroxenes also revealed that there were many more cases of carbonatitic metasomatism as a lithospheric enrichment mechanism, including Schiano *et al.* (1994) on the Kerguelen xenoliths, Blusztajn and Shimizu (1994) on the Central European Volcanic Province, and Roden and Shimizu (1993) on the Basin and Range and Colorado Plateau regions of the continental US. Ionov *et al.* (1994) likewise reported lithospheric enrichment from carbonatitic melt of xenoliths from Mongolia, in which metasomatism-induced melting of the peridotitic substrate was observed.

Throughout the studies of trace element geochemistry of mantle rocks over the years, it has become clear that any mantle rocks we can put our hands on have complex geochemical histories; not only the initial melt extraction (depletion) phase, but also the ensuing interactions with melt with addition of mineral phase(s), trace element and isotope exchanges with percolating melt with and without modal modification, and precipitation of hydrous minerals. All those processes are historically known as metasomatism and it can safely be assumed that the mantle rocks available on Earth's surface are largely metasomatised. By studying mantle rocks in whole rock units, it was noted that major and trace elements are decoupled, *i.e.* enrichment of trace elements was often observed in rocks depleted in major elements. This observation prompted Fred Frey and colleagues to suggest Components A and B. Ion probe-based studies have shown that important trace element carriers (CPX and GAR) display specific enrichment signatures, indicating that trace element enrichment has occurred in mineralogical units as opposed to residing on mineral surfaces or in submicroscopic inclusions. Of course, there have been reports of occurrences of trace elements in these domains, but it is essential to recognise that major mineralogical units do show evidence of metasomatism. Inflected REE patterns observed in peridotitic CPX from alpine massifs as well as xenoliths are not compatible with direct precipitation from basaltic melts but can be explained as intermediate stages (still incomplete) of chromatographic exchange of REE between CPX and percolating melt. The xenolith CPX data summarised above show that continental and oceanic lithosphere have been widely subjected to enrichment processes, and in some cases, carbonatitic melt is strongly implicated as the enriching agent. Mineral zoning with respect to trace elements is not uncommon, indicating that the enrichment processes occurred recently, as recently as during the transport of the xenoliths by their host magma. Even abyssal peridotites, which have always been considered to be simple melt extraction residues, have been subject to recent as well as ancient melt-rock reactions in various forms as discussed in the MORB chapter (Section 5).

5. WHOI: SIMS-BASED APPROACHES TO MID-OCEAN RIDGE MAGMA GENESIS

Until I moved to Woods Hole Oceanographic Institution in 1988, I had the impression that mid-ocean ridge basalts (MORB) were the best-understood basalts on Earth. Their Sr isotopic compositions were uniform around $^{87}Sr/^{86}Sr = 0.7025$, indicating their derivation from a well-stirred mantle source. Their Nd isotopic compositions were radiogenic, indicating that their source(s) had been light REE depleted for a long period of time. Their crystallisation sequence of olivine-plagioclase-clinopyroxene was well recognised (*e.g.*, Bender *et al.*, 1978; Grove and Bryan, 1983) and their major element characteristics indicated fairly low pressure (10 – 16 kb) multi-phase saturation (*e.g.*, Fujii and Bougault, 1983; Elthon and Scarfe, 1984; Fujii and Scarfe, 1985; among others). Trace element abundances were also well characterised as typical light REE depletion and low K and Rb with high K/Rb ratios (*e.g.*, Gast, 1968; Schilling *et al.*, 1983). Klein and Langmuir (1987) showed that basalts from individual ridge segments on the global ridge system underwent fractional crystallisation processes, maintaining chemical signatures indicative of the depth of melt separation from the mantle, as also reflected by crustal thickness. This conclusion was based on the assumption that the mantle source was homogeneous throughout the ridge system. Hofmann (1988) explicitly connected the MORB mantle source to the residues left after continental crust extraction based on the complementarity of trace element abundance patterns between the crust and the depleted mantle, with implications for the chemical evolution of the mantle.

I had stayed away from MORB so far partly because sample distribution seemed complicated and somewhat political, almost as if friendship with someone with samples was a prerequisite to be able to work on them. This impression turned out to be completely wrong. As soon as I moved to Woods Hole, I discovered that many fabulous rocks were just sleeping in the Institution's sample storage space with very easy access. Many of these samples were MORB dredged from various parts of the global mid-ocean ridge systems, some by Alvin dives. I was particularly interested in primitive MORB glasses with Mg# ~70, because they represented melts closest to their sources; if they had undergone only olivine fractionation, much of the trace element characteristics of the sources should be maintained so that I could test the validity of the assumption that MORB source mantle was chemically homogenous. My strategy was to analyse their trace element abundances with the IMS 3f ion probe that I had moved to WHOI from MIT. Bill Melson at the Smithsonian Institution kindly lent me the electron probe mounts that he had used to make a huge catalogue of major elements in MORB (Melson *et al.*, 1977, 2002). While their REE patterns were what I expected them to be (LREE depleted), I found some systematic differences in trace element ratios in primitive MORB relative to most MORB glasses. For instance, Ti/Zr of primitive MORB glasses were systematically higher (>110) than "garden variety" MORB (93, average NMORB; Hofmann, 1988). This was a moderate surprise to

me because it indicated that primitive MORB were not parental to the majority of MORB *via* fractional crystallisation of olivine and plagioclase due to their inability of fractionating Ti from Zr. Did this mean that melts delivered to mid-ocean ridges were chemically diverse? It seemed contrary to the general view that MORB source mantle is well stirred and uniform in composition and hence that melts originating from this uniform source should be uniform. Assuming that primitive MORB are derived from the same source as co-existing ordinary MORB, one plausible explanation was that primitive basalts represented melt fractions of advanced-stage fractional melting processes. The mantle-basalt partition coefficient for Zr is slightly lower than that for Ti, implying that the Ti/Zr ratio in melts should increase with greater degrees of fractional melting. If this were the case, the apparent chemical diversity of melts reflected different stages of the melting process. Thus, I thought that trace element characterisation of primitive MORB glasses with the ion microprobe had sufficient merit to be pursued further and justified the effort to obtain primitive MORB glasses from the WHOI storage. This led me to an important encounter with sample ALV519-4-1 from the FAMOUS area of the Mid-Atlantic Ridge. I will return to this sample later in the context of the issue of chemical diversity of melts beneath mid-ocean ridges. In the same period of time, I noticed that olivine phenocrysts with high forsterite contents contained large fresh non-devitrified melt inclusions and thought these might present another avenue for better understanding primitive melts. This approach developed with some stunning discoveries which I will also discuss later in this section.

Encounter with Dan McKenzie

McKenzie was completely off my radar because I was told by some, including Claude Allègre, that he was a dangerous person who could kill you outright. Early 2000s, I believe, Dan told me that he was in the US for consulting for Schlumberger in New York and wanted to talk to me. I had no idea what he wanted to talk to me about. It turned out that he was planning to send his student to my lab to do melt inclusion analyses and wanted to understand ion microprobe analysis of geological samples. Clearly, he was checking me out. So, I told him the history of geochemical applications of SIMS techniques from my own experience. He seemed to be impressed by my struggles with secondary ion energy distribution and invention of the energy filtering approach. Thus our collaboration started. Lucy Slater was the first student and John Maclennan was next, both working on melt inclusions from NE Iceland. As I came to know Dan better, my respect for him as a scientist, as well as a person, grew. It was a surprise when I discovered that he was two years younger than me… his impact on the field was so significant that I automatically thought he was at least a few years older than me. Lately, I like him even better, because he seems to advocate *"the importance of not just understanding the geochemical arguments involved, but also of thinking like a geochemist!"* (McKenzie, 2018).

Applications of ion microprobe techniques to mid-ocean ridge magma genesis had actually started at MIT before I moved to Woods Hole, when Kevin Johnson, the MIT-WHOI Joint Program student, under the supervision of Henry Dick and myself, came to the 3f lab to document trace element characteristics of

residual clinopyroxenes in abyssal peridotites for his Ph.D. thesis. His samples were derived from six cruises and covered a wide swath from the America-Antarctic Ridge (Vulcan and Bullard Fracture Zones) to the Southwest Indian Ridge (Atlantis II FZ), representing ridges with, respectively, slow and ultraslow spreading rates. By that time, in 1986, the 3f analytical protocols for Ti, Sc, Cr, V, Sr, Zr, and REE (Ce, Nd, Sm, Eu, Dy, Er, Yb) were well established with a number of well documented standard clinopyroxenes, and the system was ready to tackle the difficult analyses that those abyssal clinopyroxenes required (Johnson *et al.*, 1990). Kevin's results were astounding. Chondrite normalised REE patterns were extremely depleted in light REE (Ce) relative to heavy REE (Yb) with $(Ce/Yb)_N \sim 0.01$ or less as shown in Figure 5.1.

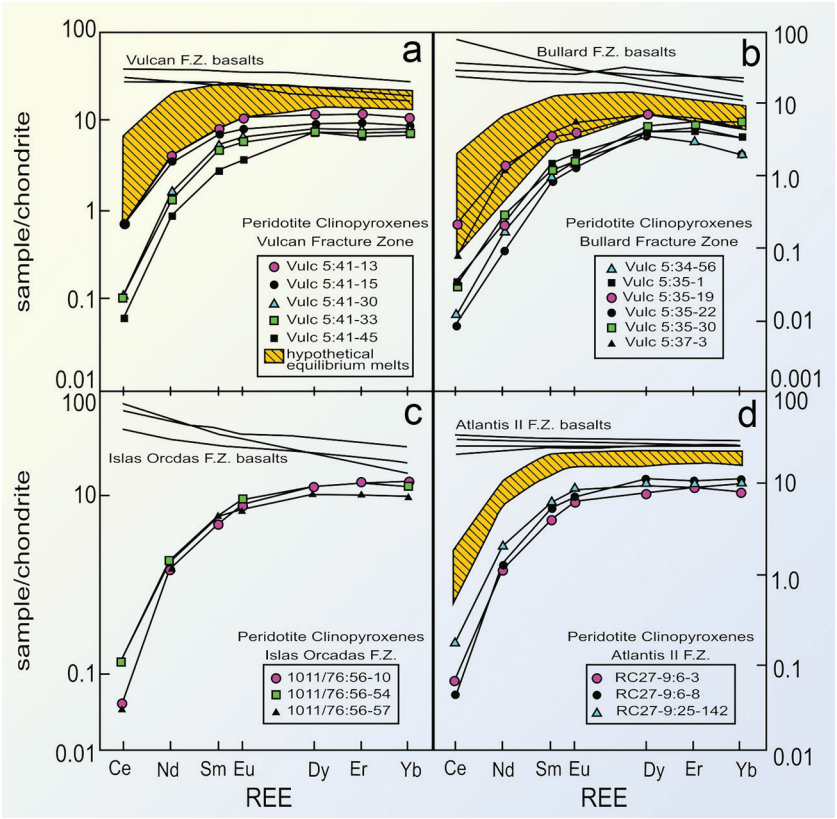

Figure 5.1 Chondrite normalised rare earth element abundance patterns determined in clinopyroxenes from abyssal peridotites. Note extreme depletion in light REE relative to heavy REE. Shaded areas represent liquid compositions directly in equilibrium with clinopyroxenes. Modified from Johnson *et al.* (1990).

Two things were immediately evident: (1) the clinopyroxenes were not in direct equilibrium with the basalts geologically associated with them, and (2) extreme depletion in light REE could not be explained by batch melting. These observations created a conundrum; why should residual clinopyroxenes not be in equilibrium with their geologically associated mid-ocean ridge basalts? The resolution we came to was a little extreme at first (Henry insisted he had known the answer since his own Ph.D. thesis more than a decade earlier); melting beneath mid-ocean ridges operates as fractional melting in which small degree melt fractions are efficiently separated from the residue as the system continues to move up. Melt fractions travel through the mantle and accumulate until they erupt as mid-ocean ridge basalts representing those accumulated melts, which hence should resemble melt produced by batch melting. Residual clinopyroxenes in abyssal peridotites then represent instantaneous residues, and are in equilibrium only with instantaneous melt fractions, not the accumulated melt as a whole. The geochemical characteristics observed for REE were also evident for other elements such as Ti and Zr.

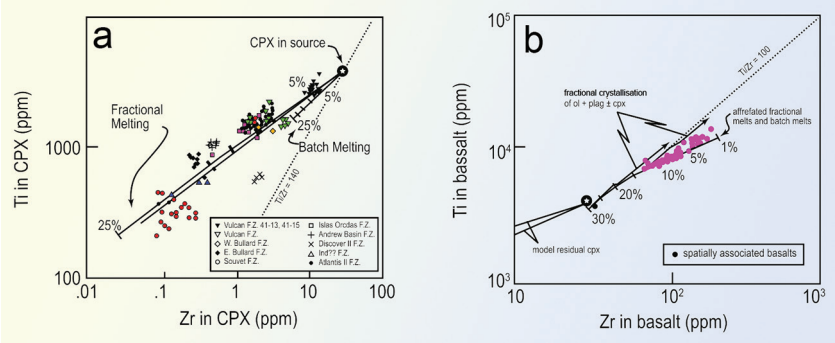

Figure 5.2 **(a)** Ti and Zr contents in CPX and **(b)** spatially associated basalts. Modified from Johnson *et al.* (1990).

Our melting models indeed indicated that these trace element characteristics in residual clinopyroxenes could only be produced through fractional melting, not batch melting (Fig. 5.3). It is important to note that fractionation of two geochemically similar elements with slightly different mantle-basalt partition coefficients (Ti and Zr, and Ce and Sm, for instance) becomes compounded in fractional melting, as exemplified by increasing Ti/Zr ratios and decreasing Ce/Yb ratios in residual clinopyroxenes and hence in melt fractions at advanced stages of the process (Fig. 5.3). This held a particular importance to me since it provided evidence in support of the argument presented above about higher Ti/Zr ratios (110) in primitive than in ordinary MORB glasses (93). It was also suggested that there was a possibility that some melt fractions could erupt without complete aggregation, thereby contributing to the observed diversity of MORB chemistry.

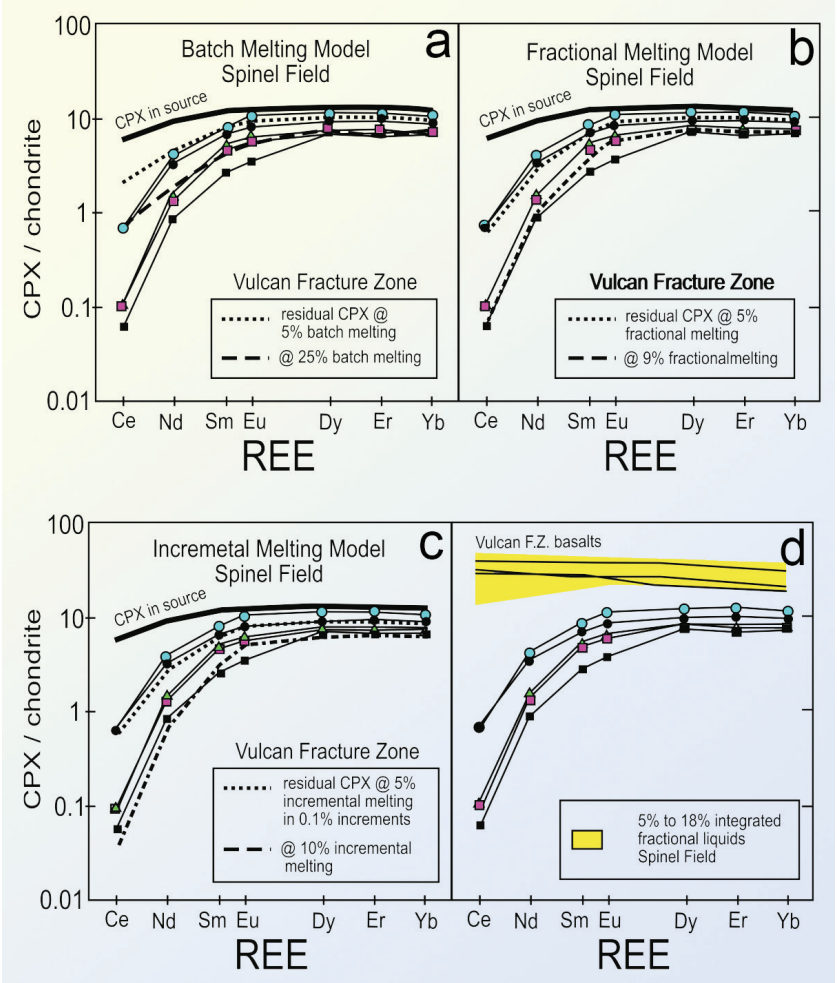

Figure 5.3 REE patterns observed for residual clinopyroxenes from abyssal peridotites from the Vulcan Fracture Zone compared with those created by melting models. Note that batch melting does not produce sufficient light REE depletion even after 25 % melting, whereas incremental melting and fractional melting produce REE patterns that match the data. Modified from Johnson *et al.* (1990).

This was particularly exciting because we were establishing strong geochemical evidence for fractional melting operating beneath ocean ridges through ion microprobe trace element analysis of residual clinopyroxenes in abyssal peridotites when most in the geochemistry community thought that

mantle melting occurred in the form of batch melting. Efficient melt extraction from the mantle was also supported by two other independent approaches. McKenzie (1984, 1985) predicted that compaction of partially molten mantle would squeeze out melt even when the degree of melting was very small. The Kohlstedt group (*e.g.*, Riley *et al.*, 1990) was showing that the dihedral angle of the olivine-basalt system is much smaller than 60°, indicating that the equilibrium melt fraction of olivine-rich mantle should be very small. Kohlstedt (1993) indicates it is 3 % (see his Fig. 2).

Thus, together with the theoretical and experimental studies just mentioned, our data contributed to the historical convergence of views that melt extraction beneath mid-ocean ridges is extremely efficient, resembling fractional melting. Kevin's work was also an important benchmark for SIMS-based geochemistry, because heavy alteration of abyssal peridotites required an *in situ* technique with sufficiently small beam size to analyse fresh remnants of original clinopyroxene grains.

Because I recognised the possibility of gaining evidence for diversity of melt compositions through fractional melting followed by incomplete aggregation, Kevin's work encouraged me greatly to pursue primitive basalt glasses and olivine-hosted melt inclusions as additional samples of melts of primitive compositions. While I was accumulating data, something historic happened. Alex Sobolev (Vernadsky Institute, Moscow) was visiting Henry Dick and walked into my office one day. It was fall 1991. We immediately started talking about primitive MORB glasses and olivine-hosted melt inclusions. We seemed to agree on major points on how magmas were generated beneath mid-ocean ridges. Then, Alex produced a tiny epoxy mount, saying that it was a special melt inclusion specimen that we should study. This sample was found in a lava dredged from the Mid-Atlantic Ridge at 9° N, between the Doldrum and Vema fracture zones by the *R/V Academician Vernadsky* (Sobolev *et al.*, 1989). By "special" he meant that incompatible elements in this inclusion should be very depleted as evidenced by its low TiO_2. There was a possibility that this melt inclusion represented melt at a very advanced stage of fractional melting, the likes of which nobody had ever seen before. So I went to work. When you are close to nature's secrets, something happens to prevent you from reaching it easily, and that was what happened to me then. I put the gold-coated mount in the machine and put it in the field of view of the microscope…the entire field of view was dark and I could not see anything. It took me more than ten minutes to realise what was happening. The mount was slightly bent so that the light reflected from the surface was directed away from the optics of the microscope! This had happened because the sample was held vertical and the light shoots up with a 45° angle and the objective lens is another 45° to the sample surface, causing the reflected light from the bent surface to go completely off the optical axis. I took the mount out of the machine and re-oriented it in the sample holder. It took me several re-orientation manoeuvres before proper alignment was finally obtained and I started to see the sample surface with the microscope. Several hours had passed already and the real difficulties were just beginning. The olivine grain itself and the melt inclusion were well

polished, but the surrounding epoxy surface was very irregular…I guessed that the grain had been polished in isolation and then embedded in the epoxy. In this type of situation, particularly with one special inclusion to be analysed, knowing the beam location is crucial, but the irregular epoxy surface made it very difficult to see where the beam was. Several more hours passed before I had located the beam and I finally brought it to the host olivine to adjust focus and shape. The inclusion was large but there was a grain of orthopyroxene trapped inside it, and there was just enough space to place a small spot (5 – 8μm) for trace elements and a larger spot (~20 μm) for REE (see Fig. 5.4).

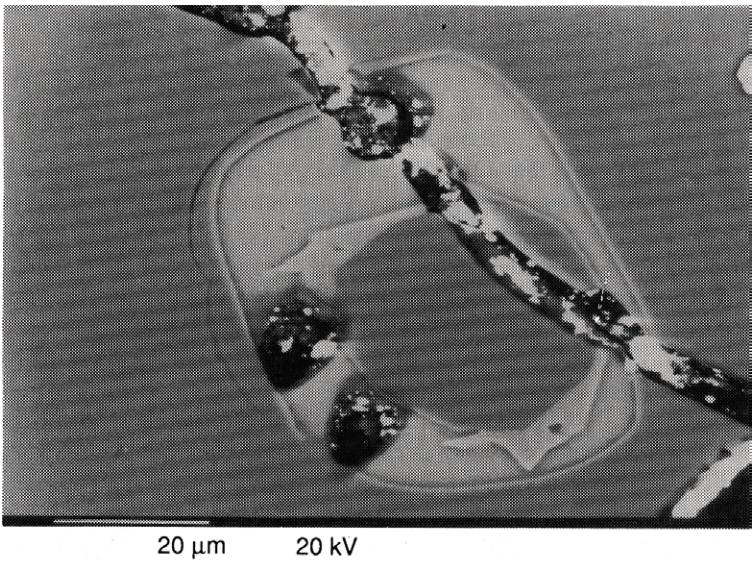

Figure 5.4 Photomicrograph of the UDM inclusion in olivine. An orthopyroxene crystal is co-included in this melt inclusion. Scale bar is 20 micrometres. A fracture through the specimen has been enhanced by repeated polishing during the course of the study. Quench CPX occurs as irregular crystals attached to the surface of OPX. Two ion probe pits are visible on the lower left part of the glass inclusion. Bright speckles are remains of gold coating for ion probe analysis. From Sobolev and Shimizu (1993).

After struggling for more than twelve hours, numbers came out on the printer and I got busy converting the intensity data to concentrations. I had never seen a basalt glass with Sr as low as 1.3 ppm and Ti of 1722 ppm (0.29 wt % TiO_2). In contrast, Y of 10.2 ppm was low, but not very unusual. From that moment I knew it was an extremely light REE depleted composition, just as Alex had forewarned me it would be, and it was clear that we had just discovered a melt composition representing an advanced stage of fractional melting. We named this composition UDM (ultra-depleted melt).

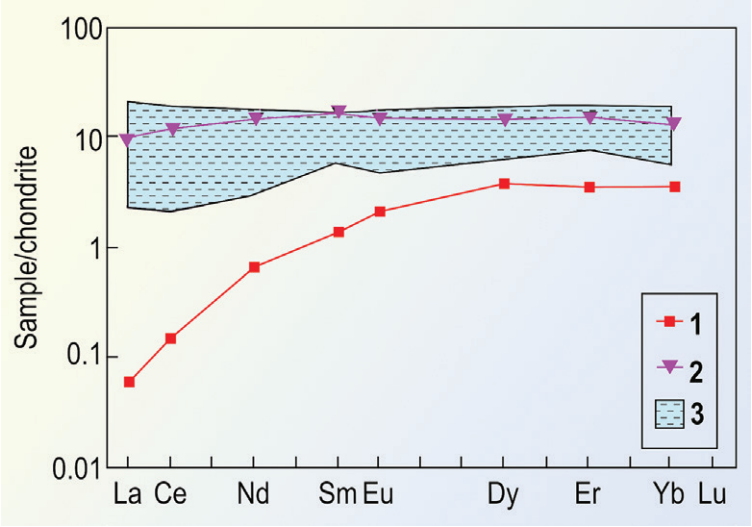

Figure 5.5 REE in the UDM (1), matrix glass (2), and primitive MORB glasses (3). Modified from Sobolev and Shimizu (1993).

While Kevin's results (Johnson *et al.*, 1990) presented evidence for fractional melting from the point of view of the residual solid, the UDM melt inclusion (Sobolev and Shimizu, 1993) was evidence for the same process from the point of view of the liquid. Combined with theoretical (McKenzie, 1984; 1985) and experimental (*e.g.*, Riley *et al.*, 1990) results, the trace element data obtained by the 3f instrument contributed to the establishment of the view that fractional (or near-fractional) melting is operating beneath mid-ocean ridges. After this discovery, Alex analysed more than one hundred melt inclusions from the same basalt, showing a near-continuous spectrum of depleted melt compositions with UDM being the most extreme depleted composition (Fig. 5.6). This spectrum, compared with the trace element concentrations of the matrix glass, was important in demonstrating the existence of melts of diverse chemistry within a single melting/melt extraction system as well as the importance of mixing of these melts in the formation of the host lava (Sobolev, 1996).

I was very encouraged by these results and a new view of mid-ocean ridge magma generation was growing firm in my mind. Passive upwelling of the mantle produces small degree melts, which are efficiently separated from the residue. Chemical changes in melts and residues follow near-fractional melting trends. Melt fractions separated from solid phases travel upwards faster than the residue and continue to react with shallower parts of the mantle column and mix with one another until eruption of the lava on the seafloor. The discovery of the UDM melt inclusion (Sobolev and Shimizu, 1993) provided support for my conviction that

melt inclusions represent melts in existence at various stages of melting and melt extraction, reflecting how the process works. The UDM discovery also encouraged me to continue geochemical studies of primitive melts *via* melt inclusions in high forsterite (Fo) hosts.

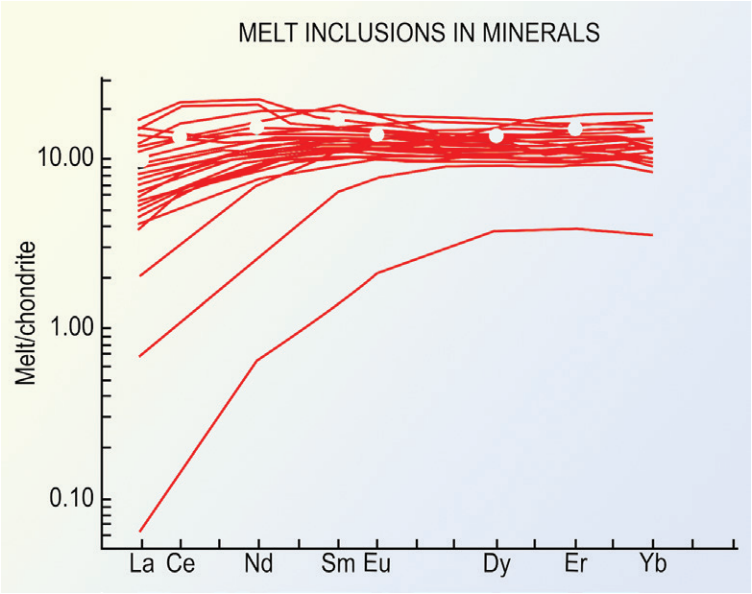

Figure 5.6 Variations of REE in melt inclusions in the UDM specimen. Matrix glass is shown with open circles. Modified from Sobolev (1996).

Sobolev (1996) also showed that diversity of trace element compositions, especially with respect to trace element ratios, among melt inclusions was greatest for those included in forsterite-rich olivines (Fo_{90}), and that the spectrum was reduced with decreasing host olivine forsterite content (see Fig. 5.7). He interpreted this as melt mixing and fractional crystallisation in a magma body tending to homogenise melt inclusion chemistry. This observation raised an important question: Is the observed chemical diversity derived wholly from the melting and melt extraction process acting on a single source, or does it also reflect chemical diversity of the sources involved?

In order to answer this question, I knew that isotopic compositions of individual melt inclusions had to be determined, but there were insurmountable technical challenges ahead. Could ion probe techniques prove good enough for the analysis of radiogenic isotopes? I knew that Sr and Nd isotopes clearly were outside the capability of ion microprobe precision. But what about Pb isotopes?

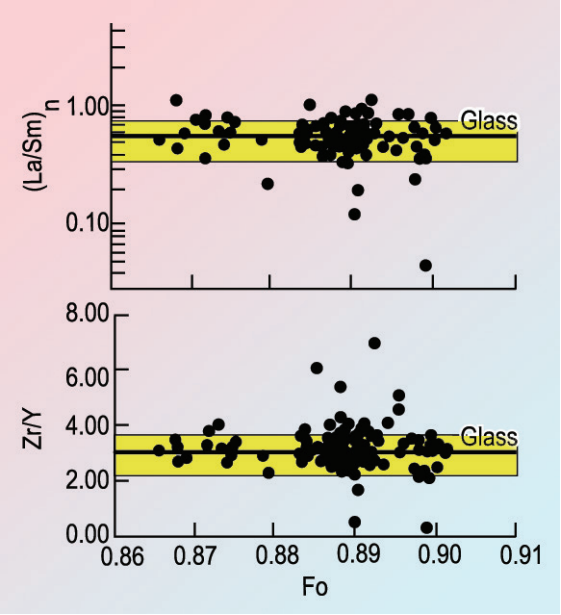

Figure 5.7 Trace element ratios of melt inclusions *vs.* forsterite content of host olivine. Note that variations are greatest for host olivine with $Fo_{\sim 90}$. Modified from Sobolev (1996).

A breakthrough occurred when, with the newly installed IMS 1270 at WHOI, we were practicing Pb isotope analysis on a zircon from Mud Tank (Northern Territory, Australia) with 1 ppm ^{206}Pb. It was 1997. I noticed that we were getting a fair number of ion counts and thought "well, if we get this much intensity for 1 ppm, we could analyse Pb isotopes in basalt glasses!". This was an exciting revelation and I got completely sidetracked from zircon U-Pb dating and instead concentrated on developing analytical protocols for Pb isotopes in basalt glasses. This was a fatal political move on my part because a rumour started to circulate in the community and at NSF that the WHOI ion probe facility was against zircon analysis.

Practising initially on a basalt glass from a seamount near Tahiti (containing 25 ppm Pb, given to me by Francis Albarède), and later on a basalt glass from Loihi Seamount with 3 ppm Pb (Garcia *et al.*, 1995), we found that the optimum mass resolution for analysis of Pb isotopes in basalt glasses with a primary O^- beam was around 3700, not 5500 as required for zircon analysis. This was because in zircon analysis $HfSi^+$ had to be separated from Pb^+ mass spectrometrically with a mass resolution of around 5500. The lower required mass resolution made the Pb^+ intensity higher, and we were ready to tackle this completely new area of

research: *in situ* analysis of melt inclusions for Pb isotope compositions (Layne and Shimizu, 1997). The ion probe values for $^{207}Pb/^{206}Pb$ and $^{208}Pb/^{206}Pb$ agreed with TIMS values within <0.1 % 2 s.e. with an instrumental mass fractionation <0.15 %/amu (Saal *et al*., 1998).

Alberto Saal was one of the first to jump on the bandwagon, looking at olivine-hosted melt inclusions from Mangaia (Saal *et al*., 1998). Alberto's results were sensational in showing extremely large isotopic variation among olivine-hosted melt inclusions in HIMU basalts, covering large portions of the spectrum of natural variations of Pb isotopes in basalts. The results provided strong evidence for the notion that the diversity of melt compositions observed in melt inclusions was partly due to diversity of the sources and encouraged me greatly to pursue my goal using *in situ* Pb isotope data. Unfortunately for me, the average Pb concentration in MORB is 0.5 ppm (for instance, see Hofmann, 1988 for NMORB average), too low to be amenable to analysis by ion probe. But, there was hope for EMORB and Alex Sobolev happened to visit me again with another epoxy mount, this time of melt inclusions in sample 30/2 from 14° N on the Mid-Atlantic Ridge, the so-called Popping Rock segment. It was known that this ridge segment was geochemically unusual with dominant occurrence of EMORB, and an incipient plume was suspected (Dosso *et al*., 1991). In fact, these authors showed that $^{207}Pb/^{206}Pb$ in basalt glasses varied smoothly from typical MORB at both ends of the segment to more enriched compositions as a function of latitude toward the centre of the segment. My thought was that if melt inclusions represented the diversity of sources, we should see a large isotopic range covering enriched as well as depleted components. Figure 5.8 shows our results.

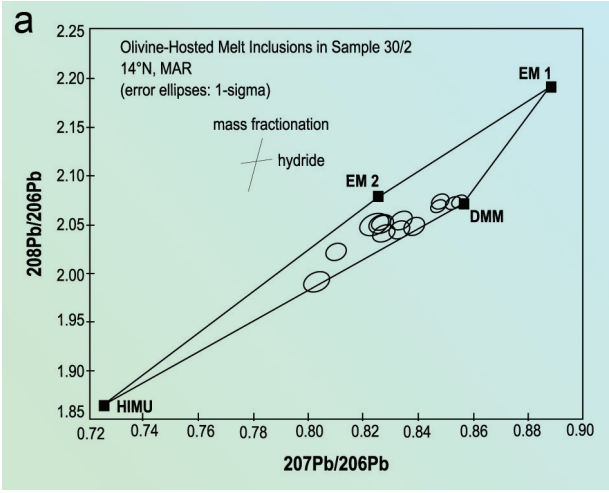

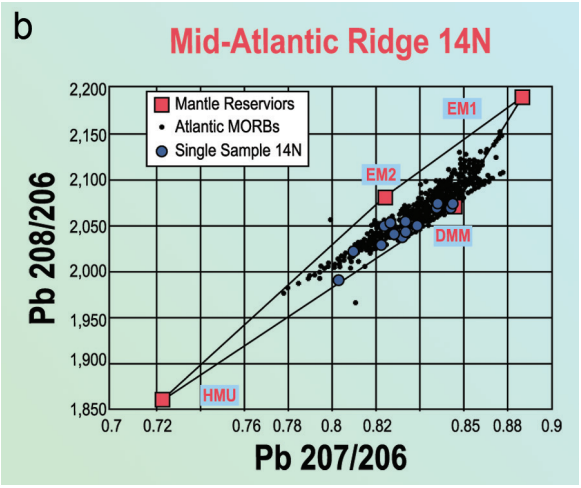

Figure 5.8 Pb isotope variations among melt inclusions in sample 30/2 from the MAR at 14 °N. **(a)** $^{208}Pb/^{206}Pb$ *vs.* $^{207}Pb/^{206}Pb$ plotted in the mantle Pb trapezium, defined by four mantle end member components (DMM, HIMU, EM I, and EM II). **(b)** Comparison between 30/2 melt inclusions and Atlantic MORB. Note that the observed variations in 30/2 cover a large portion of the spectrum for Atlantic MORB. From Shimizu (unpublished).

The data is shown in the mantle Pb trapezium, a $^{208}Pb/^{206}Pb$ *vs.* $^{207}Pb/^{206}Pb$ plot within the framework of the four mantle end member components of Hart and Zindler (1989). The trapezium had to be used because the ^{204}Pb-based isotope ratios were significantly compromised by large errors on the ^{204} Pb count rate. The end member components were defined by extreme isotopic compositions in oceanic basalts, and all oceanic Pb is confined within the trapezium. It was shocking that melt inclusions taken from one lava covered more than half of the entire spectrum of Pb isotopes for Mid-Atlantic Ridge MORB (see Fig. 5.8b)! I had seen this before, however, as the isotopic variations described by Saal *et al.* (1998) were even larger than this. The results confirmed that the sources of Mid-Atlantic Ridge basalts were isotopically diverse with the diversity defining a binary mixing relationship involving the DMM and HIMU components, *i.e.* between depleted mantle and recycled oceanic crust. I thought it was important to recognise that the presence of the DMM component in this melt inclusion suite seemed to argue against the hypothesis of an incipient underlying plume. Dosso *et al.* (1991) showed that MORB glasses from this segment possessed enriched signatures (regional anomalies) and displayed smooth transitions to more normal MORB both to the north and the south of this segment. A comparison of Dosso's data and the melt inclusion data in terms of $^{207}Pb/^{206}Pb$ is shown in Figure 5.9. If

large isotopic variations found in a single lava were a general feature, glass data alone could be misleading with respect to the length scale of mantle chemical heterogeneities.

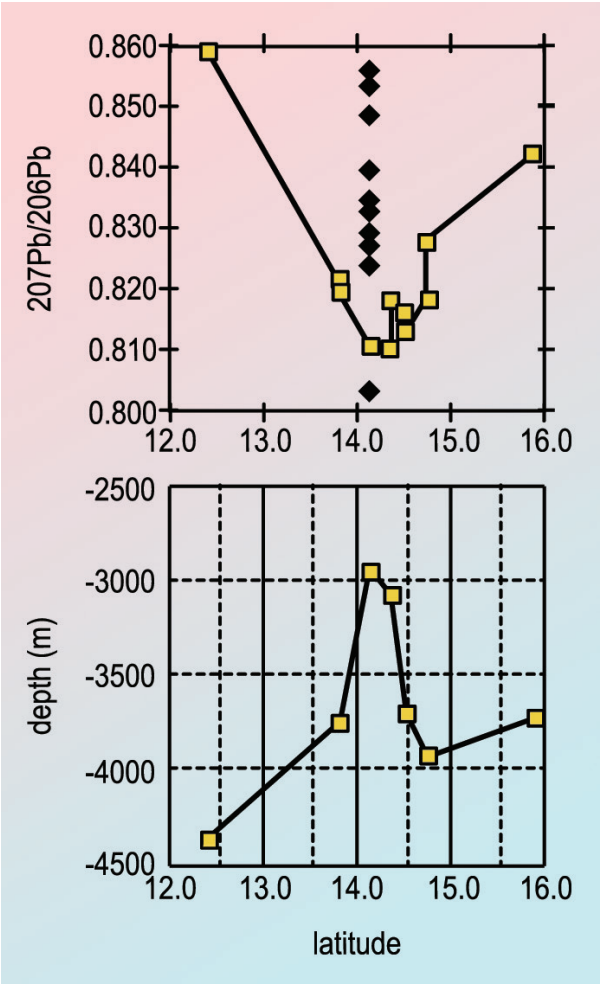

Figure 5.9 **Upper panel:** $^{207}Pb/^{206}Pb$ as a function of latitude along the MAR at 14 °N for MORB glasses (data from Dosso *et al.*, 1991) with melt inclusion data from Shimizu (unpublished). Note that the melt inclusions cover a range that encompasses the glass data and DMM (0.857), suggesting that DMM-derived melt exists even in this geochemically anomalous segment. **Lower panel**: data from Dosso *et al.* (1991).

The manuscript based on this work, discussing only the Pb isotopic variations, was rejected by *Science* on the grounds that we did not discuss the geochemical implications of trace element abundance variations with respect to the Pb isotope variations. I was greatly dismayed by this rejection, but had to be satisfied with the discovery that indeed mantle heterogeneities occur beneath mid-ocean ridges on much smaller spatial scales than generally thought. Combined with the trace element work mentioned above, the Pb isotope data on melt inclusions showed that melt inclusions carry fundamental information about source heterogeneities and processes of melting and melt extraction beneath mid-ocean ridges. These results also underlined the power of *in situ* analytical techniques. The simple realisations that a single lava can be comprised of many individual melts, and that melt inclusions provide us with the opportunity to see the immense complexity of nature, was extremely instructive and enjoyable to me. The subject of large local Pb isotope variability in MORB was revisited some years later through ion probe analysis of sulphides in abyssal peridotites as will be described later in this chapter. The ion probe-based discovery of large variations of Pb isotope compositions among melt inclusions (*e.g.*, Saal *et al.*, 1998) was later questioned on the grounds of potential surface contamination, but recent Pb isotope results by Koornneef *et al.* (2018) on individual melt inclusions using an amplifier with a 1×10^{13} Ω resistor clearly show that Pb isotopes show greater variability than Sr and Nd isotopes. That made me feel somewhat vindicated.

As mentioned above, my search for primitive MORB glasses led me to the WHOI sample storage in the McLean Laboratory, where I found ALV 519-4-1 collected by the ALVIN submersible from the FAMOUS (French-American Mid-Ocean Undersea Study) area, at 36.8 °N on the Mid-Atlantic Ridge (Bryan and Moore, 1977). The FAMOUS area is located in a transitional zone between normal mid-ocean ridge to the south and the Azores plume to the north (Schilling, 1975). Langmuir *et al.* (1977) showed that basalts in the area are chemically transitional with flat chondrite normalised REE patterns (ALV 519-4-1glass has La at 12 times chondrite, Sm at 10.5 times, and Yb at 13.8 times). The major element composition is primitive with MgO of 9.51 wt. % and Mg# = 68. The groundmass glass is fresh and many olivine phenocrysts with melt inclusions were found. The melt inclusions were fresh glass and shrinkage bubbles were very rare. Electron probe analysis of the major elements revealed that the host olivines had a narrow range of forsterite contents from 88.1 to 90.6 with the majority of them being around 89.5. Post-entrapment crystallisation of host olivine is estimated to be mostly much less than 10 wt. % (Shimizu, 1998). Trace element analysis of the melt inclusions with the 3f instrument displayed interesting features. Chondrite normalised REE abundance patterns were bimodal as illustrated in Figure 5.10.

It is remarkable that large variations in light REE (La varies by more than a factor of 10) are in strong contrast to small variations in heavy REE (Yb varies within a factor of 2). The co-existence of light REE enriched and depleted melts in a single lava presents a clear cut case for chemical diversity of melts on small spatial and temporal scales beneath ocean ridges and raises the question whether chemically different sources are present or melting and melt extraction processes

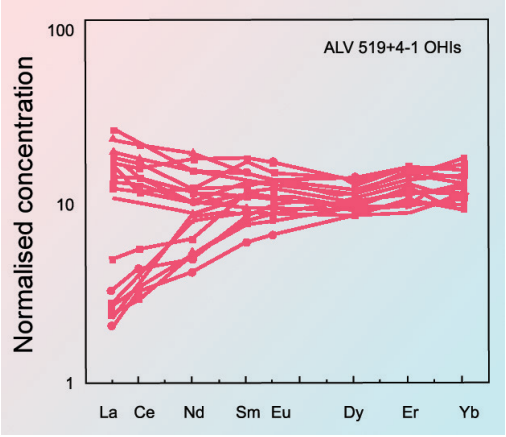

Figure 5.10 Chondrite normalised REE patterns of olivine-hosted melt inclusions from ALV 519-4-1. Note the co-existence of LREE enriched and depleted melt compositions in one suite of melt inclusions. Modified from Shimizu (1998).

from a uniform source alone could explain the diversity. Ti *vs.* Zr variations are also large and are correlated with REE variations: Ti and Zr concentrations are higher for light REE enriched than light REE depleted melts, and Ti/Zr ratios are systematically higher for light REE depleted melt inclusions. Figure 5.11 illustrates the co-variations of La/Sm and Ti/Zr.

It is noticeable that variations for Ti/Zr are small for melts with high chondrite normalised La/Sm ratios ([La/Sm]n), whereas those with low [La/Sm]n tend to have greater Ti/Zr. It looked as though melting proceeded with large changes in La/Sm but only small changes in Ti/Zr, suggesting that bulk partition coefficients for Ti and Zr were similar to each other, whereas those for La and Sm were significantly different. Shimizu (1998) argued that these trace element co-variations can be explained by critical melting (mantle has a standing porosity of 2 %, and melt in excess of this value is efficiently extracted) of a depleted source (DMM with Ti/Zr = 150 and [La/Sm]n = 0.5) with the initial stage of melting occurring in the presence of garnet. Garnet is required because its presence in the source makes Ti/Zr less variable but [La/Sm]n much more variable as melting progresses. It is also noticeable that the UDM (Sobolev and Shimizu, 1993) and other depleted melt inclusions from Iceland and elsewhere (Sobolev, pers. comm.) plot on the trend for critical melting in the spinel facies at its advanced stage. Shimizu (1998) also argued that middle REE/heavy REE fractionation displayed by these melt inclusions indicated modification of melt compositions due to AFC-type reactions with the wall-rock mantle during extraction. The suggestion made here that melting beneath mid-ocean ridges begins in the presence of garnet is in accord with U-Th disequilibrium data (*e.g.*, Beattie, 1993), but melt compositions are altered for moderately incompatible elements as well as for compatible and

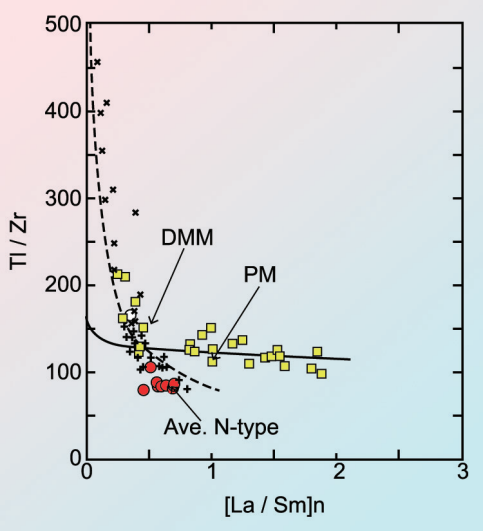

Figure 5.11 Co-variations of [La/Sm]n and Ti/Zr ratios in melt inclusions from ALV 519-4-1. Open squares: olivine-hosted melt inclusions from ALV 519-4-1; crosses: okiovine-hosted melt inclusions from southern MAR; x's: olivine-hosted melt inclusions from Iceland (Sobolev, pers. comm.); solid circles: FAMOUS glasses (Langmuir *et al*., 1977). Curves show trajectories of instantaneous melt fractions formed by critical melting (standing porosity of 2 %) of DMM in the spinel field (dashed curve), and in the garnet field (solid curve). Modified from Shimizu (1998).

major elements by melt-rock reaction during melt transport. In this sense, the trace element systematics observed here are useful in understanding melting and melt extraction processes, and help reach the realisation that the concept of a primary magma in the classical sense is no longer sustainable.

I mentioned above that isotopic variations in melt inclusions from a single lava indicate melts derived from chemically and isotopically diverse sources co-existing in close spatial and temporal proximity. However, the length scales of these heterogeneities in the mantle cannot be determined from the melt inclusion data. So, I turned my attention back to abyssal peridotites with the idea of taking a detailed look at chemical and isotopic variations of peridotite minerals from individual dredges. When Jessica Warren agreed to do this with me for her Ph.D. thesis in the MIT-WHOI Joint Program during the summer of 2001, I decided to do the best I could to help her achieve our goals. Henry Dick was eager to co-supervise her work with me and many of the samples we looked at came from Henry's cruises to the ultra-slow spreading Southwest Indian Ridge. The centrepiece of Jessica's work was going to be detailed trace element studies of clinopyroxenes and orthopyroxenes combined with Sr, Nd, and Pb isotopes.

I knew that there was only one laboratory in the world where she could do this and that was at the Institute for Study of Earth's Interior, Okayama University, where Professor Eizo Nakamura led the geochemistry group. With his kind invitation, I sent Jessica there for 4 months in 2005 to do Sr and Nd isotopes, with more than 20 handpicked pure pyroxene samples. I did the handpicking myself; I was so motivated by this project that even a 6-hour sitting for handpicking did not tire me at all. I was just happy to be an advisor who did the most menial job of the entire thesis project to help a student, and in fact, many Joint Program students were extremely jealous!

Almost at the same time as we started this project, other groups were also wondering about the genetic relationships between abyssal peridotites and associated basalts. For example, Cipriani *et al.* (2004) reported Sr and Nd isotopes for 23 clinopyroxenes separated from peridotites from the Vema lithosphere section of the Mid-Atlantic Ridge and found that their isotopic compositions do not necessarily match between basalts and associated peridotites, with peridotites having more depleted compositions than basalts. In addition, Salters and Dick (2002) presented regional scale characteristics of Sr and Nd isotopic variations in abyssal peridotites from the Southwest Indian Ridge and the Atlantis II Fracture Zone, which provided the framework for Jessica's work. Detailed studies of dredges were made for Van7-96 (9.98 °E, 53.14 °S) and Van7-85 (15.23 °E, 52.25 °S) from the oblique section of the Southwest Indian Ridge and RC27-9-6 (57.18 °E, 31.92 °S) from the Atlantis II Fracture Zone. Figure 5-12 shows Sr and Nd isotopic variations in pyroxenes from abyssal peridotites from the oblique section of the Southwest Indian Ridge.

Note that isotopic variations observed for the Van7-96 dredge at ~10 °E are large and encompass the entire range of basalt Nd isotopic compositions (corrected for radiogenic Nd ingrowth over 20 Myr) from enriched MORB ($^{143}Nd/^{144}Nd$ ~ 0.51282, ε_{Nd} = +3.5) to depleted DMM ($^{143}Nd/^{144}Nd$ ~ 0.51318, ε_{Nd} = +10.5), whereas the Van7-85 dredge samples display a narrower range within DMM-D-DMM (0.51309 – 0.51329, +8.8 - +12.7). Large ranges of isotopic compositions were also observed on "single dredge" sampling scales by Cipriani *et al.* (2004) from the Mid-Atlantic Ridge and imply large isotopic heterogeneities in the upper mantle beneath ocean ridges. Warren *et al.* (2009) argued that the variations observed for the Van7-96 dredge were due to interaction with the Bouvet mantle plume ~20 Myr ago, based on Nd and Sr isotopes as well as modal clinopyroxene abundances. In contrast, the Nd isotope variations at the Van7-85 dredge show no signs of interaction with enriched melt, suggesting that different degrees of depletion had been preserved on a length scale of less than 1 km over a long period of time. Thus, it should be noted that the MORB source mantle had had a complex geochemical history with repeated depletion (melt extraction) and enrichment (interaction with enriched melts), but, overall, the frequency distribution of $^{143}Nd/^{144}Nd$ in abyssal peridotites is skewed toward more depleted compositions relative to MORB (see Fig. 5.13; Warren *et al.*, 2009). This means that the MORB source mantle is more depleted than MORB isotopic

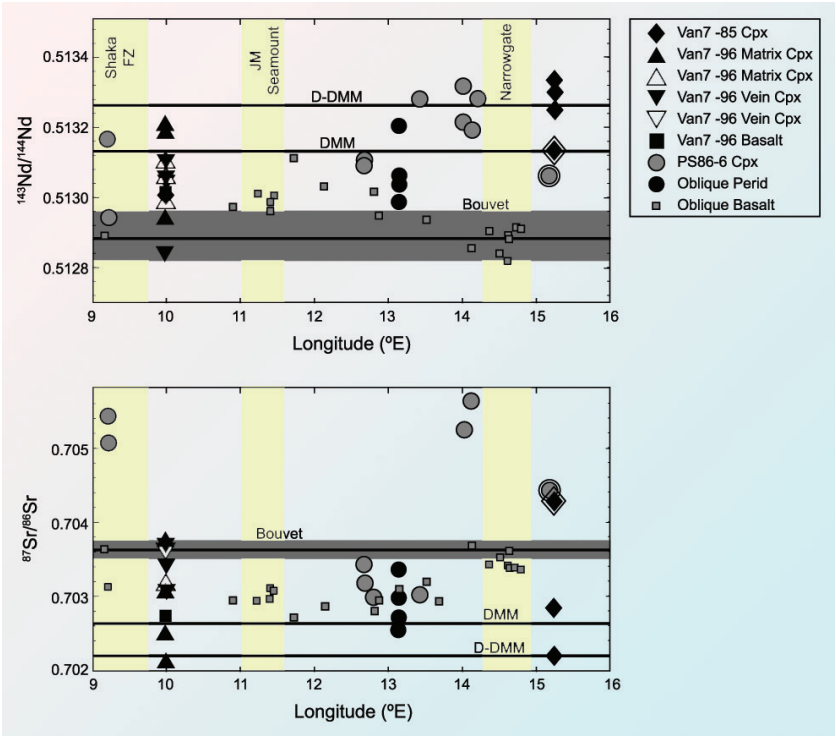

Figure 5.12 Sr and Nd isotopic variations of clinopyroxenes in abyssal peridotites from the Southwest Indian Ridge. Note the large isotopic variations observed in single dredges from the ~10 °E (dredge 96) and ~15.2 °E (dredge 85) sites. Modified from Warren *et al.* (2009).

compositions imply, as Nd mass balance contributions from depleted abyssal peridotites are easily obscured by melts derived from more enriched materials with higher concentrations of Nd.

As Warren *et al.* (2009) argued, the 20 Myr old enrichment event contributed to the chemical and isotopic diversity of abyssal peridotites at the Southwest Indian Ridge. It is not difficult to imagine that similar melt-rock interaction occurred when melting and melt extraction were active on the ridge, as upwelling mantle is internally heterogeneous with diverse geochemical prehistories and melts derived from enriched sources could react with depleted melt extraction residues and modify them on the ridge.

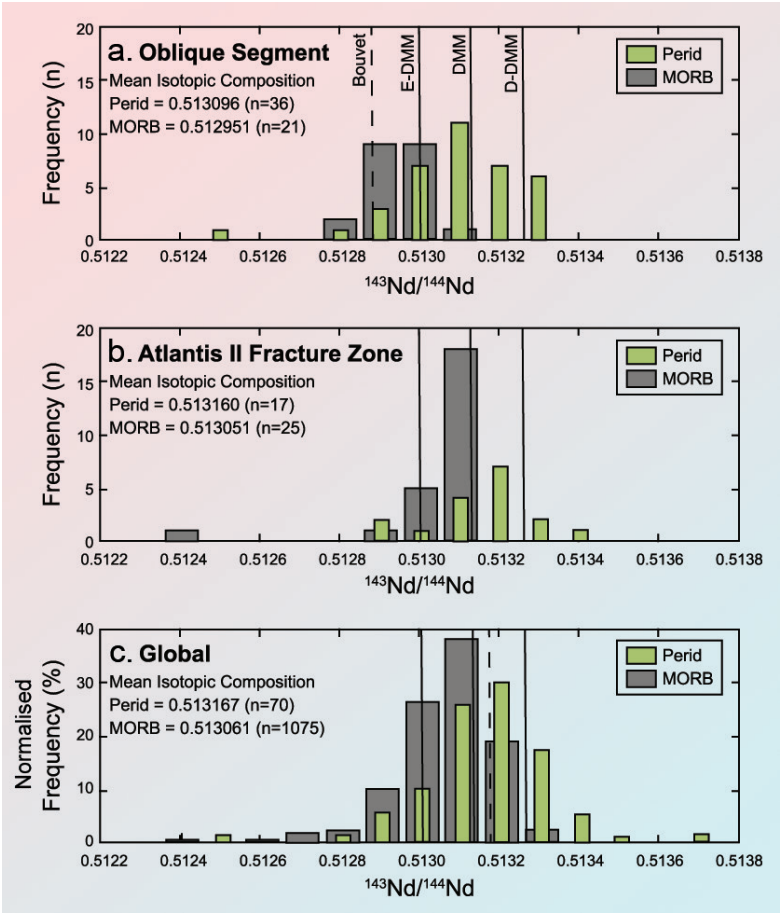

Figure 5.13 Histograms of $^{143}Nd/^{144}Nd$ of clinopyroxenes in abyssal peridotites from the oblique segment of the Southwest Indian Ridge, the Atlantis II Fracture Zone, and the global abyssal peridotite data set. Note that abyssal peridotites tend to be more radiogenic than basalts in all the diagrams, indicating that the MORB source mantle is more depleted than basalts would imply. From Warren *et al.* (2009).

Large trace element variations observed in clinopyroxenes in peridotites at the Atlantis II Fracture Zone (Warren and Shimizu, 2010) are examples of active melt-rock interaction on the ridge and display how large trace element variations (more than two orders of magnitude variations in light REE) occur on very small length scales (from the grain scale, *i.e.* 1 – 5 mm, to the single-rock scale, 10 – 50 cm). Figure 5.14 illustrates REE patterns of clinopyroxenes

in cryptically metasomatised peridotites. Sample 6K-465-2 looks like a typical abyssal peridotite, and in fact clinopyroxenes in most parts of the sample are light REE depleted, typical for abyssal peridotites (Johnson *et al.*, 1990), but at one end of the sample there are enriched clinopyroxene grains next to a narrow transition zone leading to the depleted part of the rock. No REE zoning was observed for the clinopyroxenes in the depleted or the enriched parts, but those in the transition zone are zoned with respect to REE, with light REE depleted cores and continuously increasing REE concentrations toward the rims as shown in Figure 5.14. Liquid in equilibrium with enriched clinopyroxenes (the rim of the transition zone included) are within range of the basalts in the vicinity, suggesting that they were the metasomatising agents. Other trace elements such as Ti and Zr also vary systematically during melt-rock reactions as shown by Warren and Shimizu (2010). Zoned clinopyroxenes in the transition zone suggest that the modal abundance of clinopyroxene in this sample increased as a result of interaction with melt, and negative Eu anomalies in the rim and enriched clinopyroxenes indicate co-precipitation of plagioclase from melt.

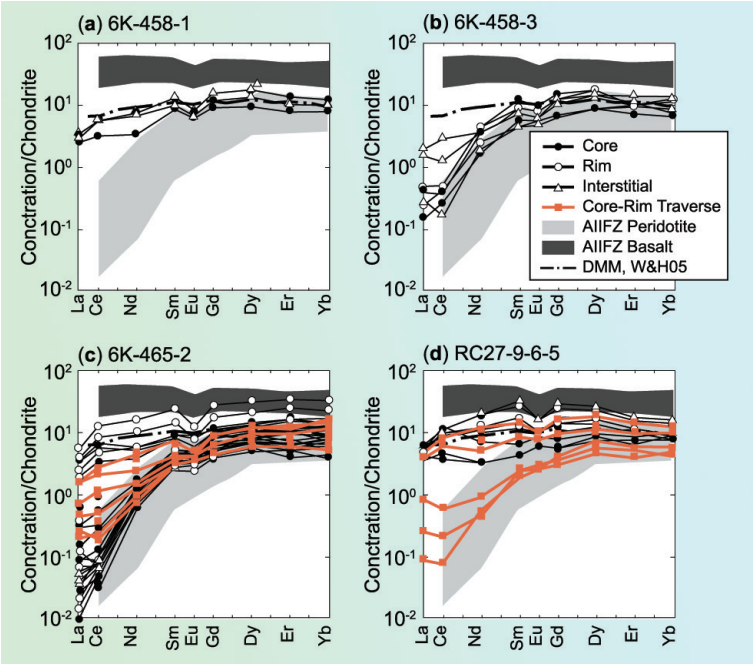

Figure 5.14 Chondrite normalised REE patterns in clinopyroxenes in abyssal peridotites from the Atlantis II Fracture Zone. Note the large variations in concentrations of light REE, ranging from the light REE depleted patterns characteristic of abyssal peridotites to much greater overall REE concentrations with less fractionated patterns. Shown in orange are core-rim variations. Note variations from light REE depleted core to enriched rim. From Warren and Shimizu (2010).

The possibility that interaction with enriched melts on the ridge contributed to isotopic diversity of abyssal peridotites was pursued through ion probe analysis of Pb isotopes in sulphides in abyssal peridotites from the Southwest Indian Ridge and the Gakkel Ridge (Blusztajn *et al*., 2014). To our surprise, many sulphide grains in peridotites with clinopyroxenes with strongly light REE depleted patterns did not have sufficient Pb for isotopic analysis. This was interpreted to mean that Pb was incompatible in sulphide-sulphide melt systems and therefore was strongly depleted in residual sulphide. However, many sulphide grains with high Pb concentrations were also found and they displayed large isotopic variability. Those sulphides were precipitated directly from infiltrating silicate melts that cryptically metasomatised abyssal peridotites such as those at the Atlantis II Fracture Zone discussed above. The sulphide Pb isotope data also indicated that mantle end members such as EM I and EM II were involved in the origin of the enriched melts. The results of this study provides credence to the large Pb isotopic variations among olivine-hosted melt inclusions described by Saal *et al*. (1998) as well as to those described above from 14 °N on the Mid-Atlantic Ridge.

To summarise, we started our work with the notion that abyssal peridotites were residues of melt extraction on the mid-ocean ridge and were genetically connected with basalts in the vicinity. Kevin Johnson's work (Johnson *et al*., 1990) demonstrated that the trace element characteristics of clinopyroxenes in abyssal peridotites provided strong evidence for near-fractional melting operating on the ridge and did not support the direct equilibrium relationship between peridotites and associated basalts. This can be understood to mean that abyssal peridotites represent instantaneous residues of near-fractional melting, whereas basalts are aggregated melt fractions. Studies of radiogenic isotopes in abyssal peridotite clinopyroxenes further showed that abyssal peridotites display isotopic heterogeneities on regional as well as local scales, indicating more complex geochemical prehistories (Salters and Dick, 2002; Cipriani *et al*., 2004; Warren *et al*., 2009). In particular, Warren *et al*. (2009) showed very large isotopic heterogeneities on single dredge scales, suggesting that the asthenospheric mantle beneath ocean ridges was not a simple single stage residue of continental crust extraction, but had experienced multiple melt extraction events and interaction with plume-derived melt in its past before its involvement in passive upwelling beneath the ridge. It is therefore suggested that the assumption that all trace element variations observed in abyssal peridotites are the result of melt extraction on the present day ridge is untenable. In addition, melt-rock interaction on an active ridge further complicates the geochemical systematics (Warren and Shimizu, 2010). Chemical and isotopic heterogeneities of the source of mid-ocean ridge basalts were also expressed in the chemical and isotopic diversity of olivine-hosted melt inclusions, and *in situ* analytical techniques including ion microprobe proved especially powerful in documenting these.

6. NO END IN SIGHT

6.1 The Big Picture

In the preceding chapters, I presented examples of applications of SIMS techniques to various aspects of geochemistry. With my narrative I hoped that the usefulness of microanalysis for providing observations pertinent to the "big picture" was self-evident. I feel, however, that some redundancy may be important here to drive the point home.

The "big picture", in the present context, is composed of two distinct elements. The first is juxtaposed scale lengths of observation (micrometre scales) and natural processes (kilometres or more). A good example is how the ion probe-based REE abundance patterns of clinopyroxenes in abyssal peridotites provide strong evidence for near-fractional melting operating beneath ocean ridges (Johnson *et al.*, 1990) as discussed in Section 5. The fluid dynamic conditions of magma bodies as inferred from trace element zoning of augite phenocrysts as described in Section 3 (*e.g.*, Shimizu and le Roex, 1986), also can be considered an example of juxtaposition of scales. The second element was the effort on my part to gain insight into the workings of natural processes *via* microanalysis. The fundamental importance of interface processes in growth of crystals from magma as discussed in Section 3, manifested itself as non-equilibrium partition coefficients at the interface and led me to conceptualise a process of magmatic mineral growth from the point of view of reaction kinetics. The enormous diversity of trace element abundance patterns in mantle minerals and micro-scale chemical heterogeneities within them are clear evidence that the mantle has not been just quietly sitting there, but rather has been interacting with fluids/melts at various times throughout the past. Particularly important in this respect is the fact that abyssal peridotites are not simple melt extraction residues, but rocks with extraordinarily complex geochemical prehistories (*e.g.*, Warren *et al.*, 2009; Warren and Shimizu, 2010). Trace element analysis of olivine-hosted melt inclusions was made possible with SIMS and provided probably the most important surprise of all: the astonishing chemical diversity discovered in a FAMOUS sample suite; the coexistence of LREE-enriched and -depleted melts within a single lava; and a Pb isotopic diversity among melt inclusions from a single EMORB sample so large that it is incontrovertible evidence that many melts must have contributed to this single lava, a conclusion which in turn provides testimony that melt fractions derived from diverse sources are aggregated to form individual lavas erupting on the ridge.

The Odyssey I began more than four decades ago seems to go on forever, and, as it did all along, still now is heading in diverse directions, both good and bad. With respect to applications of SIMS techniques, my move to Woods Hole Oceanographic Institution in 1988 was beneficial in opening up new research

areas for me. Not only did my work on MORB start there, as told in Section 5, but SIMS applications to palaeoceanography also began at WHOI with very successful outcomes.

6.2 SIMS Applications to Biogenic Carbonates

In the mid-1990s Stan Hart made a brief "excursion" into trace element studies of coral skeletons with Anne Cohen, who came to WHOI as a post-doc to work on corals as a palaeoceanographic tool. Stan's efforts opened up a new field in which the ion microprobe proved to be very effective. Hart and Cohen's first paper published in 1996 described the usefulness of some trace elements as a proxy for palaeo-sea surface temperature (SST). Among them was Sr, through Sr/Ca ratios, for which experimental data existed for calibrations of inorganic aragonite precipitation. Following this, an important breakthrough was made through the analysis of Sr/Ca in a symbiotic coral *Porites lutea* (Cohen *et al*., 2001). The authors found that Sr/Ca ratios were systematically different between day time and night time growth zones in a single coral. Photosynthesis by symbiotic algae during the day time increased CO_3^{2-} concentrations in the calcifying fluid and increased skeletal growth rate, which in turn decreased incorporation of Sr into the skeleton. This produced erroneous "temperature" signals, because too low Sr/Ca ratios indicated too high temperatures. In contrast, the night time growth zones near the centre of calcification reproduced SST more faithfully without the effects of photosynthesis by algae. This discovery explained the large puzzling discrepancies that existed between oxygen isotope-based SST records and those of bulk corals and stressed the importance of *in situ* microanalysis.

It was astounding to me to realise that even for biogenic crystal growth, partitioning of elements is affected by kinetics. Also, recognising that Sr/Ca in seawater is 8.54 mM/mol, Sr/Ca ratios in night time growth zones were always greater than those of seawater, indicating that Sr behaved as a compatible element in the aragonite-seawater system, whereas in kinetically disturbed daytime growth zones Sr varied from compatible to incompatible. But, I was still suspicious about Sr/Ca SST thermometry, because the calibration of corals was generally made using tropical species that experienced only a few degrees of temperature range. I wanted the calibration made on a much larger temperature range to be believable. This was around 2000–2001, when Cohen *et al*. (2001) was completed. Then something remarkable happened: I think it was spring of 2001, when a student at University of Chicago called me, saying, in effect, *"as a public policy major, I want to understand how science is done, and I would like to work with you this summer and learn about it"*. I was deeply impressed by this statement and decided to do my best to help. I thought that working with Anne Cohen on coral-based SST calibration would be ideal to learn how societally relevant science was done. This was how Kate Owens came to my lab, and, with Anne Cohen leading the effort, we started to work on *Astrangia poculata*, the "Woods Hole Coral", sampled in the local sea at Woods Hole, Massachusetts. This coral lives in seawater with

temperatures ranging from -2 °C in winter to 23 °C in summer and is an ideal species on which to test the Sr/Ca thermometry calibration for a wide range of temperatures. In addition, it turns out that this coral forms two colonies side by side, one *with* and the other *without* symbiotic algae, so that we could test directly, within the same environment, the effect of symbiosis on Sr/Ca ratios. The results of the ion probe analyses were stunning (see Cohen *et al*., 2002, for details): for three years recorded in the coral skeletons (1) asymbiotic specimens showed that the Sr/Ca-derived temperature dependence agreed with the Sr/Ca thermometry based on inorganic aragonite precipitation and the night time growth of *Porites* mentioned above, (2) symbiotic specimens revealed Sr/Ca variations with greater amplitudes, and (3) symbiotic specimens further displayed an ontogenetic trend that became greater over the creatures' lifetime. As a result, coral Sr/Ca thermometry was confirmed for a wide range of temperatures as long as only asymbiotic corals and night time growth zones were utilised. Inclusion of Sr/Ca data from symbiotic corals was shown to introduce the possibility of erroneous temperature estimates. Thus, not only were the long-standing discrepancies between coral-based SST and oxygen isotope thermometry resolved, but also the fundamental importance of microscale *in situ* analysis firmly established in environmental science. I was particularly happy that this work provided a first-hand experience of scientific research to Kate, and that our *Science* paper (Cohen *et al*., 2002) also became a significant career breakthrough for Anne Cohen.

However, I had no idea that a catastrophic event was about to happen.

6.3 Fire!

The IMS 1270 we purchased in 1996 caught fire on October 22, 2002. I was analysing Pb isotopes in basalt glass when I heard arcing sounds from the primary column. I stopped the machine in a routine manner. Then I saw smoke, followed by flames coming out of the electronic control chassis. Power transistors in the primary high voltage chassis somehow got heated up to very high temperatures and self-ignited. I grabbed a fire extinguisher and tried to fight the flames. It was futile. I cut the power to the machine. By that time, smoke was beginning to fill the lab and fire alarms were tripped. Security people arrived on the scene followed by fire fighters from the fire department. Smoke got into the air-handling system of the building and went everywhere, contaminating many labs. Everything in the ion probe lab and adjacent rooms was covered with soot. The entire corridor had the characteristic smell of electric fires. The IMS 3f, the Plasma MS instruments nearby, and offices on the same floor were immediately cordoned off.

This was a nightmare. I had lost tools for research as well as ways to obtain preliminary data for writing grant proposals for the foreseeable future. Collateral damage was severe, as the electric fire smoke carrying heavy metals flowed into labs and ruined carefully established chemical procedures for analysis of heavy metals in seawater. I was crushed by the heavy sense of responsibility. Even a

rumour that I torched the machine was circulated! Hazardous cleaning procedures had to be carried out immediately after the fire to save specimens, paper records, books, *etc*., which made life very difficult for Graham Layne and Pete Landry. Then, there was the question of repair or replace, and issues of insurance and institutional finance arose.

WHOI *vs*. Cameca ensued and things looked like they would be standing still for a very long time with no end in sight while lawyers from both sides conferred. The instrument was deconstructed and shipped back to the Cameca factory in France for repair. The lawsuit was settled outside court, and the instrument came back as a rebuilt 1280 in January 2005, more than two years after the fire.

While the IMS 1270 was in a state of flux, Graham and Pete worked hard to get the 3f recovered and I received a request for collaboration from Heather Stoll (then at Williams College) in 2003. She had been studying Sr/Ca ratios of coccolithophores as a productivity proxy and was inspired by Anne Cohen's work on Sr/Ca in corals. This was an ideal project to show the community that we were on the way to recovery from the fire. Heather had an ambitious plan for establishing an observational basis for how creatures responded to an abrupt "greenhouse environment". For this purpose, she wanted to determine variations of Sr/Ca ratios in handpicked individual coccolith species from sediment cores across the Paleocene-Eocene Thermal Maximum (PETM) in order to assess how productivity of individual coccolith species changed. This was a technically very challenging proposition, mainly because coccolithophores are small (*Emiliania huxleyi* is discs of ~2 μm across, for instance) and thin. How could we expose tiny and thin targets on the surface of epoxy? After wasting a lot of handpicked specimens, we finally developed a protocol (described later in Stoll and Shimizu, 2009), and Sr/Ca changes were obtained for four different species across the PETM from three different oceanographic settings (Stoll *et al*., 2007). It was shown that (1) responses of individual coccolith species to the PETM varied in each oceanographic setting, and that (2) some species displayed different responses to the PETM depending on the variety of oceanographic settings. At the high latitude site (ODP 690B) in the Weddell Sea, two species, *Chiasmolithus* and *Zygrhablithus*, showed significant increases in Sr/Ca at the PETM, indicating elevated productivity. The dominant species, *Toweius*, showed a moderate increase in productivity. Overall, the data showed that the greenhouse environment resulted in increased productivity of coccolithophores at the high latitude site. In contrast, at the tropical sites (Site 1209, tropical Pacific, and Site 1258, equatorial Atlantic at the Demerara Rise), the effect of the PETM was much more subdued, with *Toweius* and *Coccolithus* displaying a slight decrease in productivity at Site 1209, and, at Site 1258, *Coccolithus* showing variations in productivity within the range of pre-PETM periods. The different responses of coccolithophores to the PETM at different oceanographic settings were interpreted to indicate that heat stress at the photic zone at tropical sites might have affected productivity. This was one of the early attempts to try to understand how biological systems respond to environmental changes and I was surprised and dismayed by the fact that the

importance of our work was not easily registered in reviewers' minds. Regardless, it was impressive that response of coccolithophores to changes in the environment was genera specific and also depended on oceanographic settings.

6.4 Magmatic Volatiles

A complete recovery from the fire needed to be shown to NSF in order to ensure funding to resume operation of a national ion microprobe facility. I decided to shift the machine operation from almost exclusively O^- beams to a combination of O^- and Cs^+ beams and began a new journey into the geochemistry of volatile elements (CO_2, H_2O, F, Cl, and S). Erik Hauri at DTM was very generous in providing a set of basalt standard glasses and we got ourselves ready for analysis of olivine-hosted melt inclusions for volatile element abundances in 2006. The determination of D/H ratios was added to our repertoire later on. My major motivation was to document olivine-hosted melt inclusions for pre-eruption volatile element abundances, as surface degassing makes abundance data measured in lavas altogether meaningless. This was going to be my entry into a large scale study of deep recycling of volatile components as well. Particularly interesting to me was the deep recycling of sulphur. How does oxidised and isotopically heavy sulphur recycle into the mantle and contribute to isotopic heterogeneity of sulphur in the mantle? Or does the mantle act as an infinite reservoir for sulphur so that subducted oxidised heavy sulphur simply disappears into the infinite reservoir? How could we determine the diffusivity of sulphur in mantle minerals? How is sulphur transported across subduction zones into the mantle wedge and into erupted arc magmas? All these and other questions still remain unanswered.

It turned out that the analytical protocols for volatile elements became very popular, and many outside users came. As an NSF-supported national facility, this was therefore a successful strategy. For a facility like ours, I always had an open lab policy that I learned from Stan Hart and had the "Field of Dreams" approach: "If you build it, people will come". And, it worked.

As volatile element data became widely available for basaltic glasses and olivine-hosted melt inclusions, their systematics were placed in geochemical context as incompatible elements, and ratios against lithophile trace elements became a preferred way to discuss their geochemistry. I was a little apprehensive about the casual use of ratios such as CO_2/Nb or S/Dy, because the behaviour of CO_2 and S in mantle-basalt systems was not sufficiently taken into consideration. Carbon and sulphur share specific similarities in their presence in the mantle and their behaviour during mantle melting processes, which should always be kept in mind. First, their solubility in silicate minerals is extremely low, and they form their own phase in the mantle: carbonate for C and sulphide for S under the prevailing oxygen fugacity of the mantle. Yet, their solubility in silicate melts is substantial. This means that extraction of these elements from the mantle occurs *via* silicate melts. Second, melting temperatures of carbonate and sulphide are much lower than the solidus of the silicate mantle, hence they are molten (for

sulphide, it is unclear if it is partially or completely molten) when the silicate solidus is reached. Third, once silicate melt is formed, both carbon and sulphur are dissolved into silicate melt according to their solubility, and there can be cases where silicate melts are saturated with CO_2 or S, *i.e.* coexisting with carbonate melt or sulphide melt (and mineral). If this were the case, their concentrations in silicate melts are constant and independent of degree of melting as long as carbonate or sulphide phases are present. It is implied that within a limited range of mantle melting, these elements may not behave as incompatible elements, and their ratios to lithophile elements therefore would vary considerably. For example, take the S content of the mantle as 200 ppm (*e.g.*, Nielsen *et al.*, 2014), and the solubility of S in silicate melt (the S content at sulphide saturation) as 1500 ppm (Wendlandt, 1982, at 2.5 GPa; ~1100 ppm by the formula given by Mavrogenes and O'Neill, 1999). This suggests that up to 13 % melting, the S content of silicate melts would be constant at 1500 ppm. The Dy abundance in melt, on the other hand, varies according to its bulk partition coefficient, so that S/Dy increases with increasing degree of melting. Beyond 10 % melting, all S in the mantle is exhausted, and the S content in silicate melts would decrease because of dilution. Sulphur solubility increases with decreasing pressure (Mavrogenes and O'Neill, 1999); it is likely that basaltic melts are sulphur undersaturated when they come to the surface. For CO_2, the situation is similar yet complicated by the fact that CO_2 solubility in silicate melts decreases with decreasing pressure, such that degassing tends to happen as magmas move upwards toward the surface. With this in mind, we can make the same argument for CO_2 as S. If the C abundance of the mantle is ~80 ppm (*e.g.*, Wood *et al.*, 1996) and CO_2 solubility in basalts at 2.5 GPa is 2.5 wt. % (2.5×10^4 ppm: Holloway and Blank, 1994), then the critical degree of melting where melt would become undersaturated with CO_2 is 0.012, a lot smaller than that of S. This would mean that the behaviour of CO_2 resembling a perfectly incompatible element could be attained at an earlier stage of melting than for S. Nevertheless, assuming a perfect incompatible element behaviour for CO_2 during melting is premature, particularly if melt extraction happens at very low degrees (<1.2 %) of melting. Consider also that incompatible behaviour of Nb during melting suggests that the CO_2/Nb ratio would vary significantly during the early part of melting where almost all Nb is extracted into the melt. This could cause significant variations in CO_2/Nb in basalts prior to degassing and, hence, estimation of this ratio for the mantle would be compromised.

The preceding paragraph is meant as a general caution against a too casual use of volatile to lithophile trace element ratios without any consideration of the potential complexities involved. This valid concern is completely independent of the ion probe but I underscore it here because of its pertinence to SIMS work on volatile elements in melt inclusions, *etc*.

6.5 What Have I Done?

Throughout my career, I was driven by my curiosity of nature: How the Earth Works. My curiosity of natural phenomena was nurtured during my childhood in Hokkaido. Just after WWII, there were no toys to play with but there were woods and ponds, and creatures in them. I was in the woods every single day, looking at butterflies, frogs, and other creatures. Gradually, I developed an ability to observe: for instance, I developed a technique to identify butterfly species in their flight. Not just the colours of their wings. They had unique and characteristic styles of flying, by which I was able to identify their species, and I was fascinated by the diversity. This taught me the joy and power of observation of nature. Another driver of my endeavours was my suspicious character: I constantly suspected and challenged conventional wisdom. Because I believed in a dialectic approach for science to make progress, I thought that doubting and challenging conventional wisdom was the first positive step toward progress. This attitude, of course, posed problems because "the big shots", who preached the conventional wisdom, did not appreciate a neophyte iconoclast.

I also maintained that science was a team sport. When people worked on a certain area of a subject, I would always select other areas of the subject to work on. In other words, I avoided the most popular research topics. This also posed problems because I gave the impression that I was working on unimportant problems and that my work was intentionally ignored. My citation index may have suffered but I did not care. Our field of science makes progress when theoretical work, experimental work, and observations of nature mesh together. One of the examples was the convergence of views on the processes of melting and melt extraction beneath mid-ocean ridges as described in Section 5. I have stayed on the observational side throughout my career and have had opportunities for discoveries and important realisations. The way I stumbled on the energy filtering approach as described in Section 2 had a lot to do with my stubbornness in staying observationalist/experimentalist. The discovery of the UDM discussed in Section 5 was another example of a great reward to an observationalist. However, my greatest joy throughout my Odyssey was the continuous discovery that nature was much more complex than we thought, and natural processes were, by definition, disequilibrium phenomena. I feel that my Odyssey will continue on for yet a while, as long as my curiosity about nature remains alive, and in that sense, I see no end in sight.

REFERENCES

ALBARÈDE, F., BOTTINGA, Y. (1972) Kinetic disequilibrium in trace element partitioning between phenocrysts and host lava. *Geochimica et Cosmochimica* Acta 36, 141-156.

ANDERSEN, C.A., HINTHORNE, J.R. (1972) Ion microprobe mass analyzer. *Science* 175, 853-860.

ANDERSEN, C.A., HINTHORNE, J.R. (1973) Thermodynamic approach to the quantitative interpretation of sputtered ion mass spectra. *Analytical Chemistry* 45, 1421-1438.

ANDERSON, D.L. (1965) Recent evidence concerning the structure and composition of the Earth's mantle. *Physics and Chemistry of the Earth* 6, 1-131.

BAKALE, D.K., COLBY, B.N., EVENS, C.A. JR. (1975) High mass resolution ion microprobe mass spectrometry of complex matrices. *Analytical Chemistry* 47, 1532-1536.

BEATTIE, P. (1993) Uranium-thorium disequilibrium and partitioning on melting of garnet peridotite. *Nature* 363, 63-65.

BENDER, J.F., HODGES, F.N., BENCE, A.E. (1978) Petrogenesis of basalts from the Project FAMOUS area: Experimental study from 0 – 15 kbars. *Earth and Planetary Science Letters* 41, 277-302.

BENNINGHOVEN, A. (1970) Die Analyse monomolekularer Festkorperoberflachenschiktem mit Hilfe der Sekundarionenemission. *Zeitschrift für Physik A Hadrons and Nuclei* 230, 403-417.

BETZ, G. (1980) Alloy sputtering. *Surface Science* 92, 283-309.

BLAISE, G., NOURTIER, A. (1979) Experimental and theoretical approaches to the ionization process in secondary ion emission. *Surface Science* 90, 495-547.

BLUNDY, J.D., SHIMIZU, N. (1991) Trace element evidence for plagioclase recycling in calc-alkaline magmas. *Earth and Planetary Science Letters* 102, 178-197.

BLUSZTAJN, J., SHIMIZU, N. (1994) The trace element variations in clinopyroxenes from spinel peridotite xenoliths from southwest Poland. *Chemical Geology* 111, 227-243.

BLUSZTAJN, J., SHIMIZU, N., WARREN, J.M., DICK, H.J.B. (2014) In-situ Pb isotopic analysis of sulfides in abyssal peridotites: New insights into heterogeneity of the oceanic upper mantle. *Geology* 42, 159-162.

Bodinier, J.L., Vasseur, G., Vernieres, J., Dupuy, C., Fabries, J. (1990) Mechanisms of mantle metasomatism: geochemical evidence from the Lherz orogenic peridotite. *Journal of Petrology* 31, 597-628.

Boyd, F.R. (1973) A pyroxene geotherm. *Geochimica et Cosmochimica Acta* 37, 2533-2546.

Boyd, F.R. Jr., Nixon, P.H. (1972) Ultramafic nodules from the Thaba Putsoa kimberlite pipe. *Carnegie Institution of Washington Year Book* 71, 362-373.

Brochard, D., Slodzian, G. (1971) Emission ionique secondaire des alliages cuivre-aluminium en presence d'oxygene. *Journal de Physique* 323, 183-190.

Bryan, W.B., Moore, J.G. (1977) Compositional variations of young basalts in the Mid-Atlantic Ridge rift valley near latitude 36°49'N. *Geological Society of America Bulletin* 88, 556-570.

Burton, J.A., Prim, R.C., Slichter, W.P. (1953) The distribution of solute in crystals grown from the melt, Pt. I Theoretical. *The Journal of Chemical Physics* 21, 1987-1991.

Cashman, K.V., Sparks, R.S.J., Blundy, J.D. (2017) Vertically extensive and unstable magmatic systems: A unified view if igneous processes. *Science* 355, eaag3055, doi: 10.1126/science.aag3055.

Cipriani, A., Brueckner, H.K., Bonatti, E., Brunelli, D. (2004) Oceanic crust generated by elusive parents: Sr and Nd isotopes in basalt-peridotite pairs from the Mid-Atlantic Ridge. *Geology* 32, 657-660.

Coghlan, R.A.N. (1990) Study in diffusional transport: grain boundary transport of oxygen in feldspars, diffusion of oxygen, strontium and REE in garnet and thermal histories of granitic intrusions in south-central Maine using oxygen isotopes. Ph.D. Thesis, Brown University, 238 pp.

Cohen, A.L., Layne, G.D., Hart, S.R., Lobel, P.S. (2001) Kinetic control of skeletal Sr/Ca in a symbiotic coral: Implications for paleotemperature proxy. *Paleoceanography and Paleoclimatology* 16, 20-26.

Cohen, A.L., Owens, K.E., Layne, G.D., Shimizu, N. (2002) The effect of symbionts on the accuracy of Sr/Ca paleotemperatures from coral. *Science* 296, 331-333.

Compston, W., Clement, S.W.J. (2006) The geological microprobe: first 25 years of dating zircons. *Applied Surface Science* 252, 7089-7095.

de Galan, L., Smith, R., Winefordner, J.D. (1968) The electronic partition functions of atoms and ions between 1500°K and 7000°K. *Spectrochimica Acta* 23B, 521-525.

DePaolo, D.J., Wasserburg, G.J. (1976) Nd isotopic variations and petrogenetic models. *Geophysical Research Letters* 3, 249-252.

Dosso, L., Hanan, B.B., Bougault, H., Schilling, J.-G., Joron, J.-L. (1991) Sr-Nd-Pb geochemical morphology between 10° and 17°N on the Mid-Atlantic Ridge: a new MORB isotope signature. *Earth and Planetary Science Letters* 106, 29-43.

Dowty, E. (1976) Crystal structure and crystal growth: II Sector zoning in minerals; *American Mineralogist* 61, 460-469.

Elthon, D., Scarfe, C.M. (1984) High pressure phase equilibria of a high-magnesia basalt and the genesis of primary oceanic basalts. *American Mineralogist* 69, 1-15.

Fesq, H.W., Kable, E.J.D., Gurney, J.J. (1975) Aspects of the geochemistry of kimberlites from the Premier Mine, and other selected South Africa occurrences with particular reference to the rare earth elements. *Physics and Chemistry of the Earth* 9, 687-707.

Foster, J.J. (2010) The construction and development of SHRIMP I: an historical outline. *Precambrian Research* 183, 1-8.

Frey, F.A., Green, D.H. (1974) The mineralogy, geochemistry and origin of lherzolite inclusions in Victorian basanites. *Geochimica et Cosmochimica Acta* 38, 1023-1059.

Fujii, T., Bougault, H. (1983) Melting relations of a magnesian abyssal tholeiite and the origin of MORBs. *Earth and Planetary Science Letters* 62, 283-295.

FUJII, T., SCARFE, C.M. (1985) Composition of liquids coexisting with spinel lherzolite at 10 kbar and the genesis of MORBs. *Contributions to Mineralogy and Petrology* 90, 18-28.

GARCIA, M.O., FOSS, D.J.P., WEST, H.B., MAHONEY, J.J. (1995) Geochemical and isotopic evolution of Loihi Volcano, Hawaii. *Journal of Petrology* 36, 1647-1674.

GAST, P.W. (1968) Trace element fractionation and the origin of tholeiitic and alkaline magma types. *Geochimica et Cosmochimica Acta* 32, 1057-1087.

GAST, P.W., TILTON, G.R., HEDGE, C.E. (1964) Isotopic composition of lead and strontium from Ascension and Gough Islands. *Science* 145, 1181-1188.

GILETTI, B.J., YUND, R.A. (1984) Oxygen diffusion in quartz. *Journal of Geophysical Research* 89, 4039-4046.

GREEN, D.H., RINGWOOD, A.E. (1967) The genesis of basaltic magmas. *Contributions to Mineralogy and Petrology* 15, 103-190.

GRIFFIN, W.L., SMITH, D., BOYD, F.R., COUSENS, D.R., RYAN, C.G., SIE, S.H., SUTER, G.F. (1989) Trace-element zoning in garnets from sheared mantle xenoliths. *Geochimica et Cosmochimica Acta* 53, 561-567.

GROVE, T.L., BENCE, A.E. (1977) Experimental study of pyroxene-liquid interaction in quartz-normative basalt 15597. *Proceedings of the 8th Lunar and Planetary Science Conference, Houston, Texas, March 14-18, 1977,* 1549-1579.

GROVE, T.L., BENCE, A.E. (1979) Crystallization kinetics in a multiply saturated basalt magma: An experimental study of Luna 24 ferrobasalt, *Proceedings of the 10th Lunar and Planetary Science Conference, Houston, Texas, March 19-23, 1979,* 439-478.

GROVE, T.L., BRYAN, W.B. (1983) Fractionation of pyroxene-phyric MORB at low pressure: An experimental study. *Contributions to Mineralogy and Petrology* 84, 293-309.

GROVE, T.L., RAUDSEPP, M. (1978) Effects of kinetics on the crystallization of quartz normative basalt 15597: An experimental study. *Proceedings of the 9th Lunar and Planetary Science Conference, Houston, Texas, March 13-17,* 585-599.

GROVE, T.L., VANIMAN, D.T. (1978) Experimental petrology of very low Ti (VLT) basalts. In: Merrill, R.B., Papike, J.J. (Eds) *Mare Crisium: The Views from Luna 24, Proceedings of the conference on Luna 24, Houston, Texas, December 1-3, 1977. Geochimica et Cosmocimica Acta Supplement 1.* Pergamon Press, New York, 445-471.

HAASE, C.S., CHADAM, J., FEINN, D., ORTOLEVA, P. (1980) Oscillatory zoning of plagioclase feldspar. *Science* 209, 272-274.

HALL, R.N. (1953) Segregation of impurities during the growth of germanium and silicon crystals. *Journal of Physical Chemistry* 57, 836-839.

HART, S.R., BROOKS, C. (1974) Clinopyroxene-matrix partitioning of K, Rb, Cs, Sr, and Ba. *Geochimica et Cosmochimica Acta* 38, 1799-1806.

HART, S.R. ZINDLER, A. (1989) Constraints on the nature and development of chemical heterogeneities in the mantle. In: Peltier, R. (Ed.) *Mantle Convection.* Gordon & Breach Science Publishers, New York, 261-388.

HART, S.R., SCHILLING, J.-G., POWELL, J.L. (1973) Basalts from Iceland and along the Reykjanes Ridge: strontium isotope geochemistry. *Nature* 246, 104-107.

HART, S.R., SHIMIZU, N., SVERJENSKY, D.A. (1981) Lead isotope zoning in galena: an ion microprobe study of a galena crystal from the Buick Mine, southeast Missouri. *Economic Geology* 76, 1873-1878.

HAURI, E.H., SHIMIZU, N., DIEU, J.J., HART, S.R. (1993) Evidence for hotspot-related carbonatite metasomatism in the oceanic upper mantle. *Nature* 365, 221-227.

HAVETTE, A., SLODZIAN, G. (1980) Matrix effects in secondary ion emission: quantitative analysis of silicates. *Journal de Physique Lettres* 41, L247-L250.

HERZOG, R.F.K., POSCHENRIEDER, W.P., SATKIEWICZ, F.G. (1973) Observation of clusters in a sputtering ion source. *Radiation Effects* 18, 199-205.

HICKMOTT, D.D., SHIMIZU, N. (1990) Trace element zoning in garnet from the Kwoiek area, British Columbia: disequilibrium partitioning during garnet growth? *Contributions to Mineralogy and Petrology* 104, 619-630.

HOAL, K.E.O., HOAL, B.G., ERLANK, A.J., SHIMIZU, N. (1994) Metasomatism of the mantle lithosphere recorded by rare earth elements in garnets. *Earth and Planetary Science Letters* 126, 303-314.

HOFMANN, A.W. (1972) Chromatographic theory of infiltration metasomatism and its application to feldspars. *American Journal of Science* 272, 69-90.

HOFMANN, A.W. (1973) Theory of metasomatic zoning, a reply to Dr. D.S. Korzhinskii. *American Journal of Science* 273, 960-964.

HOFMANN, A.W. (1980) Diffusion in natural silicate melts: A critical review. In: Hargraves, R.B. (Ed.) *Physics of Magmatic Processes*. Princeton University Press, Princeton, New Jersey, 385-417.

HOFMANN, A.W. (1988) Chemical differentiation of the Earth: The relationship between mantle, continental crust and oceanic crust. *Earth and Planetary Science Letters* 90, 297-314.

HOLLISTER, L.S. (1966) Garnet zoning: an interpretation based on the Rayleigh fractionation model. *Science* 154, 1647-1651.

HOLLISTER, L.S. (1969a) Contact metamorphism in the Kwoiek area of British Columbia. An end member of the metamorphic process. *Geological Society of America Bulletin* 80, 2465-2494.

HOLLISTER, L.S. (1969b) Metastable paragenetic sequence of andalusite, kyanite, and sillimanite, Kwoiek area, British Columbia. *American Journal of Science* 267, 352-370.

HOLLOWAY, J.R., BLANK, J.G. (1994) Application of experimental results to COH species in natural melts. *Reviews in Mineralogy* 30, 187-230.

HUEBNER, J.S., LIPIN, B.R., WIGGINS, L.B. (1976) Partitioning of chromium between silicate crystals and melts. *Proceedings of the 7th Lunar and Planetary Science Conference, Houston, Texas, March 15-19, 1976.* 1195-1220.

IONOV, D.A., HOFMANN, A.W., SHIMIZU, N. (1994) Metasomatism-induced melting in mantle xenoliths from Mongolia. *Journal of Petrology* 35, 753-785.

IRVING, A.J. PRICE, R.C. (1981) Geochemistry and evolution of lherzolite-bearing phonolitic lavas from Nigeria, Australia, East Germany, and New Zealand. *Geochimica et Cosmochimica Acta* 45, 1309-1320.

JOHNSON, K.T.M., DICK, H.J.B., SHIMIZU, N. (1990) Melting in the oceanic upper mantle: An ion microprobe study of diopsides in abyssal peridotites. *Journal of Geophysical Research* 95, 2661-2678.

JURELA, Z. (1973) Energy distribution of secondary ions from 15 polycrystalline targets. *Radiation Effects* 19, 175-180.

JURELA, Z., PEROVIC, B. (1968) Mass and energy analysis of positive ions emitted from metallic targets bombarded by heavy ions in the keV energy region. *Canadian Journal of Physics* 46, 773-778.

KELLY, R. (1978) An attempt to understand preferential sputtering. *Nuclear Instruments and Methods* 149, 553-558.

KELLY, R. (1980) On the problem of whether mass or chemical bonding is more important to bombardment-induced compositional changes in alloys and oxides. *Surface Science* 100, 85-107.

KENNEDY, A.K., HART, S.R., FREY, F.A. (1990) Composition and isotopic constraints on the petrogenesis of alkaline arc lavas: Lihir Island, Papua New Guinea. *Journal of Geophysical Research* 95, 6929-6942.

KINZLER, R.J., GROVE, T.L. (1992) Primary magmas of mid-ocean ridge basalts 1. Experiments and methods. *Journal of Geophysical Research* 97, 6885-6906.

KIRKPATRICK, R.J. (1977) Nucleation and growth of plagioclase, Makaopuhi and Ala lava lakes, Kilauea Volcano, Hawaii. *Geological Society of America Bulletin* 88, 78-84.

KLEIN, E.M., LANGMUIR, C.H. (1987) Global correlations of ocean ridge basalt chemistry with axial depth and crustal thickness. *Journal of Geophysical Research* 92, 8089-8115.

KOHLSTEDT, D.L. (1993) Structure, rheology, and permeability of partially molten rocks at low melt fractions. In: Phipps Morgan, J., Blackman, D.K., Sinton, J.M. (Eds) *Mantle Flow and Melt Generation at Mid-Ocean Ridges. Geophysical Monograph Series 71.* American Geophysical Union, Washington D.C., 103-121.

KOORNNEEF, J.M., NIKOGOSIAN, I., HEGEMAN, L., BERNDSEN, M., VAN BERGEN, M.J., VROON, P.Z., DAVIES, G.R. (2018) Combined Sr-Nd-Pb isotope data on individual melt inclusion from Italy record extreme mantle heterogeneity induced by complex geodynamics. *Goldschmidt2018 Conference Abstract, Boston, August 12-17, 2018,* Abstract 1335.

KURODA, T., TAMAKI, S. (1986) Role of electronic partition function in quantitative SIMS using the Saha-Eggert equation. *Microchimica Acta* 90, 105-115.

KUSHIRO, I. (1968) Compositions of magmas formed by partial melting of the Earth's upper mantle. *Journal of Geophysical Research* 73, 619-634.

KUSHIRO, I., YODER, H.S.JR. (1966) Anorthite-forsterite and anorthite-enstatite reactions and their bearing on the basalt-eclogite transformation. *Journal of Petrology* 7, 337-362.

LANGMUIR, C.H., BENDER, J.F., BENCE, A.E., HANSON, G.N., TAYLOR, R.S. (1977) Petrogenesis of basalts from the FAMOUS area: Mid-Atlantic Ridge. *Earth and Planetary Science Letters* 36, 133-156.

LAYNE, G.D., SHIMIZU, N. (1997) Measurement of lead isotope ratios in common silicate and sulfide phases using the Cameca IMS 1270 ion microprobe. In: Gillen, G., Bennett, R., Stevie, F. (Eds.) *Secondary Ion Mass Spectrometry SIMS XI,* John Wiley and Sons, Chichester, 63-65.

LEPAREUR, M. (1980) Le micro-analyseurionique de seconde génération Cameca modèle 3F. *Revue Technique Thomson-CSF* 12, 225-265.

LIEBL, H. (1967) Ion microprobe mass analyzer. *Journal of Applied Physics* 38, 5277-5283.

LIEBL, H., HERZOG, R.F.K. (1963) Sputtering ion source for solids. *Journal of Applied Physics* 34, 2893-2896.

LONG, J.V.P. (1965) A theoretical assessment of the possibility of selected-area mass-spectrometric analysis using a focused ion beam. *British Journal of Applied Physics* 16, 1277-1284.

LUNDQUIST, T.R. (1979) Energy dependence of the ionization probability of sputtered Cu and Ni. *Surface Science* 90, 548-556.

MAVROGENES, J.A., O'NEILL, H.,ST.C. (1999) The relative effects of pressure, temperature and oxygen fugacity on the solubility of sulfide in mafic magmas. *Geochimica et Cosmochimica Acta* 63, 1173-1180.

MCKENZIE, D. (1984) Generation and compaction of partially molten rock. *Journal of Petrology* 25, 713-765.

MCKENZIE, D. (1985) ^{230}Th-^{238}U disequilibrium and the melting process beneath ridge axes. *Earth and Planetary Science Letters* 72, 149-157.

MCKENZIE, D. (2018) A geologist reflects on a long career. *Annual Review of Earth and Planetary Sciences* 46, 1-20.

MEDDAUGH, W.S., HOLLAND, H.D., SHIMIZU, N. (1982) The isotopic composition of lead in galenas in the uranium ores at Elliot Lake, Ontario, Canada. In: Amstutz, G.C., El Goresy, A., Frenzel, G., Kluth, C., Moh, G., Wauschkuhn, A., Zimmermann, R.A. (Eds.) *Ore Genesis-The State of the Art.* Springer-Verlag, Berlin, 25-37.

MELSON, W.G., BYERLEY, G.R., NELSON, J.A., O'HEARN, T., WRIGHT, T.L., VALLIER, T. (1977) A catalogue of the major element chemistry of abyssal volcanic glasses. *Smithsonian Contributions to the Earth Sciences* 19, 31-60.

MELSON, W.G., O'HEARN, T., JAROSEWICH, E. (2002) A data brief on the Smithsonian abyssal volcanic glass data file. *Geochemistry, Geophysics, Geosystems* 3, doi: 10.1029/2001GC00249.

MOORE, R.O., GURNEY, J.J., GRIFFIN, W.L., SHIMIZU, N. (1991) Ultra-high pressure garnet inclusions in Monastery diamonds: Trace element abundance patterns and conditions of origin. *European Journal of Mineralogy* 3, 213-230.

MORGAN, A.E., WERNER, H.W. (1976) Quantitative analysis of low alloy steels by secondary ion mass spectrometry. *Analytical Chemistry* 48, 699-708.

MORGAN, A.E., WERNER, H.W. (1977) Test of a quantitative approach to secondary ion mass spectrometry on glass and silicate standards. *Analytical Chemistry* 49, 927-931.

MORGAN, A.E., WERNER, H.W. (1978) Molecular versus atomic secondary ion emission from solids. *Journal of Chemical Physics* 68, 3900-3909.

NAKAMURA, Y. (1973) Origin of sector-zoned igneous clinopyroxenes. *American Mineralogist* 58, 986-990.

NAVON, O., STOLPER, E. (1987) Geochemical consequences of melt percolation: The upper mantle as a chromatographic column. *Journal of Geology* 95, 285-307.

NIELSEN, S.G., SHIMIZU, N., LEE, C.T.A., BEHN, M. (2014) Calcophile behavior of thallium during MORB melting and implications for the sulfur content of the mantle. *Geochemistry, Geophysics, and Geosystems* 15, 4905-4919.

NIIDA, K. (1974) Structure of the Horoman ultramafic massif of the Hidaka metamorphic belt in Hokkaido, Japan. *Journal of the Geological Society of Japan* 80, 31-44.

NORSKOV, J.K., LUNDQVIST, B.I. (1979) Secondary-ion emission probability in sputtering. *Physical Review B* 19, 5661-5665.

OBATA, M., NAGAHARA, N. (1987) Layering of alpine-type peridotite and the segregation of partial melt in the upper mantle. *Journal of Geophysical Research* 92, 3467-3474.

O'HARA, M.J. (1967) Mineral parageneses in ultrabasic rocks. In: Wyllie, P.J. (Ed.) *Ultramafic and Related Rocks*. John Wiley & Sons, New York, 393-403.

ORTOLEVA, P., CHADAM, J., MERINO, H., SEN, A. (1987) Geochemical self-organization II: the reactive-infiltration instability. *American Journal of Science* 287, 1008-1040.

PIVIN, J.C., ROCQUES-CARMES, C., SLODZIAN, G. (1978) Variation des rendments d'emission ionique secondaire des alliages Ni-Cr, Fe-Cr, Fe-Ni en function de lateneur en solute. *International Journal of Mass Spectrometry and Ion Physics* 26, 219-235.

PIVIN, J.C., ROQUES-CARMES, C., SLODZIAN, G. (1979) Couches formees sur les alliages Fe-Ni, Fe-Cr, Ni-Cr sous bombardment ionique en presence d'oxygene. *International Journal of Mass Spectrometry and Ion Physics* 31, 311-332.

POKHILENKO, N.P., PEARSON, D.G., BOYD, F.R., SOBOLEV, N.V. (1991) Megacrystalline dunites and peridotites: hosts for Siberian diamonds. *Carnegie Institution of Washington Year Book 1991*, 11-18.

RAY, G.L., SHIMIZU, N., HART, S.R. (1983) Anion microprobe study of the partitioning of trace elements between clinopyroxene and liquid in the system diopside-albite-anorthite. *Geochimica et Cosmochimica Acta* 47, 2131-2140.

RICHARD, P., SHIMIZU, N., ALLÈGRE, C.J. (1976) $^{143}Nd/^{146}Nd$, a natural tracer: an application to oceanic basalts. *Earth and Planetary Science Letters* 31, 269-278.

RICHARDSON, S.H., GURNEY, J.J., ERLANK, A.J., HARRIS, J.W. (1984) Origin of diamonds in old enriched mantle. *Nature* 310, 198-202.

RILEY, G.N.JR., KOHLSTEDT, D.L., RICHTER, F.M. (1990) Melt migration in a silicate melt-olivine system: An experimental test of compaction theory. *Geophysical Research Letters* 17, 2101-2104.

RINGWOOD, A.E. (1966) The chemical composition and origin of the Earth. In: Hurley, P.M. (Ed.) *Advances in Earth Sciences*. MIT Press, Cambridge, MA, 287-356.

RODEN, M.F., SHIMIZU, N. (1993) ion microprobe analyses bearing on the composition of the upper mantle beneath the Basin and Range and Colorado Plateau provinces, USA. *Journal of Geophysical Research* 98, 14091-14108.

SAAL, A.E., HART, S.R., SHIMIZU, N., HAURI, E.H., LAYNE, G.D. (1998) Pb isotopic variability in melt inclusions from oceanic basalts, Polynesia. *Science* 282, 1481-1484.

SALTERS, V.J.M., DICK, H.J.B. (2002) Mineralogy of the mid-ocean ridge basalt source from neodymium isotopic composition of abyssal peridotites. *Nature* 418, 68-72.

SCHIANO, P.O., CLOCCHIATTI, R., SHIMIZU, N., WEIS, D., MATIELLI, N. (1994) Cogenetic silica-rich and carbonate-rich melts trapped in mantle minerals in Kerguelen ultramafic xenoliths: Implications for metasomatism in the oceanic upper mantle. *Earth and Planetary Science Letters* 123, 167-178.

SCHILLING, J.-G. (1975) Azores mantle blob: Rare earth evidence. *Earth and Planetary Science Letters* 25, 103-115.

SCHILLING, J.-G., ZAJAC, M., EVANS, R., JOHNSTON, T., WHITE, W., DEVINE, J.D., KINGSLEY, R. (1983) Petrologic and geochemical variations along the Mid-Atlantic Ridge from 29°N to 73°N. *American Journal of Science* 283, 510-586.

SEIFERT, F., MYSEN, B.O., VIRGO, D. (1982) *American Mineralogist* 67, 696-717.

SEN, G., FREY, F.A., SHIMIZU, N., LEEMAN, W.P. (1993) Evolution of the lithosphere beneath Oahu, Hawaii: Rare earth element abundances in mantle xenoliths. *Earth and Planetary Science Letters* 119, 53-69.

SHIMIZU, N. (1974) An experimental study of the partitioning of K, Rb, Cs, Sr and Ba between clinopyroxene and liquid at high pressures. *Geochimica et Cosmochimica Acta* 38, 1789-1798.

SHIMIZU, N. (1975a) Geochemistry of ultramafic inclusions from Salt Lake Crater, Hawaii and from the southern African kimberlites, *Physics and Chemistry of the Earth* 9, 655-670.

SHIMIZU, N. (1975b) Rare earth elements in garnets and clinopyroxenes from garnet lherzolite nodules in kimberlites. *Earth and Planetary Science Letters* 25, 26-32.

SHIMIZU, N. (1978) Analysis of the zoned plagioclase of different magmatic environments: a preliminary ion-microprobe study. *Earth and Planetary Science Letters* 39, 398-406.

SHIMIZU, N. (1981) Trace element incorporation into growing augite phenocryst, Nature, 289, 575-577.

SHIMIZU, N. (1983) Interface kinetics and trace element distribution between phenocrysts and magma. In: Augustithis, S.S. (Ed.) *The Significance of Trace Elements in Solving Petrogenetic Problems and Controversies*. Theophrastus Publications, Athens, 175-195.

SHIMIZU, N. (1986) Silicon-induced enhancement in secondary ion emission from silicates. *International Journal of Mass Spectrometry and Ion Processes* 69, 325-338.

SHIMIZU, N. (1990) The oscillatory trace element zoning of augite phenocrysts. *Earth Science Reviews* 29, 27-37.

SHIMIZU, N. (1998) The geochemistry of olivine-hosted melt inclusions in a FAMOUS basalt ALV 519-4-1. *Physics of the Earth and Planetary Interiors* 107, 183-201.

SHIMIZU, N. (1999) Young geochemical features in cratonic peridotites from southern Africa and Siberia. In: Fie, Y., Bertka, C.M., Mysen, B.O. (Eds.) *Mantle Petrology: Field Observations and High Pressure Experimentation: A Tribute to Francis R. (Joe) Boyd. Geochemical Society Special Publication 6.* Geochemical Society, Houston, TX, 47-55.

SHIMIZU, N., ALLÈGRE, C.J. (1978) Geochemistry of transition elements in garnet lherzolite nodules in kimberlites. *Contributions to Mineralogy and Petrology* 67, 41-50.

SHIMIZU, N. ARCULUS, R.J. (1975) Rare earth element concentrations in a suite of basanitoids and alkali olivine basalts from Grenada, Lesser Antiles. *Contributions to Mineralogy and Petrology* 50, 231-240.

SHIMIZU, N., HART, S.R. (1973) Differential dissolution technique (DDT): chemical separation of crystals from glass. *Carnegie Institution of Washington Year Book* 72, 268-270.

SHIMIZU, N., HART, S.R. (1982a) Isotope fractionation in secondary ion mass spectrometry, *Journal of Applied Physics* 53, 1303-1311.

SHIMIZU, N., HART, S.R. (1982b) Applications of the ion microprobe to geochemistry and cosmochemistry. *Annual Review of Earth and Planetary Sciences* 10, 483-526.

SHIMIZU, N., KUSHIRO, I. (1975) The partitioning of rare earth elements between garnet and liquid at high pressures: preliminary experiments. *Geophysical Research Letters* 2, 413-416.

SHIMIZU, N., LE ROEX, A.P. (1986) The chemical zoning of augite phenocrysts in alkaline basalts from Gough Island, south Atlantic. *Journal of Volcanology and Geothermal Research* 29, 159-188.

SHIMIZU, N., RICHARDSON, S.H. (1987) Trace element abundance patterns of garnet inclusions in peridotite-suite diamonds. *Geochimica et Cosmochimica Acta* 51, 755-758.

SHIMIZU, N., SOBOLEV, N.V. (1995) Young peridotitic diamonds from the Mir kimberlite pipe. *Nature* 375, 394-397.

SHIMIZU, N., SEMET, M.P., ALLÈGRE, C.J. (1978) Geochemical applications of quantitative ion-microprobe analysis. *Geochimica et Cosmochimica Acta* 42, 1321-1334.

SHIMIZU, N., SOBOLEV, N.V., YEFIMOVA, E.S. (1997a) Chemical heterogeneities of inclusion garnets and juvenile character of peridotitic diamonds from Siberia. *Russian Geology and Geophysics* 38, 356-372.

SHIMIZU, N., POKHILENKO, N.P., BOYD, F.R., PEARSON, D.G. (1997b) Geochemical characteristics of mantle xenoliths from the Udachnaya kimberlite pipe. *Russian Geology and Geophysics* 38, 205-217.

SIGMUND, P. (1969) Theory of sputtering I. Sputtering yield of amorphous and polycrystalline targets. *Physical Review* 184, 383-416.

SIGMUND, P. (1974) Energy density and time constant of heavy-ion-induced elastic-collision spikes in solids. *Applied Physics Letters* 25, 169-171.

SLODZIAN, G. (1964) Etude d'une methode d'analyse locale chimique et isotopique utilisant l'emission ionique secondaire. *Annales de Physique* 13, 591-648.

SLODZIAN, G. (1975) Some problems encountered in secondary ion emission applied to elementary analysis. *Surface Science* 48, 161-186.

SLODZIAN, G., HENNEQUIN, J.-F. (1966) Sur emission ionique secondaire des metaux en presence d'oxygene. *Comptes Rendus de l'Académie des Sciences Paris* 263, 1246-1249.

SLODZIAN, G., LORIN, J.C., HAVETTE, A. (1980) Isotopic effect on the ionization probabilities in secondary ion emission. *Journal de Physique Lettres* 23, 555-558.

SMITH, D., GRIFFIN, W.L., RYAN, C.G., SIE, S.H. (1991) Trace element zonation in garnets from The Thumb: Heating and melt infiltration below the Colorado Plateau. *Contributions to Mineralogy and Petrology* 107, 60-79.

SMITH, D., GRIFFIN, W.L., RYAN, C.G. (1993) Compositional evolution of high-temperature sheared lherzolite PHN 1611. *Geochimica et Cosmochimica Acta* 57, 603-613.

SMITH, V.G., TILLER, W.A., TUTTER, J.W. (1955) A mathematical analysis of solute redistribution during solidification. *Canadian Journal of Physics* 33, 723-745.

SNEERINGER, M., HART, S.R., SHIMIZU, N. (1984) Strontium and samarium diffusion in diopside. *Geochimica et Cosmochimica Acta* 48, 1589-1608.

SOBOLEV, A.V. (1996) Melt inclusions in minerals as a source of principle petrological information. *Petrology (Petrologia)* 3, 209-220.

SOBOLEV, A.V. SHIMIZU, N. (1993) Ultra-depleted primary melt included in an olivine from the Mid-Atlantic Ridge. *Nature* 363, 151-154.

SOBOLEV, A.V., DANYUSHEVSKIY, L.V., DIMITRIEV, L.V., SUSHCHEVSKAYA, N.M. (1989) High-alumina magnesian tholeiite as the primary basalt magma at mid-ocean ridge. *Geochemistry International* 26, 128-133.

SROUBEK, Z. (1974) The theoretical and experimental study of the ionization processes during the low energy ion sputtering. *Surface Science* 44, 47-59.

STOLL, H.M., SHIMIZU, N. (2009) Micropicking of nanofossils in preparation for analysis by secondary ion mass spectrometry. *Nature Protocol* 4, doi: 10.1038/nprot.2009.83.

STOLL, H.M., SHIMIZU, N., ARCHER, D., ZIVERI, P. (2007) Coccolithofore productivity response to greenhouse event of the Paleocene-Eocene Thermal Maximum. *Earth and Planetary Science Letters* 258, 192-206.

SVERJENSKY. D.A., HUANG, F. (2015) Diamond formation due to a pH drop during fluid-rock interactions. *Nature Communications* 6, doi: 10.1038/ncomms 9702.

TAKAZAWA, E., FREY, F.A., SHIMIZU, N., OBATA, M., BODINIER, J.L. (1992) Geochemical evidence for melt migration and reaction in the upper mantle. *Nature* 359, 55-58.

TATSUMOTO, M. (1966) Isotopic composition of lead in volcanic rocks from Hawaii, Iwo Jima and Japan. *Journal of Geophysical Research* 71, 1721-1733.

THOMPSON, M.W. (1968) II. The energy spectrum of ejected atoms during the high energy sputtering of gold. *The Philosophical Magazine: A Journal of Theoretical Experimental and Applied Physics* 18, 374-414.

TILLER, W.A., JACKSON, K.A., RUTTER, J.W., CHALMERS, B. (1953) The redistribution of solute atoms during solidification of metals. *Acta Metallurgica* 1, 428-437.

TSUCHIYAMA, A. (1981) Experimental studies on crystallization kinetics in the system diopside-anorthite and their application to crystallization of natural magmas. D. Sc. Thesis, University of Tokyo, 178 pp.

VAN ORMAN, J.A., GROVE, T.L., SHIMIZU, N. (2001) Rare earth element diffusion in diopside: Influence of temperature, pressure, and ionic radius, and an elastic model for diffusion in silicates. *Contributions to Mineralogy and Petrology* 141, 687-703.

VASSEUR, G., VERNIERES, J., BODINIER, J.-L. (1991) Modelling of trace element transfer between mantle melt and heterogranular peridotite matrix. *Journal of Petrology, Special Volume, Issue 2*, 41-54.

WARREN, J.M., SHIMIZU, N. (2010) Cryptic variations in abyssal peridotite compositions: Evidence for shallow-level melt infiltration in the oceanic lithosphere. *Journal of Petrology* 51, 395-423.

WARREN, J.M., SHIMIZU, N., SAKAGUCHI, C., DICK, H.J.B., NAKAMURA, E. (2009) An assessment of upper mantle heterogeneity based on abyssal peridotite isotopic compositions. *Journal of Geophysical Research* 114, B12203, doi: 10.1029/2008JB006186.

WATSON, C.C., HAFF, P.K. (1980) Sputtering-induced isotopic fractionation at solid surfaces. *Journal of Applied Physics* 51, 691-699.

WENDLANDT, R.F. (1982) Sulfide saturation of basalt and andesite melts at high pressures and temperatures. *American Mineralogist* 67, 877-885.

WERNER, H.W. (1974) Theoretical and experimental aspects of secondary ion mass spectrometry. *Vacuum* 24, 493-504.

WILLIAMS, P. (1979) The sputtering process and sputtered ion emission. *Surface Science* 90, 588-634.

WOOD, B.J., PAWLEY, A., FROST, D. (1996) Water and carbon in the earth's mantle. *Philosophical Transactions of the Royal Society, London A* 354, 1495-1511.

WYLLIE, P.J. (1967) *Ultramafic and Related Rocks*. John Wiley and Sons, Inc., New York, 464p.

YOSHIKAWA, M., NAKAMURA, E., TAKAHASHI, N. (1993) Rb-Sr isotope systematics in a phlogopite-bearing spinel peridotite and its implications for age and origin of metasomatism in the Horoman peridotite complex,m Hokkaido, Japan. *Journal of Mineralogy, Petrology and Economic Geology* 88, 121-130.

YU, M.L. (1981) Velocity dependence of the ionization probability of sputtered atoms, *Physical Review Letters* 47, 1325-1328.

YU, M.L. (1987) A bond breaking model for secondary ion emission. *in Physics Research Section B: Beam Interactions with Materials and Atoms* 18, 542-548.

YU, M.L., REUTER, W. (1981a) Secondary ion emission from binary alloy systems. Part I: O_2^+ bombardment. *Journal of Applied Physics* 1478-1488.

YU, M.L., REUTER, W. (1981b) Secondary ion emission from binary alloy systems. Part II: Ar^+ bombardment with O_2 absorption. *Journal of Applied Physics* 52, 1489-1498.

INDEX

G

H

I

J

K

L

M

N

O

P

R

S

T

U

V

W

Z

Geochemical Perspectives is an official journal of the European Association of Geochemistry

The European Association of Geochemistry, EAG, was established in 1985 to promote geochemistry, and in particular, to provide a platform within Europe for the presentation of geochemistry, exchange of ideas, publications and recognition of scientific excellence.

Officers of the 2019 EAG Council

President	**Sigurður Reynir Gíslason**, University of Iceland, Iceland
Vice-President	**Derek Vance**, ETH Zurich, Switzerland
Past-President	**Bernard Marty**, CRPG Nancy, France
Treasurer	**Estelle Rose-Koga**, University of Clermont Auvergne, France
Secretary	**Mihály Pósfai**, University of Pannonia, Hungary
Goldschmidt Officer	**Dan Frost**, University of Bayreuth, Germany
Goldschmidt Officer	**Helen Williams**, University of Cambridge, UK

www.eag.eu.com

NOBUMICHI SHIMIZU is a Scientist Emeritus at Woods Hole Oceanographic Institution and was founder and director of the Northeast National Ion Microprobe Facility.

Immediately after finishing his Ph.D. at University of Tokyo under the supervision of Professor Hisashi Kuno in April 1968, the entire university got embroiled in the '68 student-administration confrontation and all possibilities for Nobumichi (better known as Nobu) to pursue his research goals in Tokyo vanished. The untimely death of Professor Kuno in 1969 exacerbated an already bad situation, and his future at the university looked bleak. Stan Hart and colleagues at DTM agreed to hire him as a post-doc, so he moved to Washington in 1971. After three productive years at DTM, he had to leave the US due to the J-1 visa rules, but he did not want to go back to Tokyo because he knew he could not continue there the projects that he had started at DTM. He then met Claude Allègre at the AGU Spring Meeting who gave him a job at the Institut de Physique du Globe, Paris. So, he moved to Paris in August 1974 as a 'Physicien Adjoint'. This was when he first encountered the Cameca IMS 300, the first-generation Cameca ion microprobe, and what was to become his four-decade long odyssey began. At first he struggled mightily with the physics of secondary ion formation processes, but eventually the energy filtering approach was established based on the relationship between secondary ion energy and intensity and it became possible to carry out *in situ* determinations of trace elements in silicate minerals and glasses. He moved to MIT in 1978, when the MIT-Harvard-Brown Consortium led by Stan Hart was funded by NSF, and purchased a second-generation Cameca ion microprobe, the IMS 3f, and he joined Stan's group as a Principal Research Scientist. Nobu moved the ion microprobe operation to WHOI in 1988 and remained there until his retirement in 2013. His research accomplishments in geochemistry and efforts to develop micro-scale trace element analysis techniques for geological samples were recognized in the form of AGU Fellowship in 1995, EAG and GS Geochemistry Fellowship in 1999, and AAAS Fellowship in 2006.